



This work is protected by copyright and other intellectual property rights and duplication or sale of all or part is not permitted, except that material may be duplicated by you for research, private study, criticism/review or educational purposes. Electronic or print copies are for your own personal, non-commercial use and shall not be passed to any other individual. No quotation may be published without proper acknowledgement. For any other use, or to quote extensively from the work, permission must be obtained from the copyright holder/s.

NON-IDEALITY IN LIQUID MIXTURES:
THE PREDICTION AND MEASUREMENT OF
THERMODYNAMIC EXCESS FUNCTIONS

by

Frank Anthony Hewitt G.R.I.C.

A thesis submitted to the University of Keele
in partial fulfilment of the requirements
for the degree of
Doctor of Philosophy

September 1976

UNIVERSITY
OF KEELE

ACKNOWLEDGEMENTS

I should like to thank Professor H.D.Springall, whose kindness in providing a maintenance grant for the first year of this work made it possible, and whose provision of whatever facilities were required at various stages of the work made it successful. I should also like to thank Professor I.T.Millar for his continued support of my work, and the University of Keele, which kindly provided a research studentship for the second and third years.

To my supervisor Dr.D.T.Dixon, I am most grateful, since his initial support gained me the aid of Professor Springall, and his continuing kindness and assistance made my work both fruitful and enjoyable.

I am very grateful, also, to the staff of the Computer Centre at Keele, and to Dr.P.G.Collis, in particular, for their help with the many problems which arose in the writing and running of numerous programmes.

I should also like to offer my thanks to the technical staff of the Chemistry Department, particularly Mr. C.Cork and Messrs. P.Holbrook, and R.Dix, for their generous assistance.

Finally, my thanks also to Mr.H.Wardell and his staff of the University Workshop, who constructed, and in some cases, reconstructed, much of the mechanical equipment which I designed.

ABSTRACT

This thesis may be separated readily into three sectors: firstly, the mathematical prediction of the excess functions of some well-known systems, and also of some new systems, the experimental data for which were gathered in the course of this work; secondly, the measurement of the excess enthalpies and volumes of mixing of three systems, for comparison with the predicted values; thirdly, the development of a method for obtaining excess free energies of mixing by measurement of the bubble- and dew-points of mixtures of approximately known composition. The thesis is presented more or less in the order in which the work was carried out, which was not that of the sectors just described.

The Appendix to the thesis contains details of the numerous computer programmes required and written in the course of this work, including the major programme, for analysis of the data from bubble- and dew- point measurements, which yields an equation for the excess free energy in terms of composition.

The predictive work was based on the use of two equations of state, that of van der Waals, produced in 1900, and that of Guggenheim, produced in 1965. Van der Waals's own approach to obtaining the adjustable parameters a and b for the mixture was employed, and two different methods for obtaining the mixed critical values were tested. The measurements of both the excess enthalpies and volumes were carried out using small, mercury-filled, batch-type devices,

the dilatometer being particularly simple, but quite accurate.

The apparatus eventually produced for the measurement of bubble- and dew- points was large and complex, and the third chapter suggests means by which the method might be adapted for a small, semi- automatic system.

	PAGE NO.
<u>CONTENTS</u>	
CHAPTER ONE ENTHALPY OF MIXING	
GENERAL DESCRIPTION OF THE OPERATING SYSTEM	1.1
THE CALORIMETERS	1.3
CALORIMETER FILLING DEVICES	1.6
CALORIMETER SUPPORT JACKET	1.7
CALORIMETER ROTATING DEVICES	1.7
THE VACUUM DEGASSING SYSTEM	1.9
THE THERMOSTAT TANK AND CONTROL SYSTEMS	1.10
THE TEMPERATURE MONITORING SYSTEM	1.11
THE HEATER CONTROL SYSTEM	1.13
THE EXPERIMENTAL PROCEDURE	1.14
ANALYSIS OF RESULTS	1.16
THE SYSTEMS STUDIED	1.18
CHAPTER TWO FREE ENERGY OF MIXING	
THE DEW-POINT, BUBBLE-POINT METHOD	2.1

THE SOLUTION OF THE EQUATIONS	2.5
THE EXPERIMENTAL MEASUREMENT OF BUBBLE-, AND DEW-POINTS	2.8
THE MARK 1 APPARATUS	2.10
THE MARK 2 APPARATUS	2.11
THE MARK 3 APPARATUS	2.14
THE MECHANICAL AND ELECTRONIC CONTROL APPARATUS	2.16
THE EXPERIMENTAL PROCEDURE WITH THE MARK 3 APPARATUS	2.18
RESULTS OBTAINED	2.24
APPENDIX	2.25
CHAPTER THREE FURTHER DEVELOPMENT	3.1
FURTHER DEVELOPMENT OF THE METHOD	3.1
CHAPTER FOUR VOLUMES OF MIXING	
THE MEASUREMENT OF THE EXCESS VOLUMES OF MIXING	4.1
THE RESULTS OBTAINED	4.4

CHAPTER FIVE

THE PREDICTION OF THE EXCESS
FUNCTIONS

5.1

APPENDIX ONE

THE REDLICH-KISTER CURVE-FITTING

PROGRAMME

APP1.2

PARABOLIC FITTING PROGRAMME

APP1.3

THE MATRIX SET SIMEQN

APP1.4

THE PRESSURE-VOLUME CALCULATION

AND FITTING PROGRAMMES

APP1.5

THE STATE EQUATION

PROGRAMMES

APP1.6

THE BUBBLE-POINT, DEW-POINT

PROGRAMME

APP1.7

The cell was used for the measurement of the heat of mixing of the components of the system. The cell was calibrated by the method of van't Hoff, and the heat of mixing of the components was determined by the method of van't Hoff. The cell was used for the measurement of the heat of mixing of the components of the system. The cell was calibrated by the method of van't Hoff, and the heat of mixing of the components was determined by the method of van't Hoff.

CHAPTER ONE

ENTHALPIES OF MIXING

The cell was used for the measurement of the heat of mixing of the components of the system. The cell was calibrated by the method of van't Hoff, and the heat of mixing of the components was determined by the method of van't Hoff.

The cell was used for the measurement of the heat of mixing of the components of the system. The cell was calibrated by the method of van't Hoff, and the heat of mixing of the components was determined by the method of van't Hoff.

A GENERAL DESCRIPTION OF THE OPERATING SYSTEM

This method for determining excess enthalpies of mixing was based upon the use of a small calorimeter, of low specific heat, in which the liquids were mixed in the absence of any vapour phase. The liquids to be mixed were isolated in two compartments, over mercury, provision for change of volume on mixing being allowed in the form of a capillary and bulb expansion device. The mixtures studied were all endothermic and the process of mixing was made as nearly isothermal as possible by the timed release of electrical energy into a heater coil in the calorimeter, thus providing the energy to be taken up by the mixing process. The temperature of the calorimeter was monitored by observation of the off-balance signal of an alternating current Wheatstone bridge, of which two thermistors in series, on the calorimeter, formed one arm. This signal was amplified, rectified, and fed to a pen recorder.

The calorimeter itself was thermally isolated, as far as this was possible, by containing it within a block of expanded polystyrene foam, this cylindrical block being enclosed within a Dewar vessel, with a flanged top. To this flange was fitted a domed cap, through which passed the connections to the calorimeter. The entire vessel was protected within a tubular plastic jacket, and was immersed in a thermostat (which was controlled to within 0.002 K of the desired temperature).

The liquids used in this work were of spectroscopic grade or better, were purified by repeated fractional distillation, and degassed thoroughly before use.

The apparatus used in this work is shown in the diagram, which is a schematic representation of the apparatus, and is not intended to show the details of construction.

In the diagram (Diagram 1), the heater and condenser are connected at the joint, as is the condenser and the receiver. The vessel is filled with the liquid to be used, and the liquid is drawn off by means of a syringe, through the joint, into the receiver. The heater and condenser are then fitted, and the calorimeter removed from the system.

As may be seen from the diagram, the calorimeter which contained the calorimeter is connected to the exterior surface of the top, with a view of available work. The heater and condenser fitted were also in place with cover.

This calorimeter was designed to measure a large quantity of energy and contained a large quantity of liquid, leading to great expenditure of time in purification work. The acute angle of joints needed to retain small quantities of liquid after the first operation, and the apparatus was not particularly accurate, and the calorimeter was not liberally covered with insulation in view of

THE CALORIMETERS

The calorimeter finally used in this study was the product of considerable experimentation with several designs, in order to solve the various problems of filling, heating and monitoring.

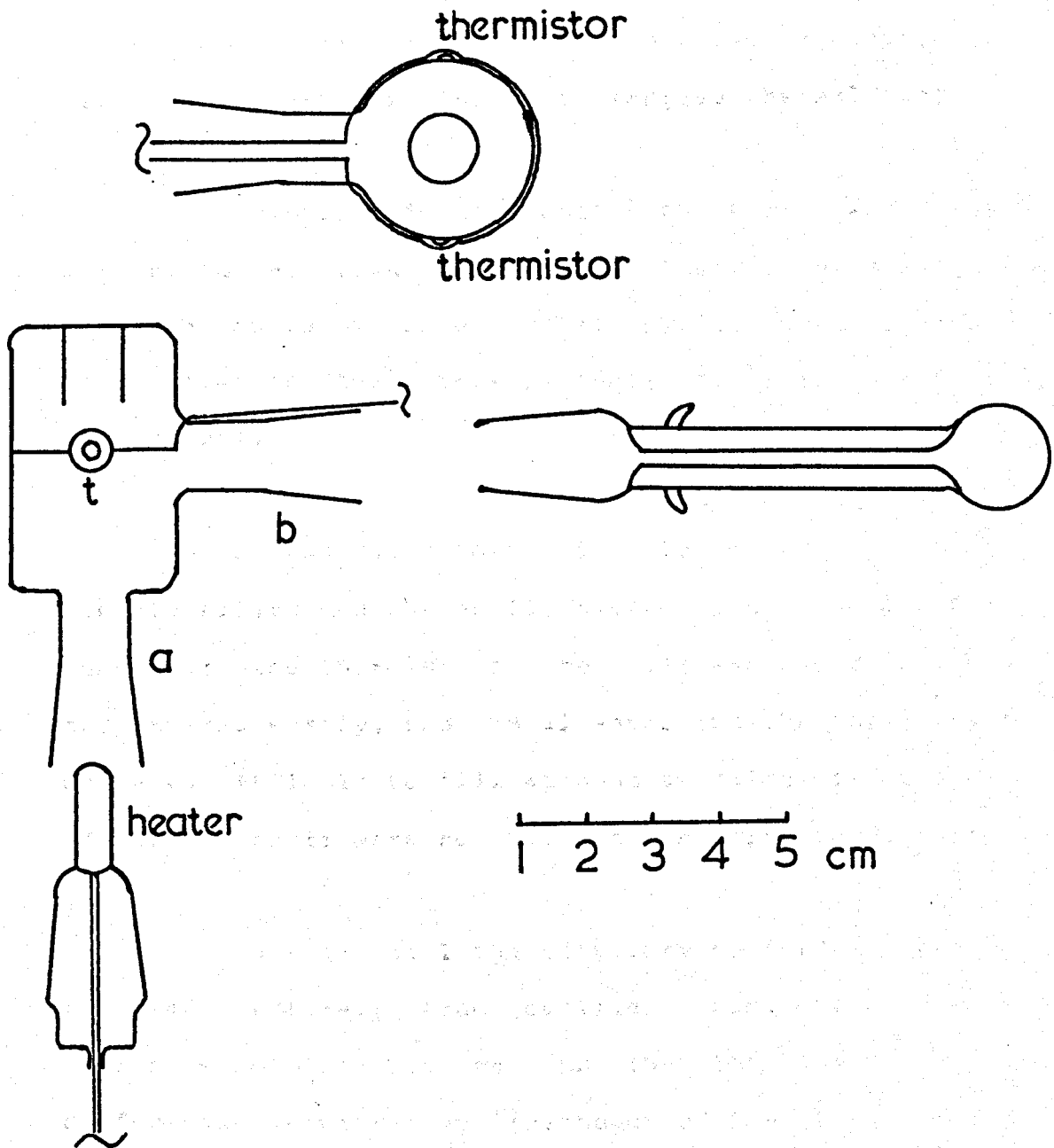
In the first model (diagram 1), the heater was sealed into an extension of the joint a, and a capillary and bulb expansion device fitted to the joint b. The vessel was filled beneath the surface of a bowl of mercury, and the liquids injected, by means of bent syringe needles, through the joint a, into the two concentric compartments. The heater and expansion device were then fitted, and the calorimeter removed from the mercury.

As may be seen from the diagram, the thermistors which monitored the calorimeter temperature were cemented to the exterior surface of the body with a drop of araldite cement, and both heater and expansion fitting were clamped in place with springs.

This calorimeter had numerous drawbacks: a large quantity of mercury was contaminated each time the calorimeter was filled, leading to great expenditure of time in purification work; the acute angle at joint a tended to retain small quantities of unmixed liquids after the first inversion, causing incomplete mixing; and the calorimeter was considerably more massive than was really desirable in view of

DIAGRAM I

the heat of mixing calorimeters:
the first model



the requirement for a low specific heat; also the thermistors and their wiring were exposed enough to be prone to accidental damage.

The second model of the calorimeter was an attempt to rectify at least some of the faults of its predecessor. Joint a and the heater fitting were replaced by a fine-walled glass pocket in the base of the body, into which was tightly fitted a heater coil, wound on threaded p.t.f.e. rod, and lubricated with paraffin oil to improve thermal contact.

This calorimeter, unlike the first, was filled with mercury under vacuum, and the liquid samples introduced by mounting the vessel on a special filling rig, to which were also attached the micro-syringes with which the filling was carried out.

It was found that this calorimeter was easily and cleanly filled and gas easily excluded, but two problems still remained: the thermistors were still exposed to shock damage, and damaged easily, and the air-space in the capillary fitting was very difficult to fill without trapping air bubbles. Both of these defects were remedied in the third model (diagram 3).

In this model the capillary device was replaced by one made entirely from capillary rod, which prevented any inclusion of air-bubbles and the thermistors were of a different, sturdier type, (although of identical sensitivity), I.T.T. Stantel G.52 rather than the previously used M.52.

DIAGRAM 2

the enthalpy of mixing calorimeters:
the second model

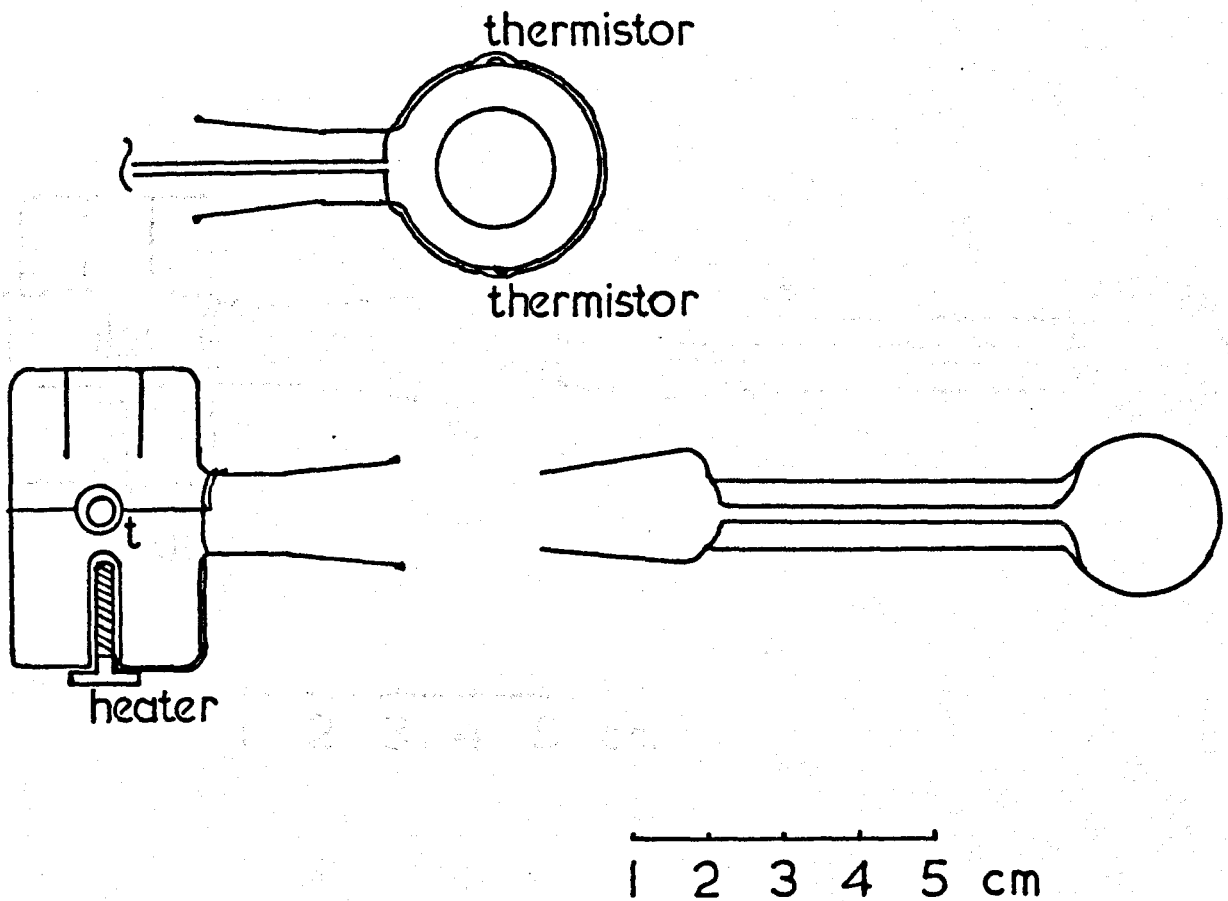
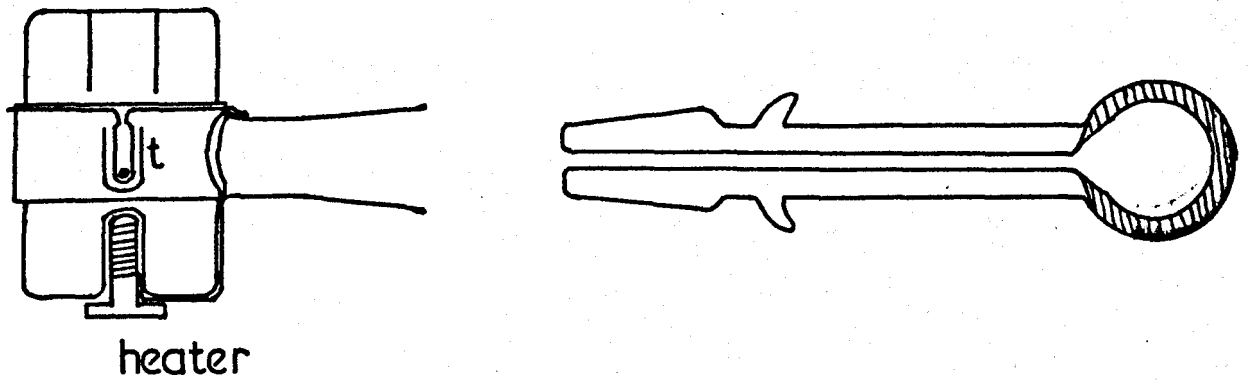


DIAGRAM 3

the enthalpy of mixing calorimeters:
the third model



1 2 3 4 5 cm

CALORIMETER ANCILLARY DEVICES

Calorimeter Filling Devices

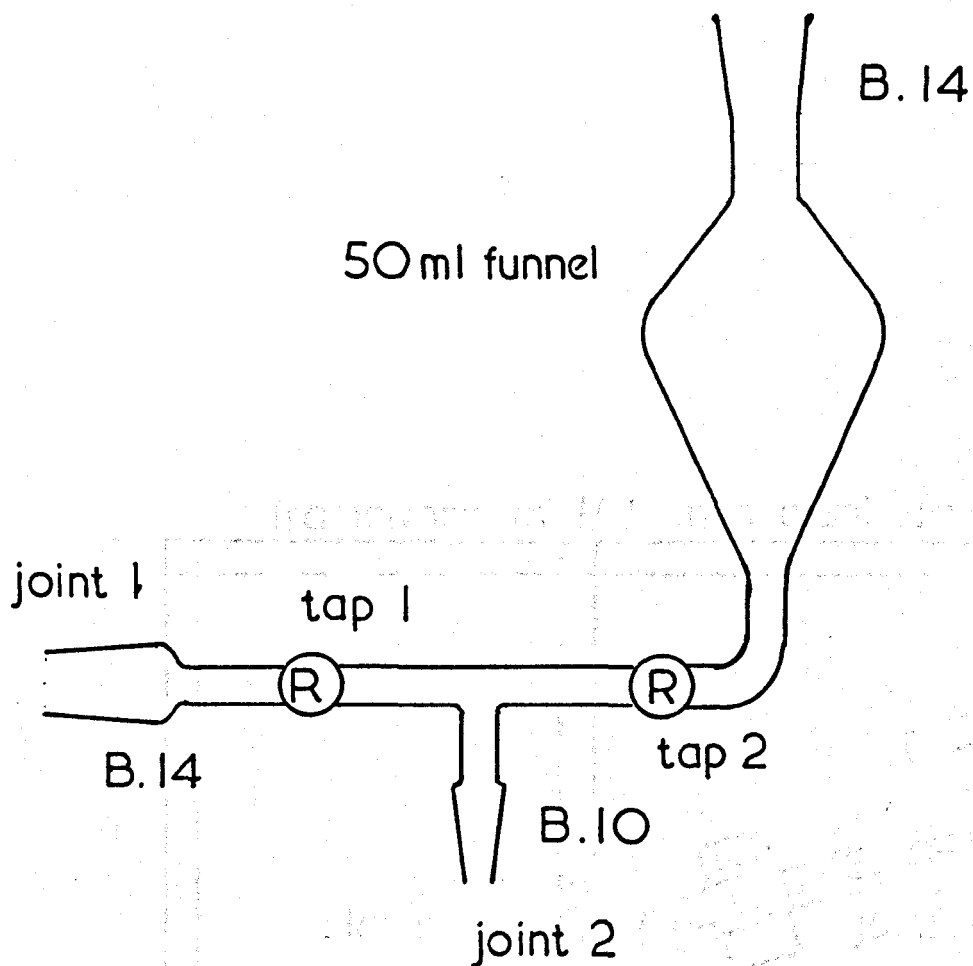
Mercury Filling

The device shown in diagram 4 was attached to the vacuum system at joint 1. Taps 1 and 2 were closed. The vacuum system was evacuated and joint 2 connected to the calorimeter at joint b. The funnel was filled with mercury, and tap 1 opened. When system pressure was below 0.1 Pa, tap 2 was opened and the calorimeter filled with mercury. Taps 1 and 2 were then closed, and the system re-pressurised. The calorimeter was then removed to the liquid filling rig for liquid injection.

Liquid Filling

The liquids to be mixed were metered into the calorimeter on the filling rig in diagram 5. The vessel was fitted to clamp a, at a slight angle to the horizontal, and moved into position in line with the first syringe. The appropriate adaptor for the compartment to be filled was fitted to joint b, and the syringe was moved down its guide, the needle passing into the required compartment in the calorimeter. The correct volume of liquid was then driven slowly into the vessel and the syringe withdrawn. The calorimeter was moved to the second clamp and a similar procedure followed for the second syringe and liquid.

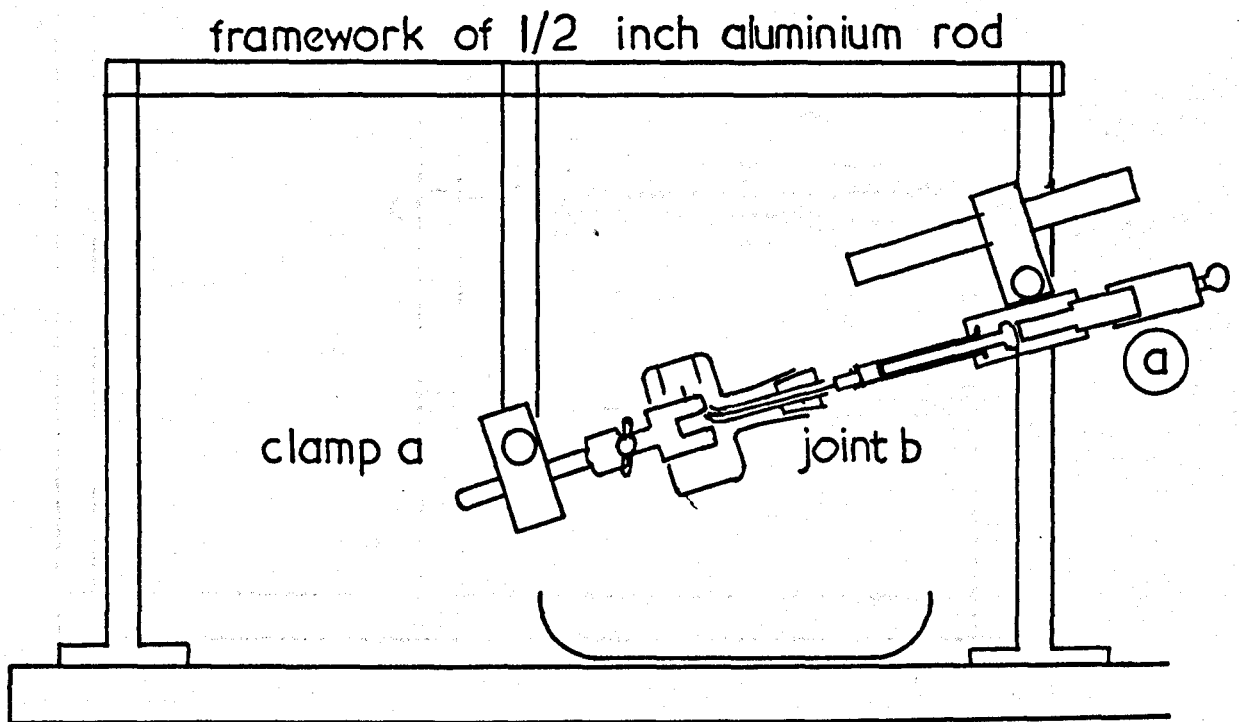
DIAGRAM 4



Ⓡ 3mm "Rotaflo" glass/p.t.f.e taps

the mercury-filling attachment

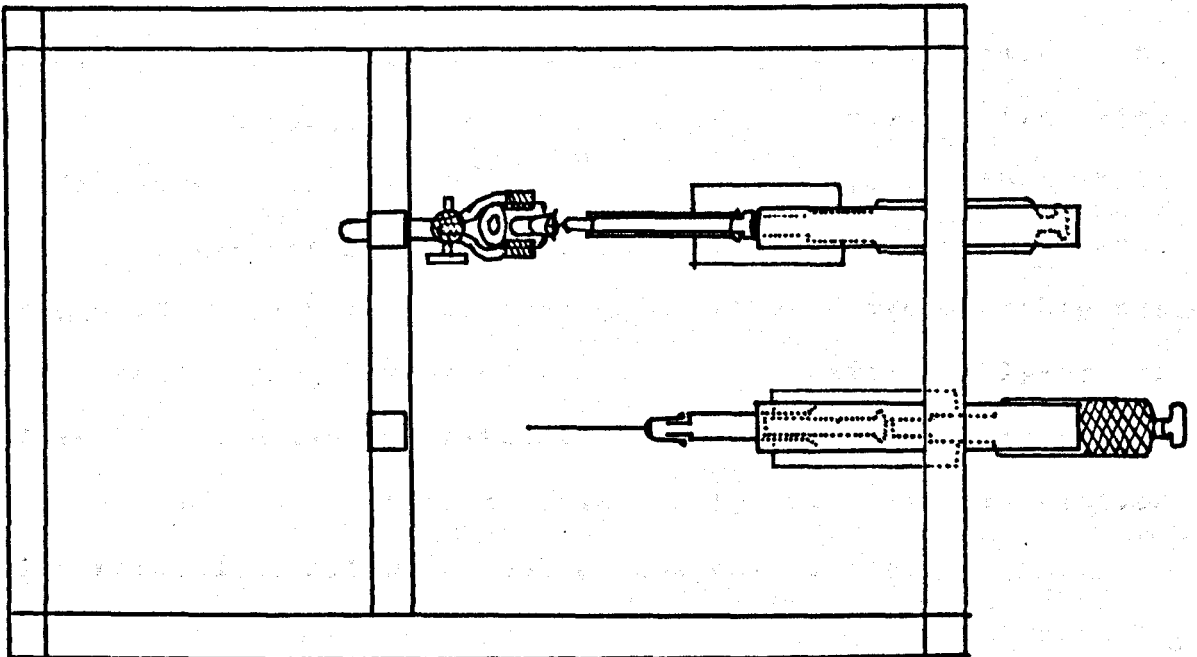
DIAGRAM 5



Ⓐ 0.5 cm³ "AGLA" micrometer syringe

Elevation of filling rig

DIAGRAM 6



Plan of filling rig

Calorimeter Support Jacket

The purpose of the jacketing system was twofold: firstly, to seal the calorimeter from the water of the thermostatic bath in which it was immersed; secondly, to isolate the calorimeter thermally from its surroundings.

These requirements were met by having a Dewar vessel with flanged top holding the vessel, which was already encased in the two halves of the expanded polystyrene inner jacket, firmly. The leads were passed through a flanged domed cap, and rubber tubing, to the surface of the thermostatic bath. The flange was lightly greased before assembly, and the whole vessel was further protected by an outer layer of polystyrene, surrounded by a hard polythene tube. The entire assembly was coated with a final layer of solution deposited polymer to render the assembly water-tight. The assembly was permanently attached to the rotating unit, only the domed cap section being removed to allow removal of the calorimeter.

Calorimeter Rotating Device

This was a device which, like the calorimeter, underwent considerable redesign in the course of the development of the equipment. The original version was as in diagram 8. Here the handle at the top was above the surface of the water in the thermostat, and was turned through 180 degrees to invert the calorimeter, and returned. In practice it was found that, given the necessary locations of the rest

DIAGRAM 7

the calorimeter support jacket

c is the outer polythene jacket

a and b are expanded polystyrene

shaded area is the Dewar vessel

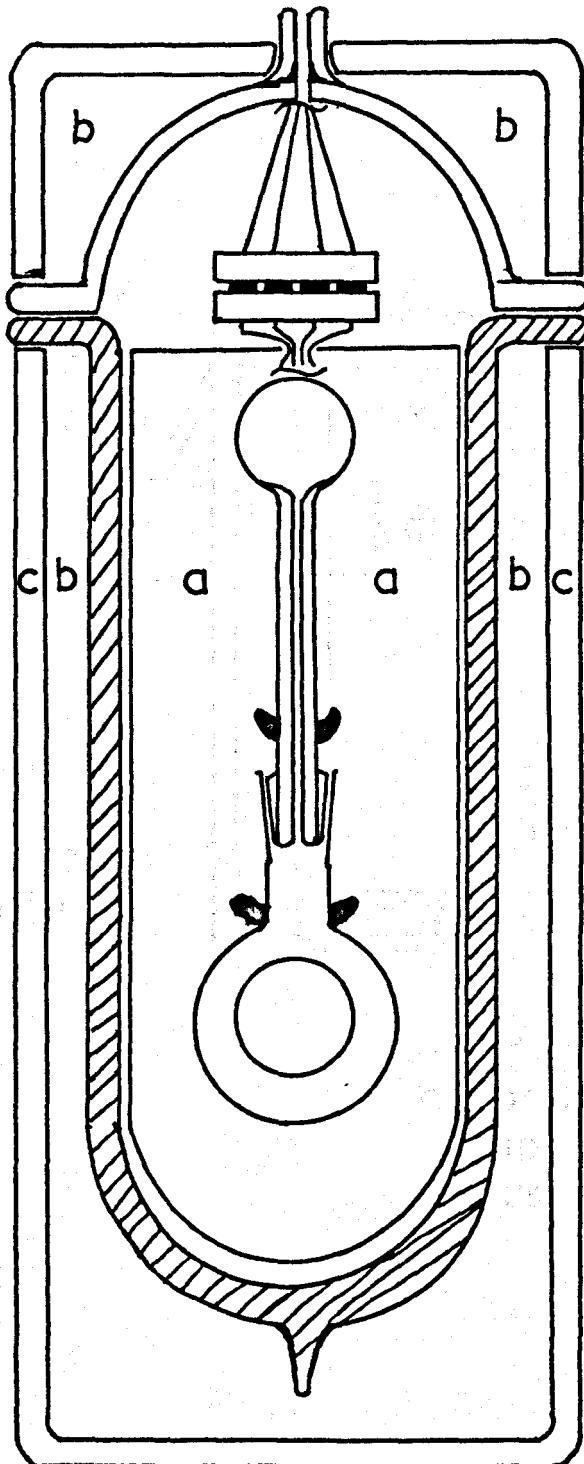


DIAGRAM 8

the calorimeter rotating devices: I

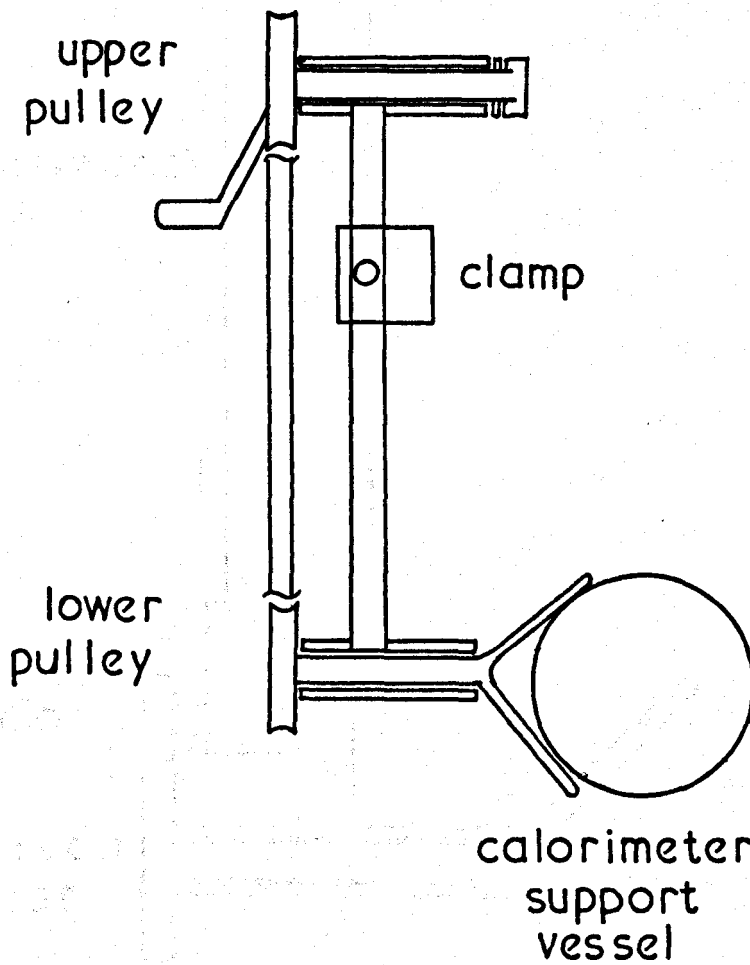
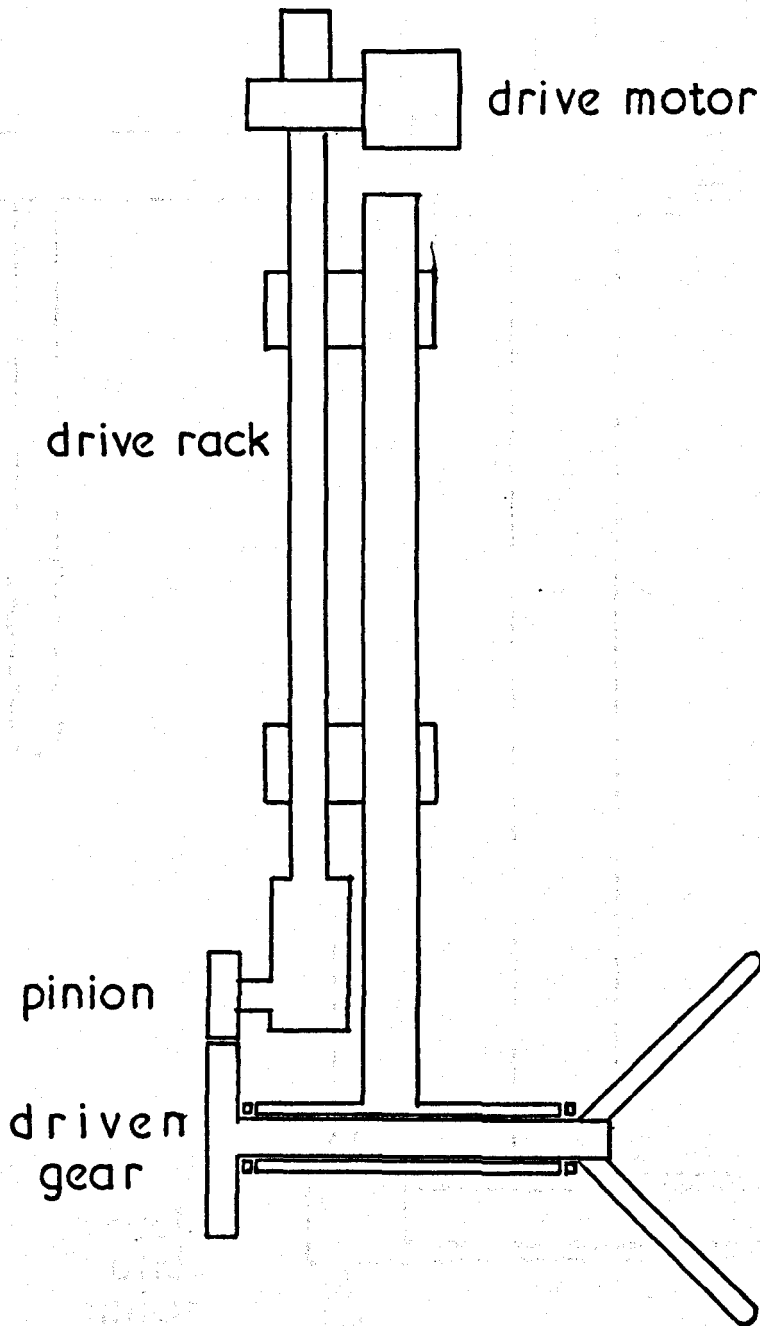


DIAGRAM 9

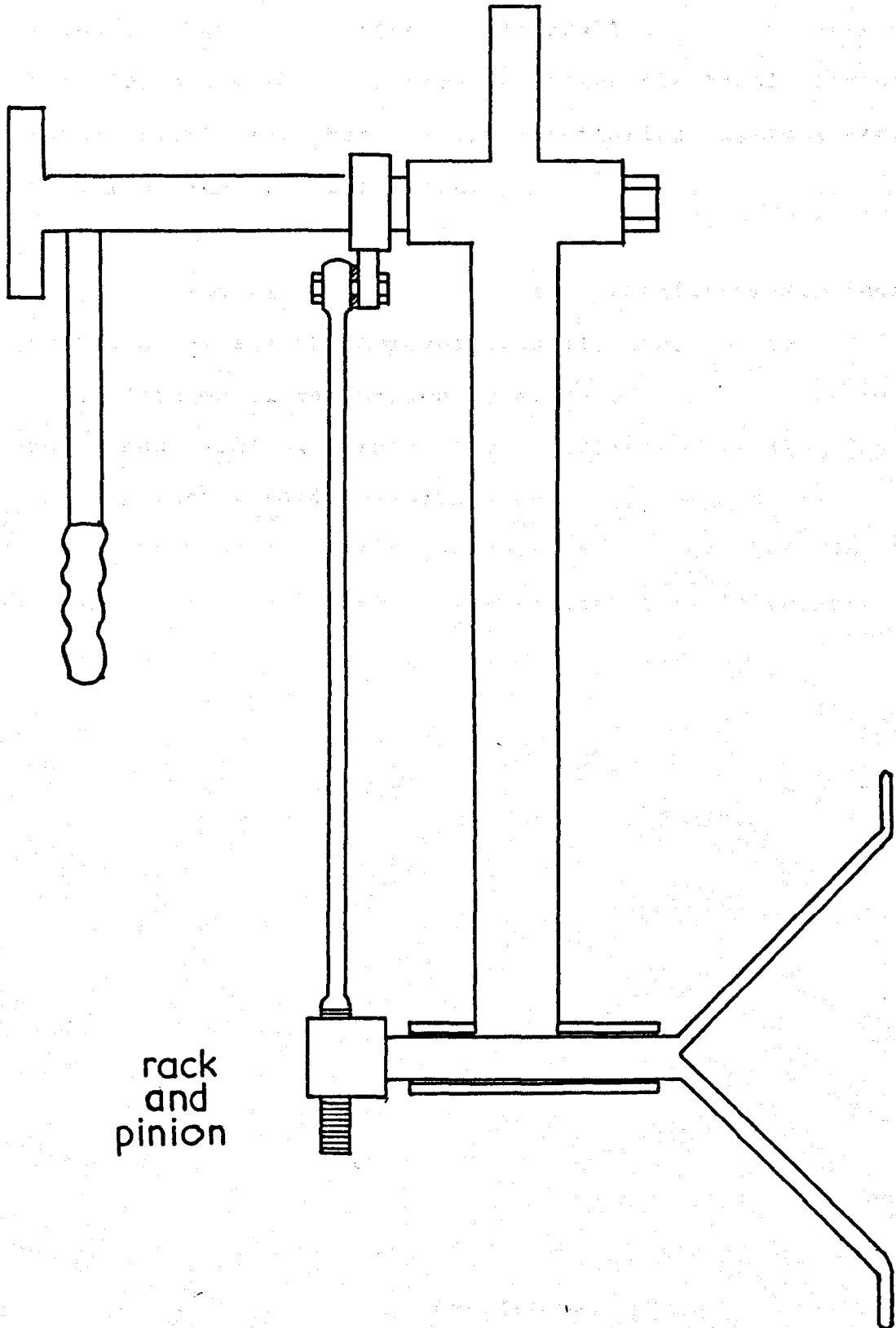
powered inverter



the calorimeter rotating devices: 2

DIAGRAM 10

the calorimeter rotating devices: 3



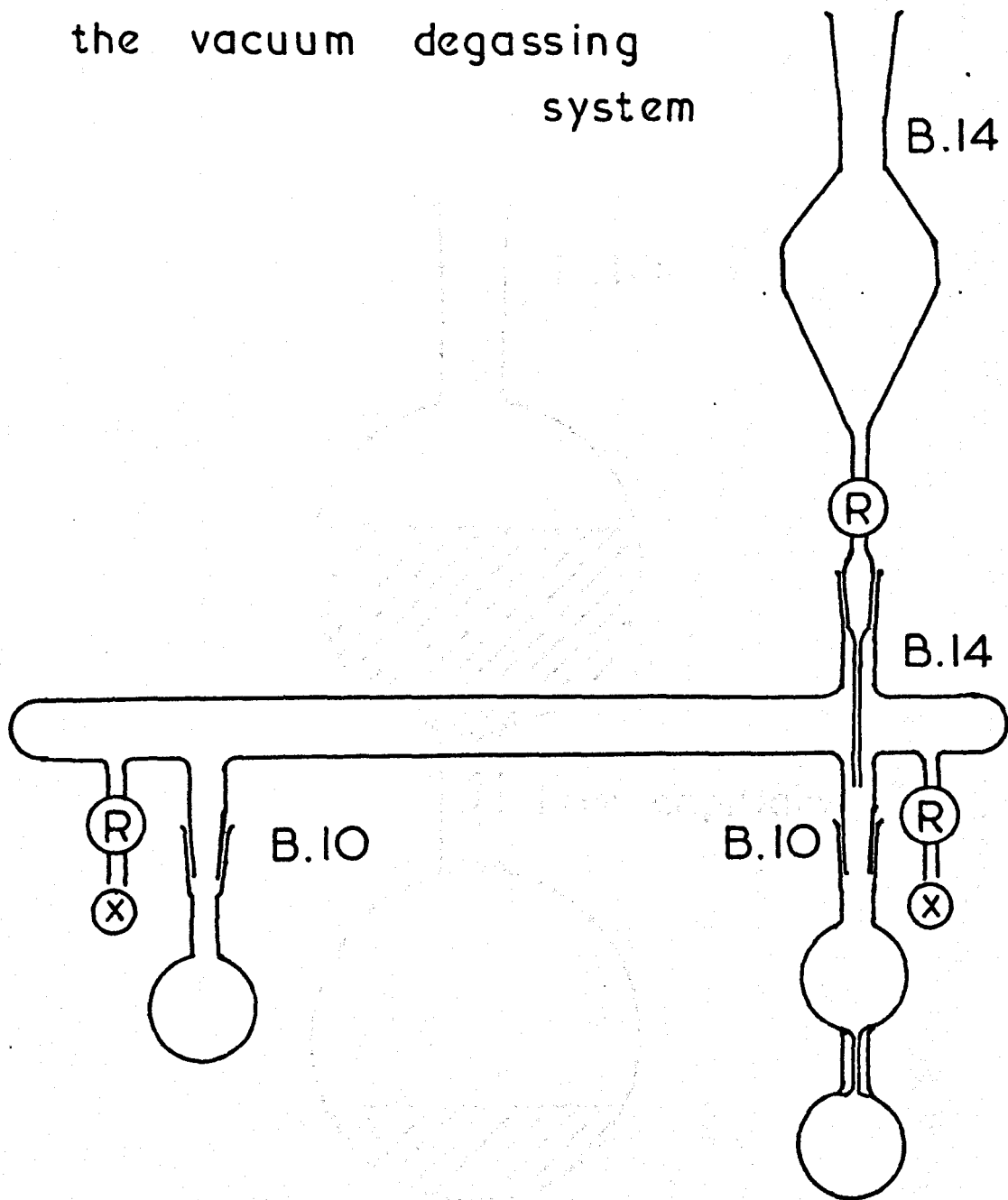
of the equipment, and the other operations required in the course of a mixing, it was too difficult to operate the rotator in this form. It was therefore decided that a form of inverter would be produced which could be operated remotely from the central switchboard. The resulting machine, however, although highly effective operationally, caused very severe interference with the highly sensitive electronic circuitry of the calorimeter temperature monitoring system, and this behaviour was not acceptable. After several modifications (initially using a motor) the liquid was allowed to run into the lower half. The final version of the rotator was, therefore, designed as a much-improved manually operated device (diagram 10). This model was driven by means of a crank, operating a rack and pinion, turning the calorimeter vessel. The system had a velocity ratio of 1:6, a movement of 30 degrees at the handle driving the vessel through 180 degrees between positive stops. This version was quite satisfactory in practice. However, some tests to be fairly critical in this regard, and the results were rather poor. The diameter of the vessel was greater than that needed to permit the disturbance flow of mercury into the lower half, and the needle was raised into the lower half, this adversely resulting in the loss of part of the liquid. Originally, one of the systems was intended to be a remote control manifold, but this entire arrangement was later discarded for a more suitable arrangement to the higher-velocity turbo-spin, described below.

THE VACUUM DEGASSING SYSTEM

In this system, the liquid was distilled, under vacuum, backwards and forwards between two flasks, in order to remove any dissolved gases. One of the flasks was of a special form, such that the liquid could be sealed in, in a fashion suitable for multiple accessing, without exposure to atmosphere. Diagram 11 illustrates the apparatus in which this operation was carried out. After several distillations (usually about ten), the liquid was allowed to run into the lower bulb of the flask; mercury was then allowed to run into the flask, from the special funnel, displacing the liquid into the capillary, and sealing the liquid into the lower bulb, by filling the upper with mercury. When a sample was required, a syringe with a long needle was passed into the lower bulb, and the required volume of liquid withdrawn, which was replaced by mercury from the upper bulb. The dimensions of the capillary were found to be fairly critical in this work, any length much shorter than 2 cm or diameter greater than 1 mm tending to result in the continuous flow of mercury into the lower bulb, whenever the needle was passed into the lower bulb, this naturally resulting in the loss of much of the liquid. Originally, two of the systems were joined to a common vacuum manifold, but this entire apparatus was later discarded for a much simpler attachment to the higher-vacuum bubble-point, dew-point system.

DIAGRAM II

the vacuum degassing system

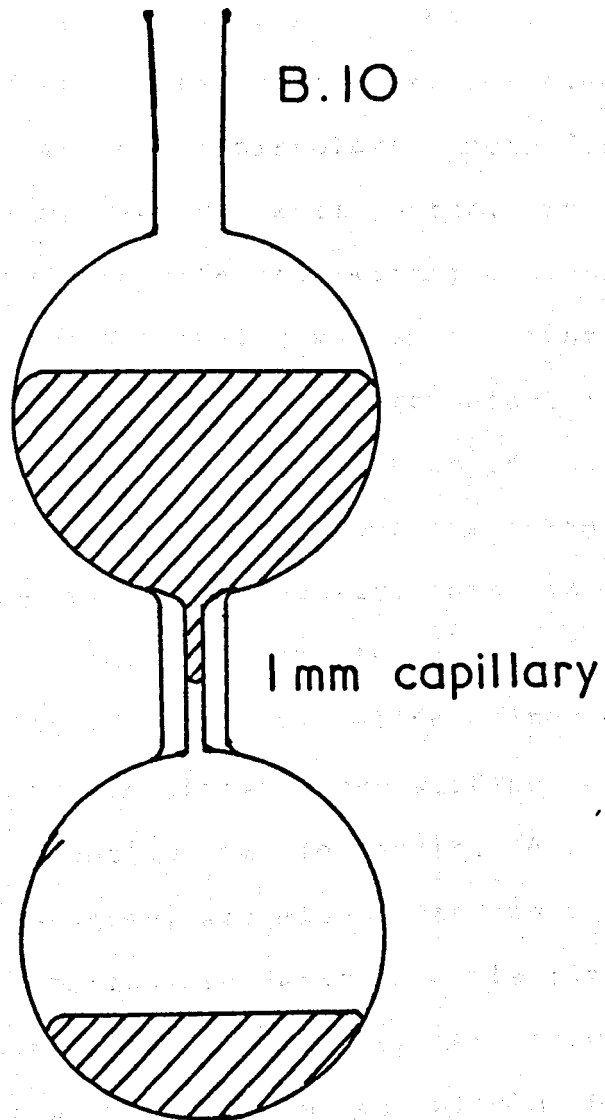


Ⓡ 3 mm "Rotaflo" glass / p.t.f.e. taps

ⓧ connection to vacuum manifold

DIAGRAM 12

the storage flask for degassed liquids



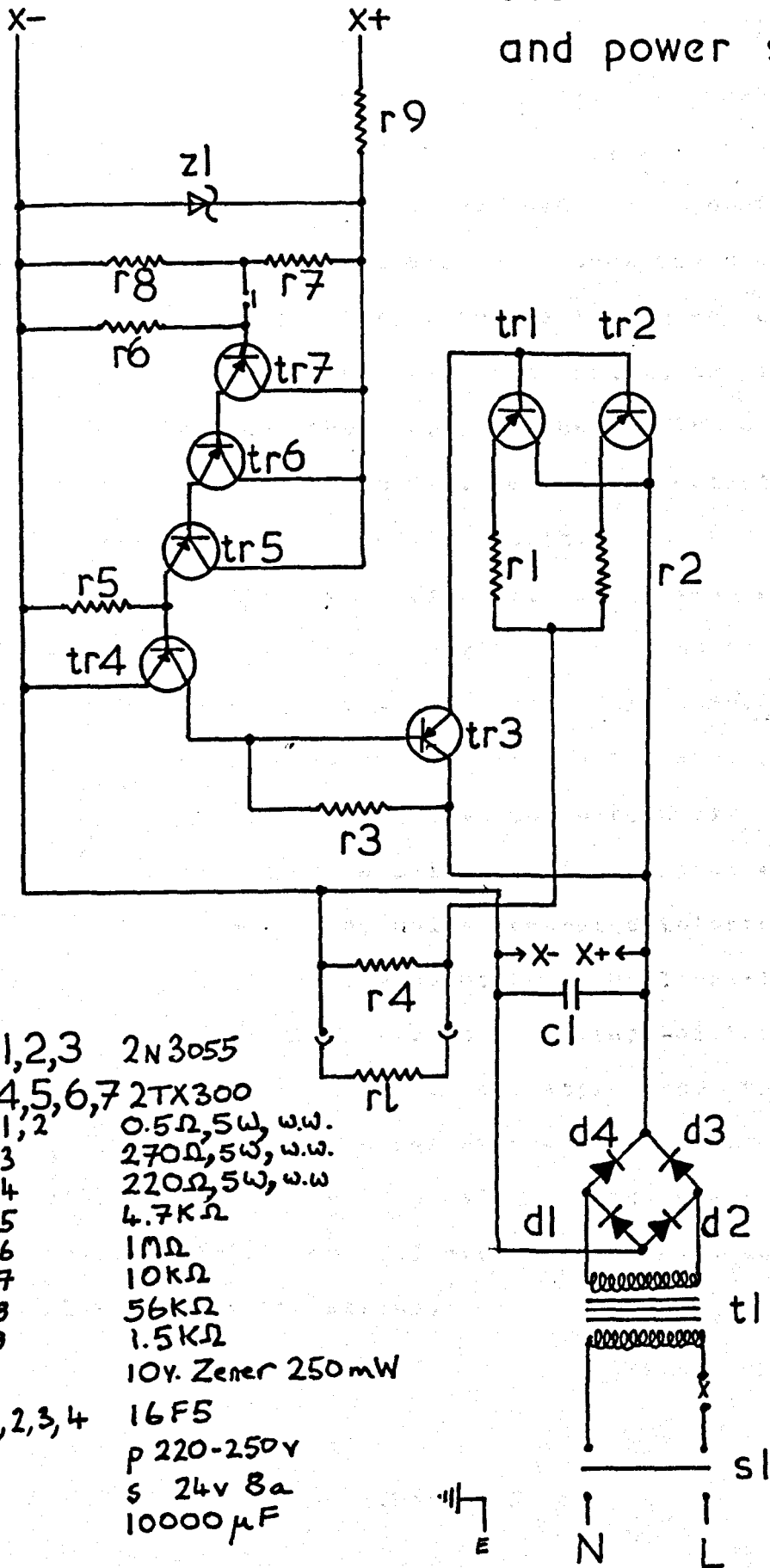
the shaded area illustrates the volume occupied by mercury

THE THERMOSTAT TANK AND CONTROL SYSTEMS

The system as finally operated consisted of a 40 cm cubic tank, insulated on all four sides and the base with a two-inch layer of expanded polystyrene foam, and on the water-surface with a two-inch thick layer of floating polystyrene packing granules. The tank was stirred, initially, by four shafts, having several submerged paddles on each shaft. These and a circulating pump for the water, were all driven by a single 100 watt motor, induction type, to avoid electrical interference with the sensitive electronics of the calorimeter monitoring system. The stirrers and their flexible drives were mounted in mechanical isolation from the tank, in order to prevent transmission of mechanical energy to the calorimeter. In order to prevent sticking of the mercury in the mercury-toluene regulator, this was also mounted with the stirrers, so that it vibrated gently. The controlled heater was fitted in the flow-line of the circulating pump, being wound on the insulated outer surface of a thin-walled copper tube, about 8 cm in length. A small cooling coil, cooled with tap-water, was also fitted into this flow-line, in order to shorten temperature cycle times when operating near to room temperature. This system proved excellent in use, controlling temperature to within 0.002 K, for many months, without any mechanical or electrical problems. The circuit diagram for the electronic relay is given in diagram 13, together with the component values used.

DIAGRAM 13

the electronic relay
and power supply

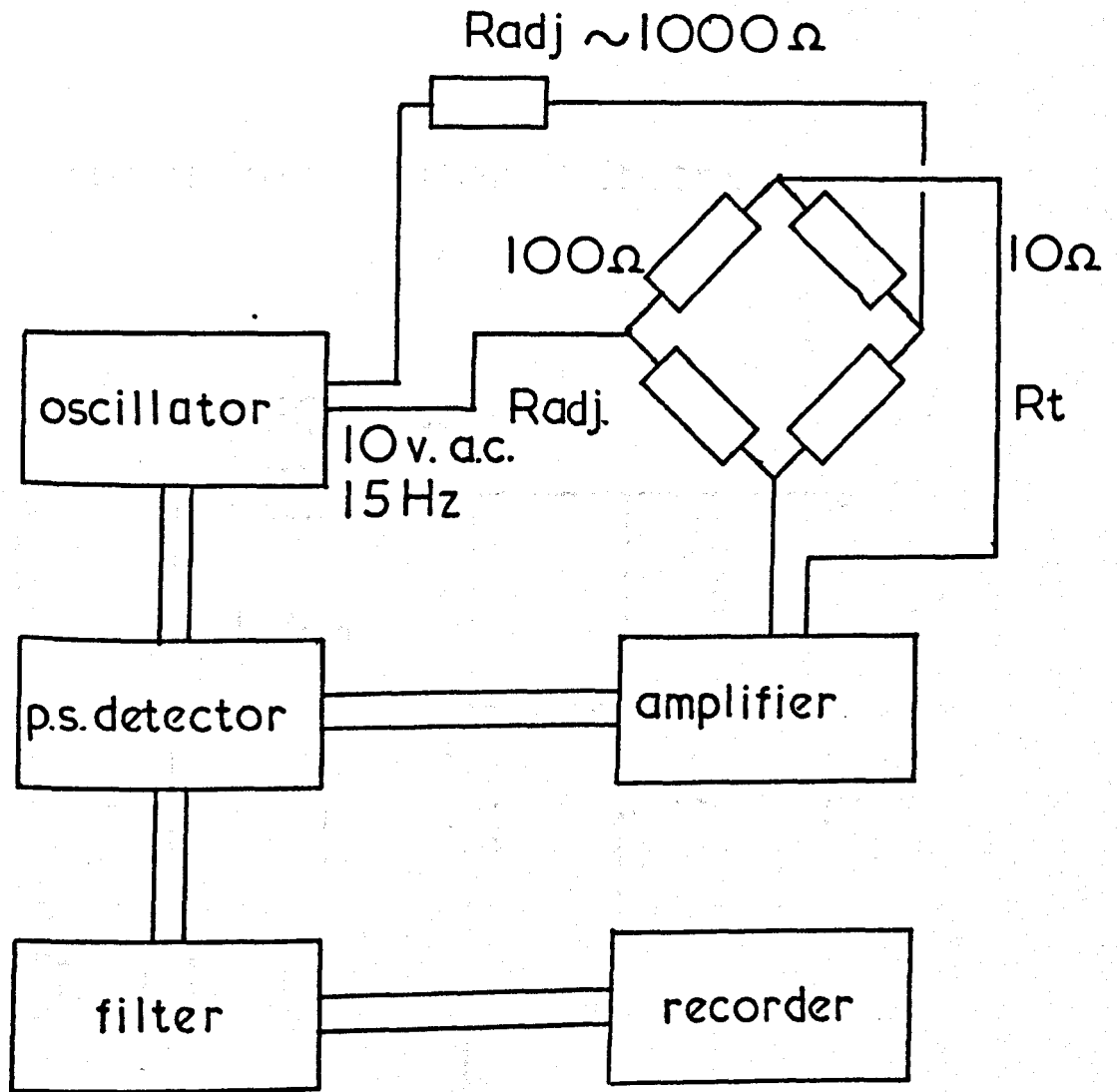


- tr1,2,3 2N3055
- tr4,5,6,7 2TX300
- r 1,2 0.5Ω, 5W, w.w.
- r 3 270Ω, 5W, w.w.
- r 4 220Ω, 5W, w.w.
- r 5 4.7KΩ
- r 6 1MΩ
- r 7 10KΩ
- r 8 56KΩ
- r 9 1.5KΩ
- z 1 10V. Zener 250mW
- d 1,2,3,4 16F5
- t 1 p 220-250v
- s 24v 8a
- c 1 10000μF

THE TEMPERATURE MONITORING SYSTEM OF THE CALORIMETER

The electrical circuitry, in block diagram form, of the thermistor-bridge temperature monitoring system, is given in diagram 14. This circuit is based on one devised by Faulkner, McGlashan, and Stubley (1965), with numerous detail modifications. Screened cable was used throughout, with only the cores conducting, and all resistance boxes were screened also. The screens, together with the instrument earth wires, were all connected to a central earth point, as were all other earthing cables and the thermostat bath. The oscillator was an Advance Electronics type J2E, having two outputs, one of 5 ohms impedance, with one side earthed, and the other of 600 ohms impedance, with both ends floating, which was used to energise the bridge, while that of 5 ohms fed the synchronous gate of the phase-sensitive detector. Any change in temperature of the calorimeter led to a change in resistance of the monitoring thermistors, which in turn led to an a.c. signal being fed to the amplifier. This signal was amplified and filtered to remove any mains generated interference, then fed to the phase-sensitive detector to be linearly rectified. This d.c. output was then fed to a voltage-dividing network, where signal strength could be attenuated to produce a suitable deflection per degree at the chart-recorder (normally about 1000 to 3000 cm per degree); at this stage the signal could also finally be filtered of any a.c. components and noise picked up by the wiring.

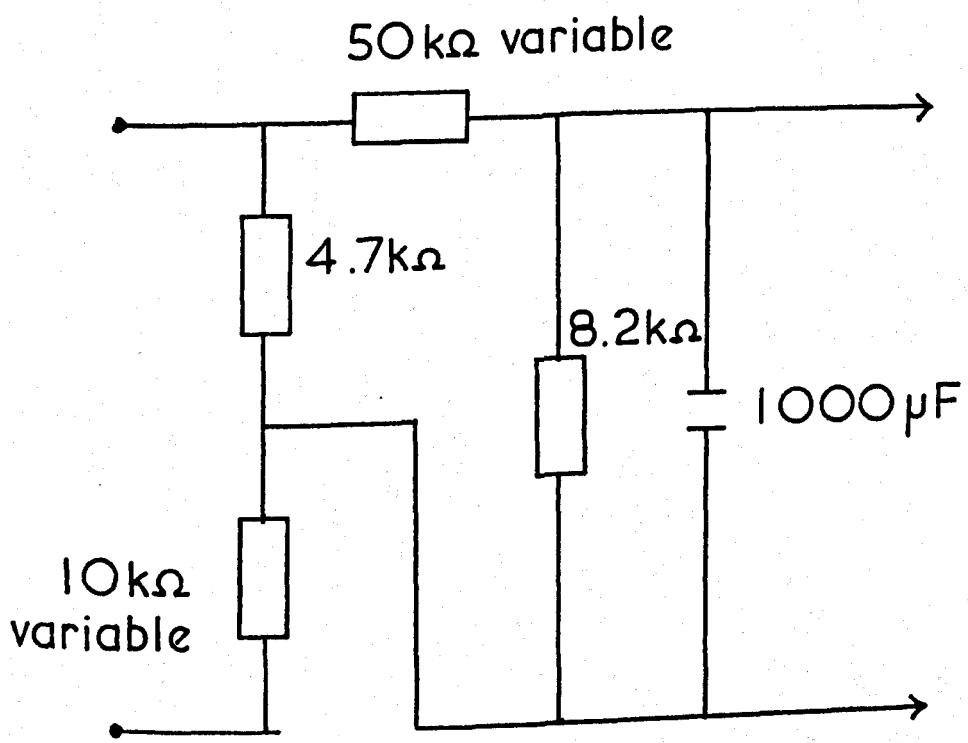
DIAGRAM 14



a block diagram of the calorimeter temperature monitoring system

DIAGRAM 15

Filter/attenuator network



The final response of the pen recorder was relatively noise free and, by its steadiness, suggested that thermal control of the calorimeter was being maintained to better than 0.0001 K. Self-heating of the thermistors led to a slow rise in temperature of the calorimeter, the magnitude of which corresponded well with that predicted, on the basis of all the heat thus generated being absorbed by the calorimeter. For this purpose the circuit could be regarded thus:

Total resistance = 1708.79 ohms

Total current = 0.0058521 amps

Current in thermistors = 0.000064309 amps

Power dissip. in thermistors = 0.00000372 watts

Thermal capacity of calorim. = about 50 J K⁻¹

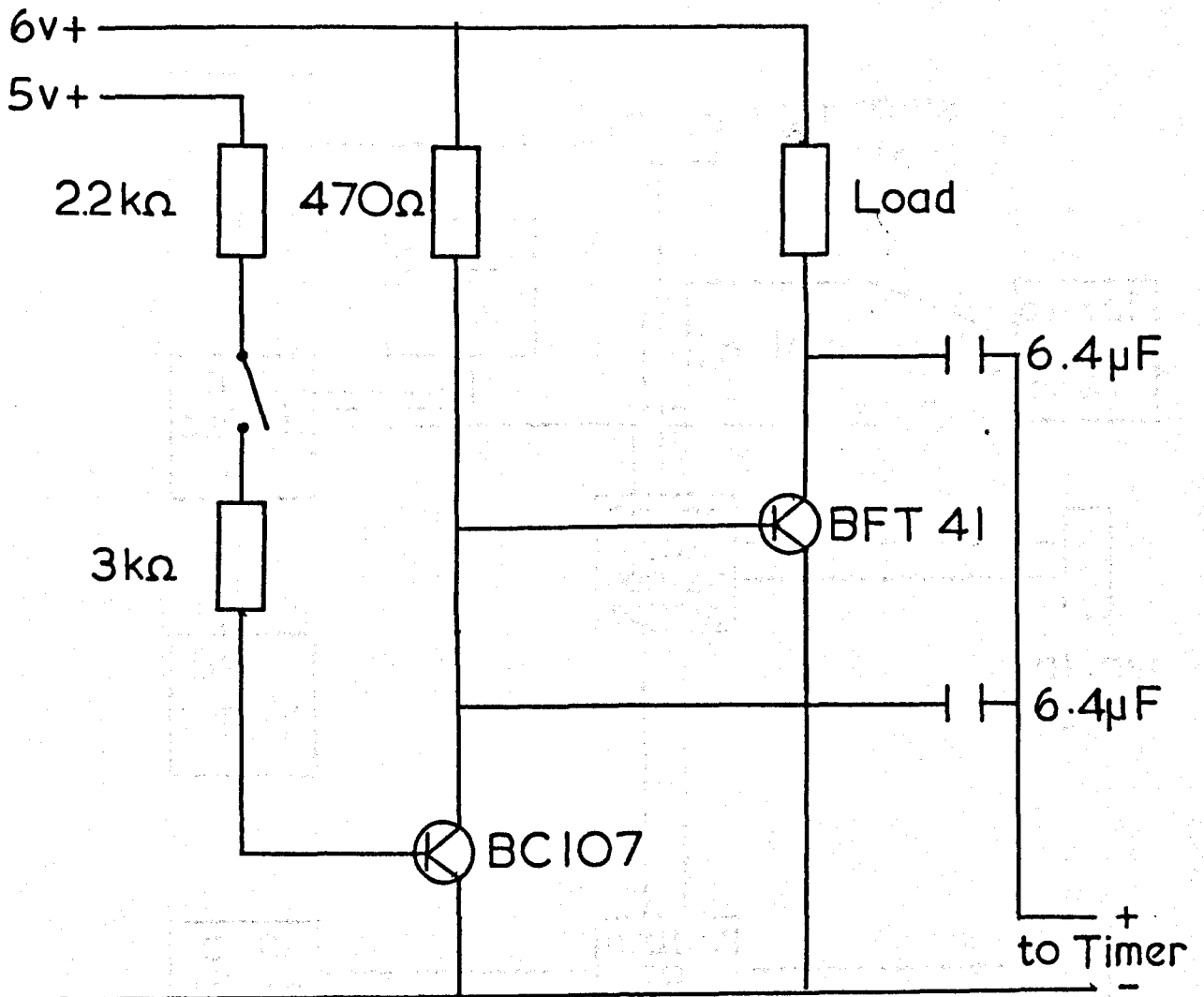
Temp. rise neglecting heat losses = 0.00000446 K per hour

Which was in fair agreement with that observed i.e. 0.000004 K per hour approx.

THE CALORIMETER HEATER CONTROL SYSTEM

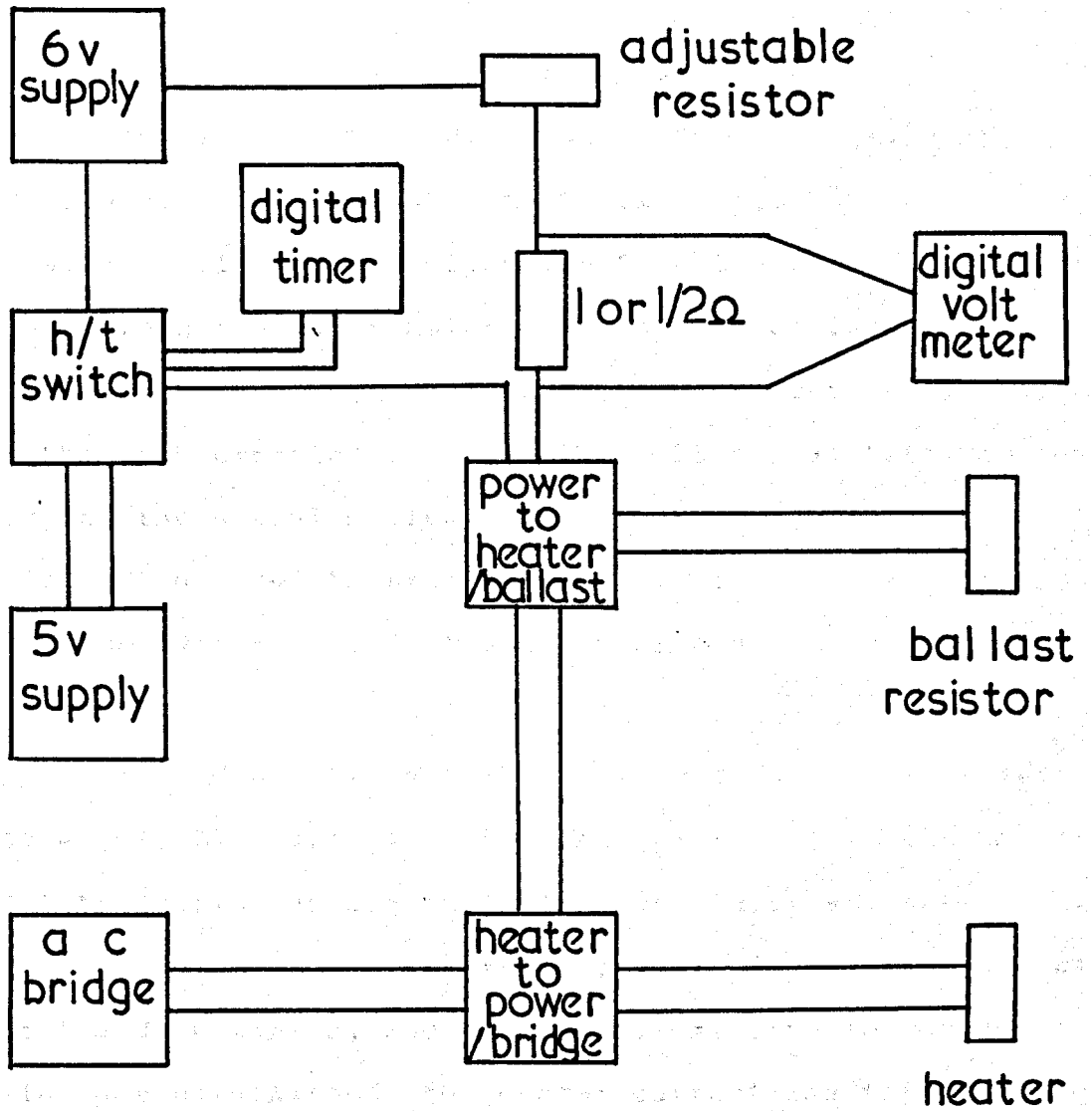
This heater was powered by a battery of lead-acid cells, stabilised by passing a current through a ballast resistor of about the same resistance as that of the heater, for about one hour prior to the need for the heater. The circuit was then switched over to the heater, and, at the appropriate time, the heater current was triggered through the transistor trigger, which simultaneously (to within 0.000001 sec) triggered a digital micro-second timer (diagram 16). Both heater and timer were switched off simultaneously by a further pulse from the trigger. The heater and ballast currents both passed through a standard resistor of one or one-half ohm, the voltage across which was measured by a ten micro-volt digital voltmeter, to yield the current flowing in the circuit, and through two resistance boxes, which could be adjusted to give the desired heater current. (Diagram 17 shows a block diagram of this system).

DIAGRAM 16



Heater and timer switching
circuit

DIAGRAM 17



the calorimeter heater control system

THE EXPERIMENTAL PROCEDURE

The calorimeter was filled with mercury, and the expansion tube was fitted and clamped into place. The liquids were obtained in Spectroscopic grade or Analar grade or better, and further purified by repeated fractional distillation through a thermostatted Fenske column. They were then degassed in the vacuum system and sealed into their flasks. Samples were then extracted for the first mixture composition. The calorimeter was filled with mercury, under vacuum, and removed to the filling rig. The appropriate quantities of liquid were withdrawn from the two flasks and injected into the calorimeter. The expansion tube was fitted and clamped into place, and the calorimeter carefully loaded into the submersible vessel, the electrical fittings were joined and the vessel sealed. The assembly was then fitted to the frame in the thermostat and left to reach thermal equilibrium over a period of about twelve hours.

The a.c. bridge was then balanced, the pen recorder set to a suitable position on the chart, and the heater current triggered through the ballast resistor and the circuit left for about one hour to stabilise. The chart recorder was then set and restarted, and after a few minutes in which the baseline was established, the heater current was triggered for the required number of seconds, during which time the vessel was rotated about twenty times to mix the liquids thoroughly. After the baseline had settled, a calibration was carried out, twice, to determine the energy input due to the stirring. The calorimeter was inverted twenty times and the baseline allowed to settle. The thermal capacity calibration was then carried

out, by running the heater again for a shorter period and allowing the baseline to settle finally. The calorimeter was then removed from the thermostat, emptied, washed, and dried, before filling for the next run. The results were then calculated as shown in the results section. The calibration constant for the calorimeter was determined by the method described in the appendix. A typical trace is shown in figure 1. The signal is shown as it was measured.

The signal from the calorimeter was amplified, for each linear expansion of the wire, and carried out as follows:

Heat = $\frac{1}{2} \rho \pi r^2 \Delta L \Delta T$

Heat = $\frac{1}{2} \rho \pi r^2 \Delta L \Delta T$

Heat = $\frac{1}{2} \rho \pi r^2 \Delta L \Delta T$

where ρ is the density of the wire, r is the radius of the wire, ΔL is the change in length of the wire, and ΔT is the change in temperature of the wire.

where subscript 1 refers to initial, and subscript 2 to final. The calorimeter constant, then, becomes this result divided by the mass of the sample of metal m and by the change in temperature ΔT .

The observed results were then fitted, by a least-squares method, to the following equation of the form:

$$C = \frac{1}{2} \rho \pi r^2 \Delta L \Delta T \left(\frac{1}{m} \right) \left(\frac{1}{\Delta T} \right)$$
 where C was the calorimeter constant, ρ was the density of the wire, r was the radius of the wire, ΔL was the change in length of the wire, ΔT was the change in temperature of the wire, and m was the mass of the sample.

A standard deviation analysis of the data:

THE ANALYSIS OF THE EXPERIMENTAL RESULTS

The experimental results for this system were essentially in two sections; the first, a record of heater currents, resistances and times for the mixing and calibration section; the second, the pen-recorder trace of the amplified output from the thermistor bridge. A typical trace is shown in diagram 18, and the heights marked on it were measured.

The calculation of the molar enthalpy of mixing, for each liquid composition measured, was carried out as follows:

Heater resistance = R ohms

Heater current = i amps

Heater run time = t seconds

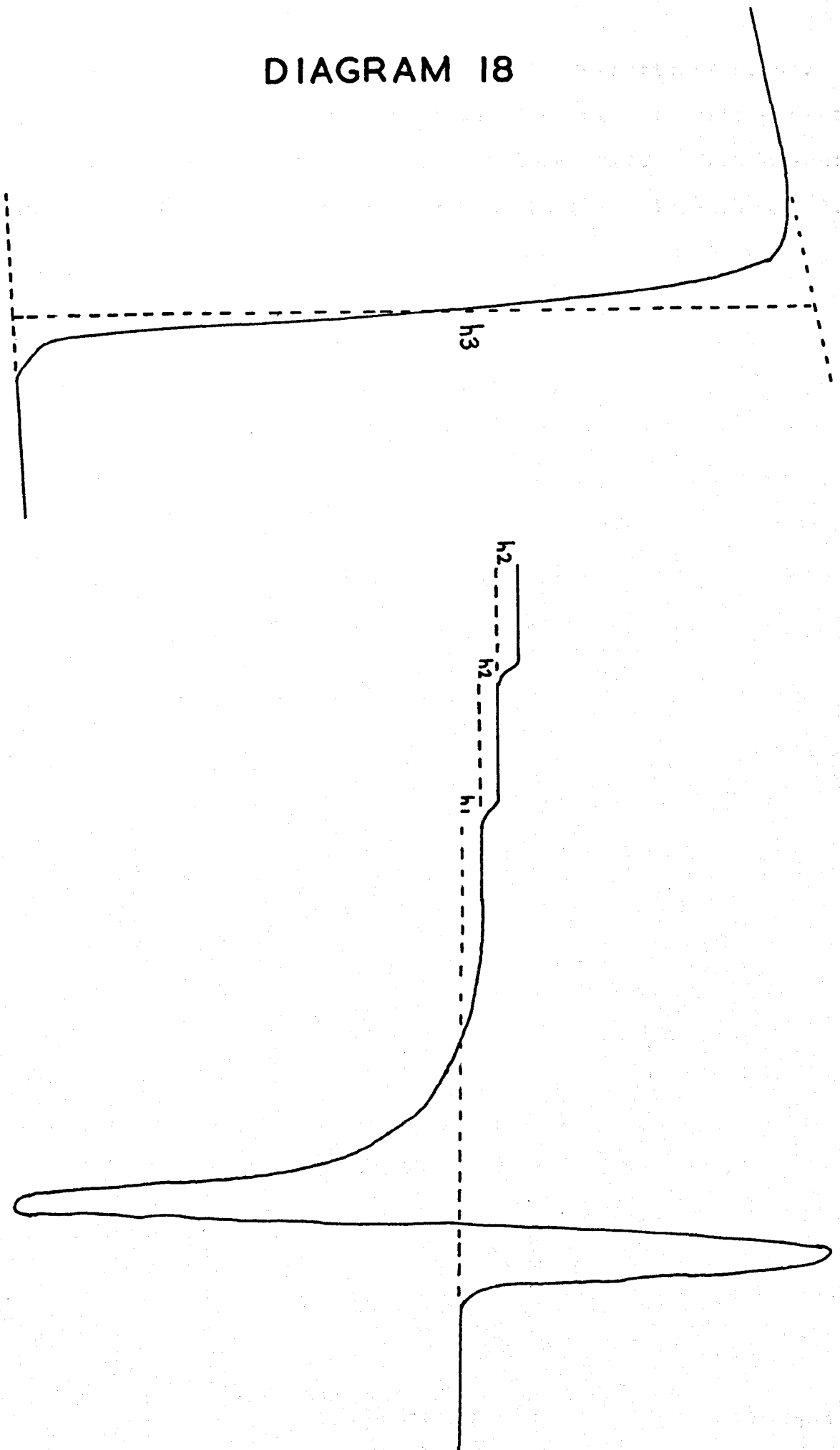
Excess enthalpy of mixing = $((h_1/h_3)-(h_2/h_3))i_2Rt_2 + i_1Rt_1$

where subscript 1 refers to mixing, and subscript 2 to calibration. The molar excess enthalpy then becomes this result divided by the sum of the number of moles of both liquids mixed.

The measured results were then fitted, by a least-squares method, to a Redlich-Kister equation of the form:

$H^E = x(1-x)(a+b(1-2x)+c(1-2x)^2 + \dots)$, where x was the mole fraction of component 2, and H^E was the molar excess enthalpy of mixing. A standard deviation criterion of the form:

DIAGRAM 18



recorder trace of a mixing experiment

s.d.=square root (sum of squares of deviations/(number of points -number of coefficients)) was used to determine the number of coefficients for an optimum fit. The computer programme for this fitting operation is given in Appendix 1.

This method is suggested since your data distribution (1968) is very irregular, it being broader, and the system was found to be unreliable, by several groups, (Lambert et al. 1968, Lamberton et al. 1968, Lamberton et al. 1969, Lamberton et al. 1970, Lamberton et al. 1971, Lamberton et al. 1972, Lamberton et al. 1973, Lamberton et al. 1974, Lamberton et al. 1975, Lamberton et al. 1976, Lamberton et al. 1977, Lamberton et al. 1978, Lamberton et al. 1979, Lamberton et al. 1980, Lamberton et al. 1981, Lamberton et al. 1982, Lamberton et al. 1983, Lamberton et al. 1984, Lamberton et al. 1985, Lamberton et al. 1986, Lamberton et al. 1987, Lamberton et al. 1988, Lamberton et al. 1989, Lamberton et al. 1990, Lamberton et al. 1991, Lamberton et al. 1992, Lamberton et al. 1993, Lamberton et al. 1994, Lamberton et al. 1995, Lamberton et al. 1996, Lamberton et al. 1997, Lamberton et al. 1998, Lamberton et al. 1999, Lamberton et al. 2000, Lamberton et al. 2001, Lamberton et al. 2002, Lamberton et al. 2003, Lamberton et al. 2004, Lamberton et al. 2005, Lamberton et al. 2006, Lamberton et al. 2007, Lamberton et al. 2008, Lamberton et al. 2009, Lamberton et al. 2010, Lamberton et al. 2011, Lamberton et al. 2012, Lamberton et al. 2013, Lamberton et al. 2014, Lamberton et al. 2015, Lamberton et al. 2016, Lamberton et al. 2017, Lamberton et al. 2018, Lamberton et al. 2019, Lamberton et al. 2020, Lamberton et al. 2021, Lamberton et al. 2022, Lamberton et al. 2023, Lamberton et al. 2024, Lamberton et al. 2025).

THE SYSTEMS STUDIED

The Test System n-Hexane + Cyclohexane At 298.15 K

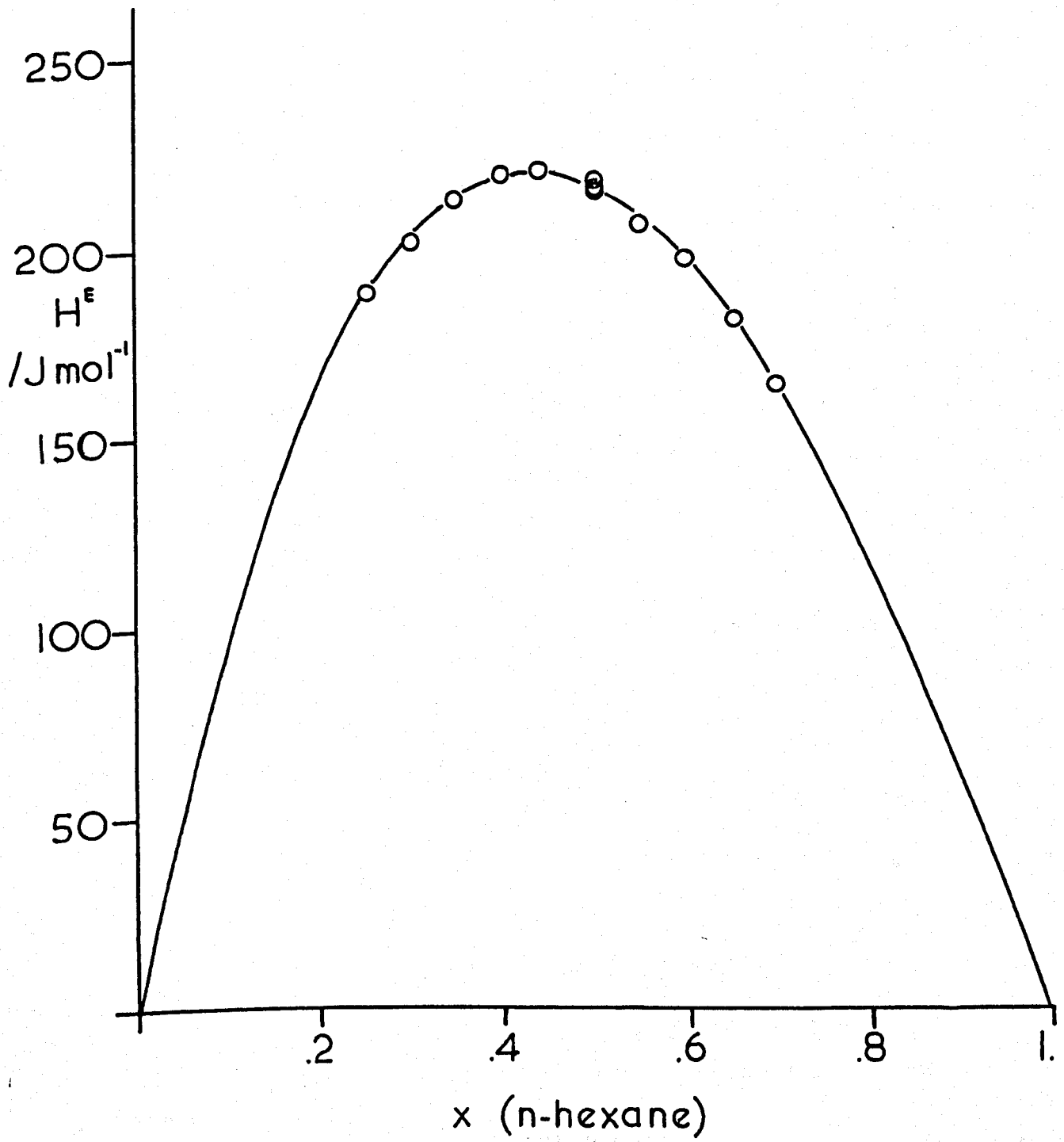
This system was suggested some years ago (McGlashan 1965) as a convenient enthalpy of mixing standard, and the system has since been studied carefully, by several groups, (Watts et al. 1968, Stoeckli and McGlashan 1968, Sturtevant and Lyons 1969, Ewing, Marsh, Stokes and Tuxford 1970, Harsted and Thomsen 1974, among others) with close agreement between the various measurements, thus suggesting that this would be a good system with which to test a new calorimetric system. The only real objection to this mixture as an enthalpy of mixing standard for calorimeters is the fact that the densities at 298.15 K are so similar (n-hexane 0.6549 g cm^{-3} , cyclohexane 0.7743 g cm^{-3}) that very little is demanded of the calorimeter in efficiency of mixing, in which respect the older but apparently less reliable standard, benzene + carbon tetrachloride is preferable. The test results obtained with the new system are recorded in Table 1.1. The optimum fit was obtained with an equation of three parameters:

$$H^E / \text{J mol}^{-1} = x(1-x)[863.78 - 241.30(1-2x) + 49.539(1-2x)^2]$$

where x is the mole fraction of cyclohexane and H^E is the molar excess enthalpy. Table 1.1 shows the mole fractions, measured excess enthalpies and deviations from the fitted values ($H^E_{\text{fit}} - H^E_{\text{exp}}$) a graph showing the measured values and the fitted curve is given in diagram 19. The fitted curve agrees well with the results obtained by Marsh et al., showing a deviation of 0.1 J mol^{-1} at $x=0.5$, 0.3 J mol^{-1} at $x=0.7$ and a maximum

DIAGRAM 19

cyclohexane + n-hexane at 298.15 K



deviation of -3.7 J mol^{-1} at $x=0.3$. Agreement with the results of Stoeckli and McGlashan is similar, with slightly larger deviation at higher x values. Given the standard deviation of this set, 1.1 J mol^{-1} , it seems that the agreement between these sets is close enough to suggest that the calorimeter could be used in the measurement of previously untested systems.

The System Cyclohexane + Tetramethyl Silane At 298.15 K

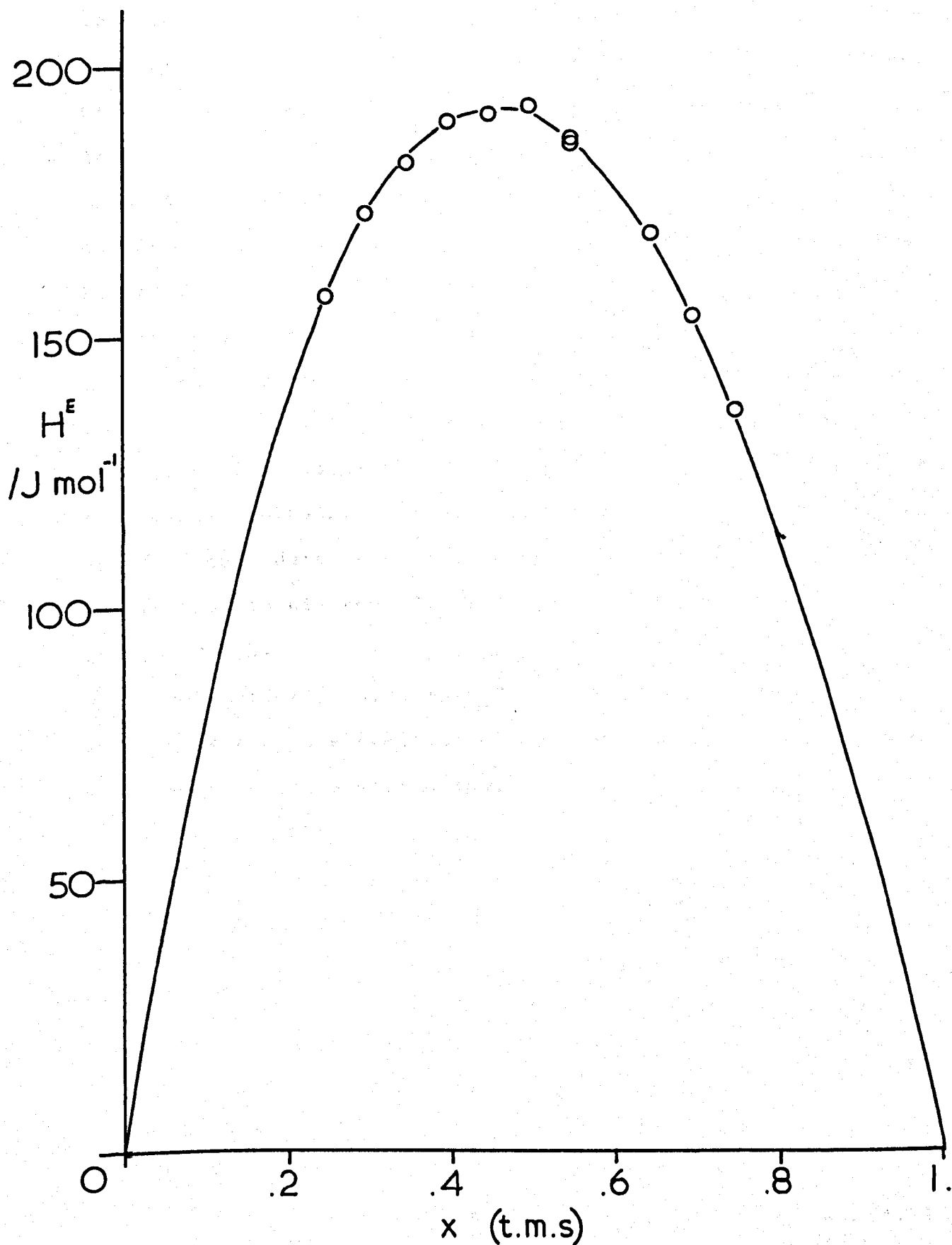
This system was chosen, as was the next, because of the near-sphericity of its molecules. The tetramethyl silane had to be handled with care, as the boiling point was around 299 K, but no purification was carried out on the sample, specified as better than 99.9 moles per cent pure, as no sign of impurity could be found on g.l.c. analysis. The liquid was stored over molecular sieve. The cyclohexane was Analar grade material, purified as previously described, with the exception that the liquid was refluxed violently over mercury for 5 hours, prior to distillation, to remove traces of sulphur. Table 1.2 shows the results obtained, and the graph (diagram 20) shows the measured values, and the fitted curve. The equation of this curve is:

$$H^E / \text{J mol}^{-1} = x(1-x)[764.50 + 110.54(1-2x) + 77.02(1-2x)^2]$$

where x is the mole fraction of tetramethyl silane and H^E the molar excess enthalpy. The standard deviation of the results was 0.84 J mol^{-1} .

DIAGRAM 20

cyclohexane + tetramethyl silane at 298.15K



The System Neopentane + Cyclohexane At 298.15 K

The same sample of cyclohexane was used as in the tetramethylsilane mixtures, but the neopentane posed rather more problems. A sample was obtained from British Drug Houses Ltd., which was stated to be 99 moles per cent pure. This then had to be fractionated, a process which, to avoid setting up temperature control apparatus for the entire system, was carried out in the cold room (274 K), using an electrically heated jacket for the column, with an infinitely variable controller. This process was necessitated by the low (circa 283 K) boiling point of this component. The sample was eventually purified to the same standard as the other materials, i.e. about 99.95 moles per cent. The results of the excess enthalpy measurements are shown in Table 1.3 and a graph of the data and the fitted curve, again of three parameters, in diagram 21. The standard deviation of the data is 0.69 J mol^{-1} .

$$H^E / \text{J mol}^{-1} = x(1-x)[390.84 + 45.33(1-2x) - 38.10(1-2x)^2]$$

where x is the mole fraction of cyclohexane in the mixture and H^E is the molar excess enthalpy.

DIAGRAM 21

neopentane + cyclohexane at 298.15 K
and 200kPa

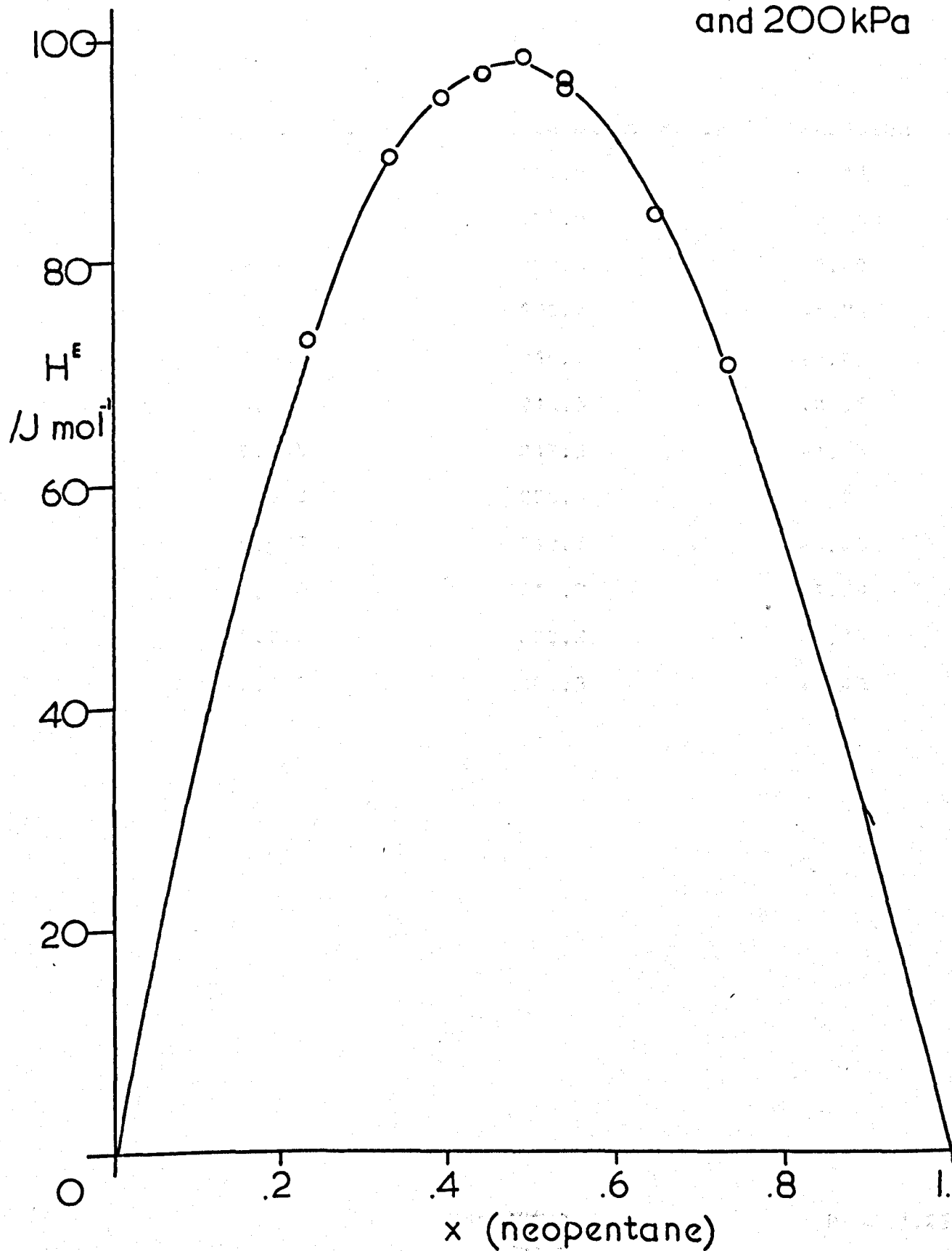


TABLE 1.1

The System Cyclohexane + n-Hexane At 298.15 K

<u>x(cyclohexane)</u>	<u>H^E / J mol⁻¹(observed)</u>	<u>deviation</u>
0.300	162.9	+0.11
0.350	180.5	-0.56
0.400	197.0	+0.80
0.450	206.2	-1.74
0.500	216.0	+0.05
0.500	216.5	+0.55
0.500	217.3	+1.35
0.560	220.4	+0.25
0.600	219.6	+0.23
0.650	212.7	-1.29
0.700	202.2	-1.13
0.750	188.3	+1.40
0.75	188.3	+1.40

TABLE 1.2

The System Cyclohexane + Tetramethyl Silane At 298.15 K

<u>x(t.m.s.)</u>	<u>H^E/J mol⁻¹(exp)</u>	<u>deviation</u>
0.25	157.4	-0.1
0.30	173.0	-0.5
0.35	182.1	+0.9
0.40	190.1	-0.5
0.45	191.1	+1.1
0.50	192.9	-1.8
0.55	186.4	+0.3
0.55	186.0	+0.6
0.55	186.3	+0.3
0.65	168.7	-0.8
0.70	153.7	+0.2
0.75	136.6	+0.0
0.75	136.4	+0.2

TABLE 1.3

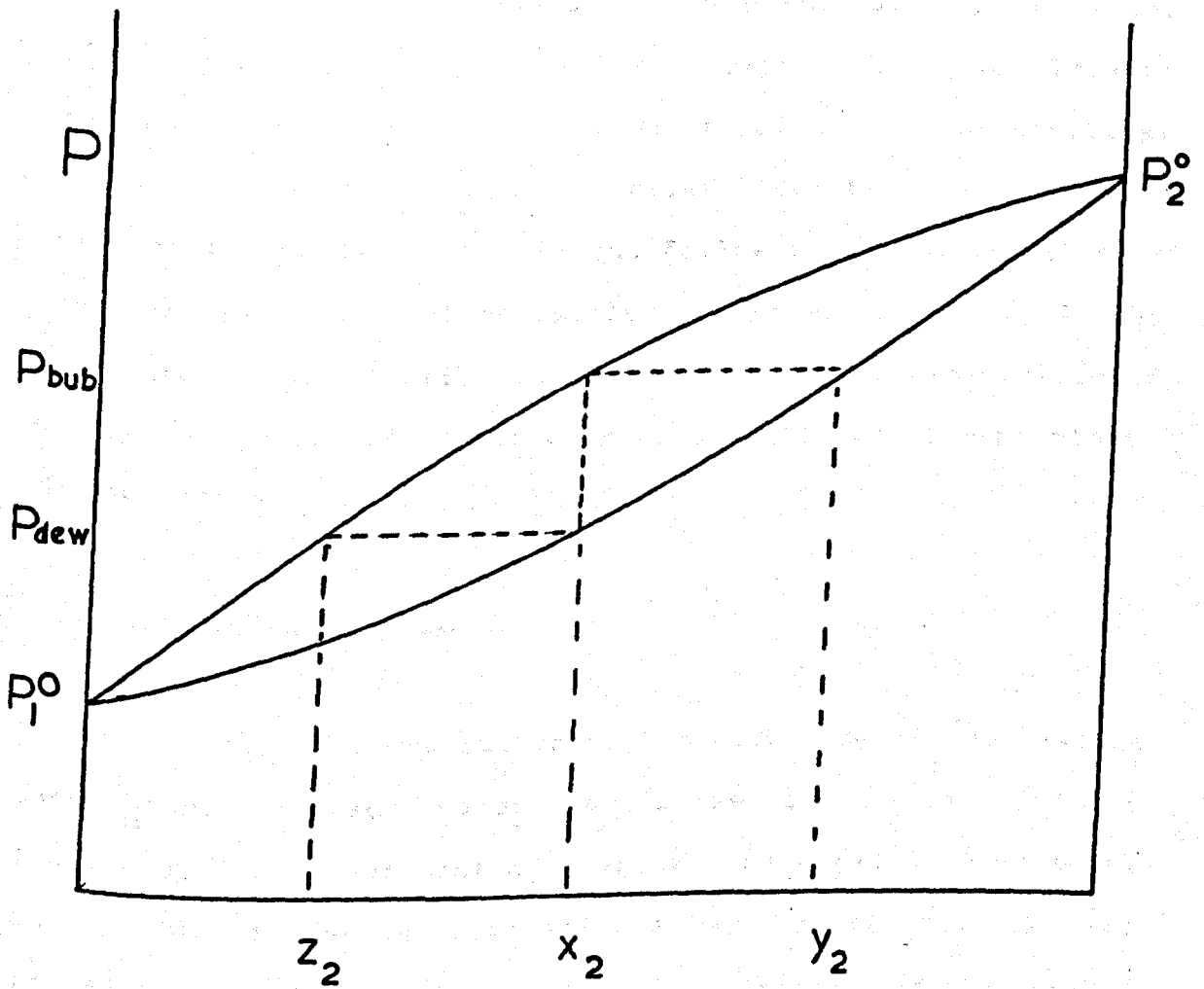
The System Neopentane + Cyclohexane At 298.15 K

<u>x(neopentane)</u>	<u>H^E/J mol⁻¹(exp)</u>	<u>deviation</u>
0.237	73.08	+0.00
0.334	89.49	-0.14
0.393	94.92	+0.21
0.443	97.03	+0.56
0.494	98.57	-0.74
0.544	96.67	-0.78
0.542	95.67	+0.34
0.650	84.06	+0.98
0.736	70.60	-0.46

CHAPTER TWO

DIAGRAM 2.1

Pressure / Composition Phase Diagram
For A Two Component Liquid Mixture



MEASUREMENT OF THE EXCESS GIBBS FUNCTION

The Dew-Point, Bubble-Point Method

This method was first discussed theoretically by Dixon and McGlashan (1965), and was examined in detail in the Ph.D. thesis of the former. The method was not, however, successfully put into practice, owing to experimental problems, and also, in lesser degree, to computational problems. There follows a brief description of the theoretical basis of the method, followed by a description of the computational problems involved in the solution of the equations. This section then concludes with a description of the experimental method for obtaining bubble and dew points to the desired accuracy.

The Basis Of The Method

The usual approaches to the obtaining of the excess Gibbs function from vapour pressures of volatile mixtures involve either measurement of vapour pressure, temperature, and liquid and vapour compositions in a recirculating still; or measurement of static vapour pressure and liquid composition followed by solution via the "Barker" method (Barker 1953); or, less frequently, measurement of total pressure and liquid and vapour compositions in a gas-transpiration method.

Owing to the difficulties of bringing recirculatory stills to equilibrium and of obtaining a reproducible steady-state situation in the transpiration method, the second method has been the most frequently used, for accurate work, in recent years.

The relationships involved are as in diagram 2.2. The only further requirement is the assumption of a suitable functional relationship between G^E and x_2 . This may take the form, for instance, of a Redlich-Kister equation:

$$G^E = x_2(1-x_2)(A_1 + A_2(1-2x_2) + A_3(1-2x_2)^2 + \dots) \quad (4)$$

or, perhaps, the Myers-Scott equation:

$$G^E = x_2(1-x_2)(1-k(1-2x_2))(A_1(1-2x_2) + A_2(1-2x_2)^2 + \dots) \quad (5)$$

The more commonly used form is the Redlich-Kister equation, which will be used throughout this work.

now

$$\left(\frac{\partial G^E}{\partial x_2}\right) = (1-x_2)\left(\frac{\partial \mu_1^E}{\partial x_2}\right) - \mu_1^E + x_2\left(\frac{\partial \mu_2^E}{\partial x_2}\right) + \mu_2^E \quad (6)$$

and from the Gibbs-Duhem equation

$$(1-x_2)\left(\frac{\partial \mu_1^E}{\partial x_2}\right) + x_2\left(\frac{\partial \mu_2^E}{\partial x_2}\right) = 0 \quad (7)$$

so

$$\left(\frac{\partial G^E}{\partial x_2}\right) = -\mu_1^E + \mu_2^E \quad (8)$$

combining 1 and 8 we obtain:

$$\mu_1^E = G^E - x_2\left(\frac{\partial G^E}{\partial x_2}\right) \quad (9)$$

$$\mu_2^E = G^E + (1-x_2)\left(\frac{\partial G^E}{\partial x_2}\right) \quad (10)$$

DIAGRAM 2.2

$$G^E = x_1 \mu_1^E + x_2 \mu_2^E \quad (1)$$

$$\mu_1^E = RT \ln(P_m y_1 / P_1^\circ x_1) + (V_1^\circ - B_{11}) (P_1^\circ - P_m) + P_m \delta_{12} y_2^2 \quad (2)$$

$$\mu_2^E = RT \ln(P_m y_2 / P_2^\circ x_2) + (V_2^\circ - B_{22}) (P_2^\circ - P_m) + P_m \delta_{12} y_1^2 \quad (3)$$

μ_i^E are the excess chemical potentials

P_i° are the vapour pressures of the pure components

V_i° are the liquid molar volumes of the pure components

B_{ii} are the second virial coefficients in the equations of state of the pure components

x_i, y_i are the liquid and vapour phase mole fractions of component i

δ_{12} is $2 B_{12} - B_{11} - B_{22}$

If we now consider equations 2,3,4,9 and 10, it is clear that a relationship, albeit a complex one, exists between the terms on the right-hand sides of equations 2 and 3, and the A_i coefficients of the Redlich-Kister equation 4. This relationship leads to two equations in A_i , P_m , x_1 , x_2 , y_1 , y_2 , B_{11} , B_{12} , B_{22} , Δ_{12} , P_1° , P_2° , V_1° , V_2° , for each pressure/composition value, with only P_m and the composition terms changing between measurements on any particular system (diagram 2.3). This method of solution, whereby a set of $2n$ equations in $n+m$ parameters, where m is the number of A_i terms, and P_m and x_2 are measured, may be reduced to n equations in m unknowns by approximate elimination of the y terms between each pair of equations, followed by solution of the Jacobian of the set of equations in P and the A_i terms which remain (diagram 2.4). This yields improved values of the initially estimated A_i terms, which may then be used to calculate an improved value of y , the solution is then repeated, with the differential elements of the Jacobian being calculated from the improved values of the A_i terms, and the cycle may be repeated until the values obtained converge to a solution. This method is, in effect, the "Barker" method.

In the case of the recirculatory still, or the transpiration train, where both x and y as well as P and T are measured, there is no need for such solution, since the excess potentials may be calculated directly from equations 2 and 3, and G^f from these values and the liquid compositions. The case is, in fact, overdetermined by these methods, and the Gibbs-Duhem equation may be used in checking the internal

(e)

The combination of the equation (e) with

(c) and (d) leads to a relationship between the P_i terms, P_m , V_i^0 , B_{ii} , x_2 and y_2 and P_i

DIAGRAM 2.3

$$G^E - x_2 \left(\frac{\partial G^E}{\partial x_2} \right) = RT \ln \left(\frac{P_m (1 - y_2)}{P_1^0 (1 - x_2)} \right) + (V_1^0 - B_{11}) (P^0 - P_m) + P_m \delta_{12} y_2^2 \quad \text{(a)}$$

$$G^E + (1 - x_2) \left(\frac{\partial G^E}{\partial x_2} \right) = RT \ln \left(\frac{P_m y_2}{P_2^0 x_2} \right) + (V_2^0 - B_{22}) (P_2^0 - P_m) + P_m \delta_{12} (1 - y_2)^2 \quad \text{(b)}$$

$$P_m = P_1^0 \left(\frac{1 - x_2}{1 - y_2} \right) \exp \left\{ [G^E - x_2 \left(\frac{\partial G^E}{\partial x_2} \right) - (V_1^0 - B_{11}) (P^0 - P_m) - P_m \delta_{12} y_2^2] / RT \right\} \quad \text{(c)}$$

$$P_m = P_2^0 \frac{x_2}{y_2} \exp \left\{ [G^E + (1 - x_2) \left(\frac{\partial G^E}{\partial x_2} \right) - (V_2^0 - B_{22}) (P_2^0 - P_m) - P_m \delta_{12} (1 - y_2)^2] / RT \right\} \quad \text{(d)}$$

$$G^E / RT = x_2 (1 - x_2) (A_{11} + A_{22} (1 - 2x_2) + A_{33} (1 - 2x_2)^2 \dots \dots \dots)$$

DIAGRAM 2.4

$$\delta P_1 = \left(\frac{\partial P_1}{\partial A_1} \right) \delta A_1 + \left(\frac{\partial P_1}{\partial A_2} \right) \delta A_2 + \left(\frac{\partial P_1}{\partial A_3} \right) \delta A_3 \dots$$

$$\delta P_2 = \left(\frac{\partial P_2}{\partial A_1} \right) \delta A_1 + \left(\frac{\partial P_2}{\partial A_2} \right) \delta A_2 + \left(\frac{\partial P_2}{\partial A_3} \right) \delta A_3 \dots$$

$$\delta P_3 = \left(\frac{\partial P_3}{\partial A_1} \right) \delta A_1 + \left(\frac{\partial P_3}{\partial A_2} \right) \delta A_2 + \left(\frac{\partial P_3}{\partial A_3} \right) \delta A_3 \dots$$

$$\delta P_4 = \left(\frac{\partial P_4}{\partial A_1} \right) \delta A_1 + \left(\frac{\partial P_4}{\partial A_2} \right) \delta A_2 + \left(\frac{\partial P_4}{\partial A_3} \right) \delta A_3 \dots$$

the N equations in M coefficients showing the Jacobian matrix in the "Barker" solution

consistency of the results (Rowlinson 1969 p.125).

The bubble point, dew-point method is a special case of the previously described P, x method, which resulted in the set of $2n$ equations in $n+m$ unknowns. If, instead of measuring P and x or y , we measure the bubble-point and dew-point of the same mixture, then we have, effectively, a double set of equations, where the liquid phase composition at the bubble-point may be equated with the vapour phase composition at the dew-point (diagram 2.5). This results in a reduction of the number of coefficients involved in the equations, leading to the situation shown in diagram 2.6. It may be seen that we obtain $4n$ equations in $3n+m$ unknowns, i.e. we have obtained a relationship between G^E and x , without exact control of x . It is also possible, in the case of all such non-linear methods, to solve the equations for other variables e.g. virial coefficients, which are sufficiently determinate. This is achieved by a process exactly like that already used for the composition and Redlich-Kister coefficients, the appropriate differential coefficients being obtained, and inserted into the Jacobian, and the solution being carried out as usual. The solution is now of $4n$ equations in $3n+m+v$ coefficients.

DIAGRAM 2.5

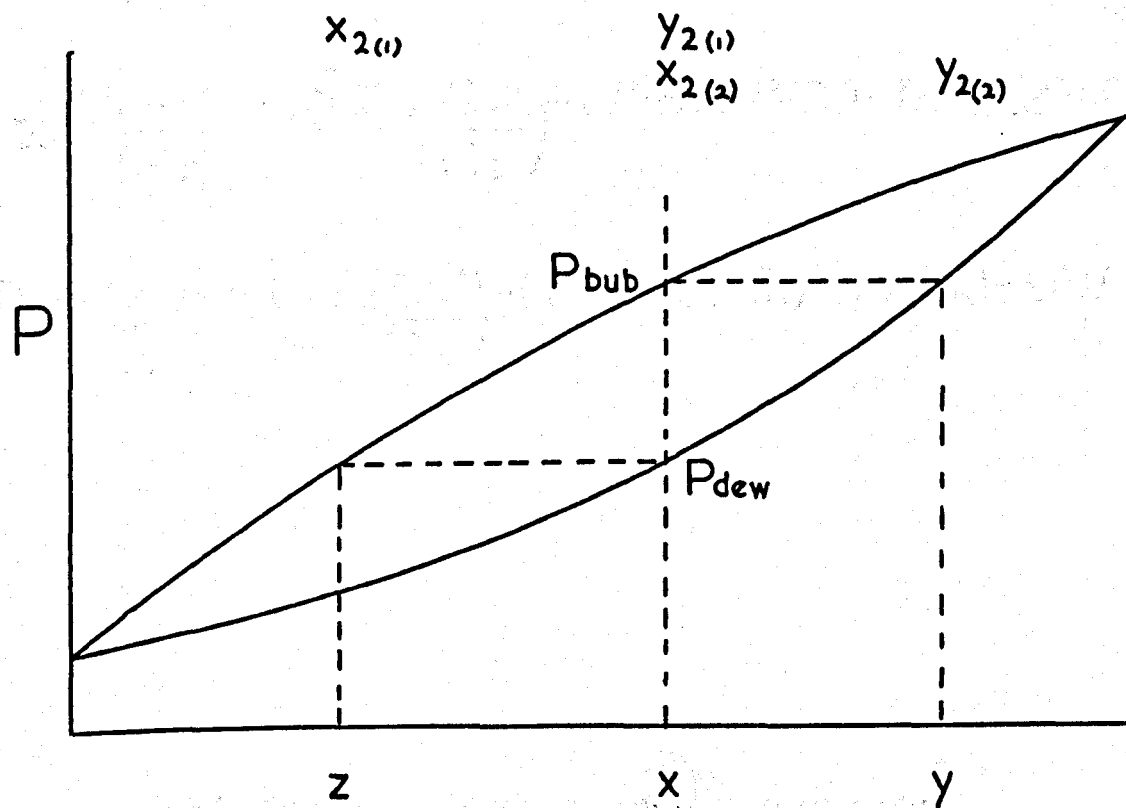
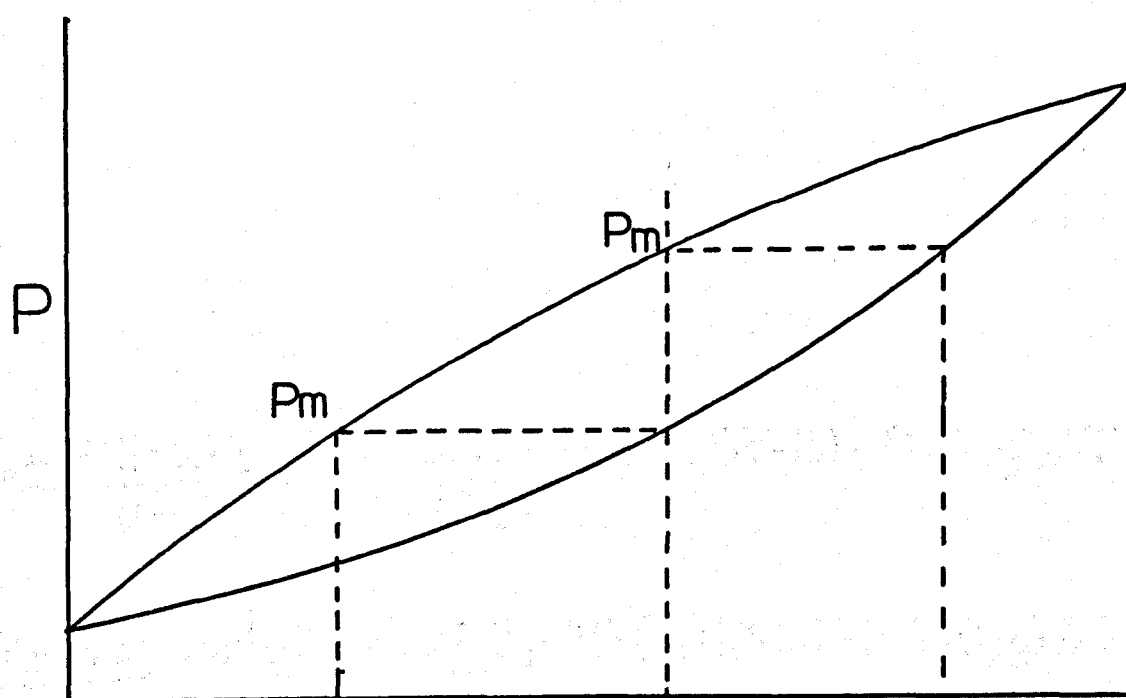


DIAGRAM 2.6

$$P_m = P_1^0 \frac{(1-x)}{(1-y)} \exp \left[\left(G^E - x \left(\frac{\partial G^E}{\partial x} \right) - (V_1^0 - B_{11}) (P_1^0 - P_m) - P_m \delta_{12} y^2 \right) / RT \right]$$

$$P_m = P_2^0 \frac{x}{y} \exp \left[\left(G^E + (1-x) \left(\frac{\partial G^E}{\partial x} \right) - (V_2^0 - B_{22}) (P_2^0 - P_m) - P_m \delta_{12} (1-y)^2 \right) / RT \right]$$

$$P_m = P_1^0 \frac{(1-z)}{(1-x)} \exp \left[\left(G^E - z \left(\frac{\partial G^E}{\partial z} \right) - (V_1^0 - B_{11}) (P_1^0 - P_m) - P_m \delta_{12} x^2 \right) / RT \right]$$

$$P_m = P_2^0 \frac{z}{x} \exp \left[\left(G^E - z \left(\frac{\partial G^E}{\partial z} \right) - (V_2^0 - B_{22}) (P_2^0 - P_m) - P_m \delta_{12} (1-x)^2 \right) / RT \right]$$

the bubble-point, dew-point equations

THE SOLUTION OF THE EQUATIONS

The first major problem now arises, in that the equations are of exponential form after rearrangement; this means that the set can not be solved by direct linear methods, and that a non-linear method must be employed. The equation set in diagram 2.6 is that for one bubble-point, dew-point measurement. The method employed is that of successive improvement of initial estimates of the parameters by solution of the Jacobian set of equations, derived from the set of exponential equations, and shown in diagram 2.7. Values of the delta P terms are calculated using initial estimates of the coefficients, as are the differential terms. The solution is then obtained, by normal linear-least-squares methods, and the delta (coefficient) terms used to increment the initial estimates of the coefficients; a further cycle is then commenced. The process is halted when the change in the coefficients from one cycle to the next reaches some suitable fraction of the absolute value of the coefficients. The Jacobian for a set of bubble-point, dew-point measurements is large, and most of the elements are zeros (diagram 2.8), but solution with modern, powerful computers, of even (as for 10 pairs of points), a matrix of 40 equations in up to 40 coefficients presents no real problem. For instance, for 5 cycles of such a set of equations, using the programme written by the Author, the C.D.C. 7600 computer, after compilation, required only about 2 seconds of central processor time. The time required on older computers, such as the Keele Elliott 4130 was much greater, up to 16 or 17 minutes, but even this

DIAGRAM 2.7

$$\delta P_{1b} = \left(\frac{\partial P_{1b}}{\partial x}\right)_1 \delta x + \left(\frac{\partial P_{1b}}{\partial y}\right)_1 \delta y + 0 + \left(\frac{\partial P_{1b}}{\partial A_1}\right)_1 \delta A_1 + \left(\frac{\partial P_{1b}}{\partial A_2}\right)_1 \delta A_2 \dots$$

$$\delta P_{2b} = \left(\frac{\partial P_{2b}}{\partial x}\right)_2 \delta x + \left(\frac{\partial P_{2b}}{\partial y}\right)_2 \delta y + 0 + \left(\frac{\partial P_{2b}}{\partial A_1}\right)_2 \delta A_1 + \left(\frac{\partial P_{2b}}{\partial A_2}\right)_2 \delta A_2 \dots$$

$$\delta P_{3d} = \left(\frac{\partial P_{3d}}{\partial x}\right)_3 \delta x + 0 + \left(\frac{\partial P_{3d}}{\partial z}\right)_3 \delta z + \left(\frac{\partial P_{3d}}{\partial A_1}\right)_3 \delta A_1 + \left(\frac{\partial P_{3d}}{\partial A_2}\right)_3 \delta A_2 \dots$$

$$\delta P_{4d} = \left(\frac{\partial P_{4d}}{\partial x}\right)_4 \delta x + 0 + \left(\frac{\partial P_{4d}}{\partial z}\right)_4 \delta z + \left(\frac{\partial P_{4d}}{\partial A_1}\right)_4 \delta A_1 + \left(\frac{\partial P_{4d}}{\partial A_2}\right)_4 \delta A_2 \dots$$

the 4 equations in $3+M$ coefficients with the Jacobian set of a single bubble-point, dew-point pair

is not really excessive. The computational problems spoken of in the introduction to this section arose where an attempt was made to reduce the amount of computer time and workspace required for a solution. Most of the time required for the method used here is taken up in the linear-least squares solution of large sets of equations, and if some means could be found to reduce the size of these sets, some quite useful reductions in time and workspace used might be obtained. D.T.Dixon in his thesis, (1966), attempted such a saving by initial algebraic elimination of the terms in concentration, followed by solution for the terms in the Redlich-Kister parameters, concluding by back-substitution to obtain the concentration terms. This method reduces the amount of time required considerably, but the method seemed numerically rather unstable, and sometimes failed to converge, even when the estimated values of the parameters seemed quite good.

The only circumstances in which difficulties were encountered with the current programme were those involving the calculation of virial coefficients, when the appropriate differentials and coefficients were inserted into the equation set, and the solution carried out for these terms also. It was found that this solution only proceeded satisfactorily when the absolute value of the vapour pressures of the pure components was large, 3 kPa or greater, and the method therefore highly sensitive to the values of the virial coefficients.

At pressures below 1 kPa it was found that changes in the virial coefficients had only very small effects on the values of the Redlich-Kister parameters, and this caused the solution to become unstable. This is, however, no major problem, since the occurrence of such non-determinacy simply implies that the value of the solution is not seriously dependent on the actual values of the virial coefficients used, and estimates may therefore safely be used.

The liquids were first weighed in a balance and then distilled in the same way as was used in the preliminary reaction. The first portion of the liquid, for the first time, was distilled from a very small amount of liquid, and the second portion was distilled from a larger amount. The boiling point of the liquid was found to be 100.4°C, and the boiling point of the liquid was found to be 100.4°C. The liquids were then separated in the reservoir in the vacuum system for a pressure of 100.4 kPa. The liquids were then carried out by means of a vacuum system, after which the liquids were finally distilled from a very small amount.

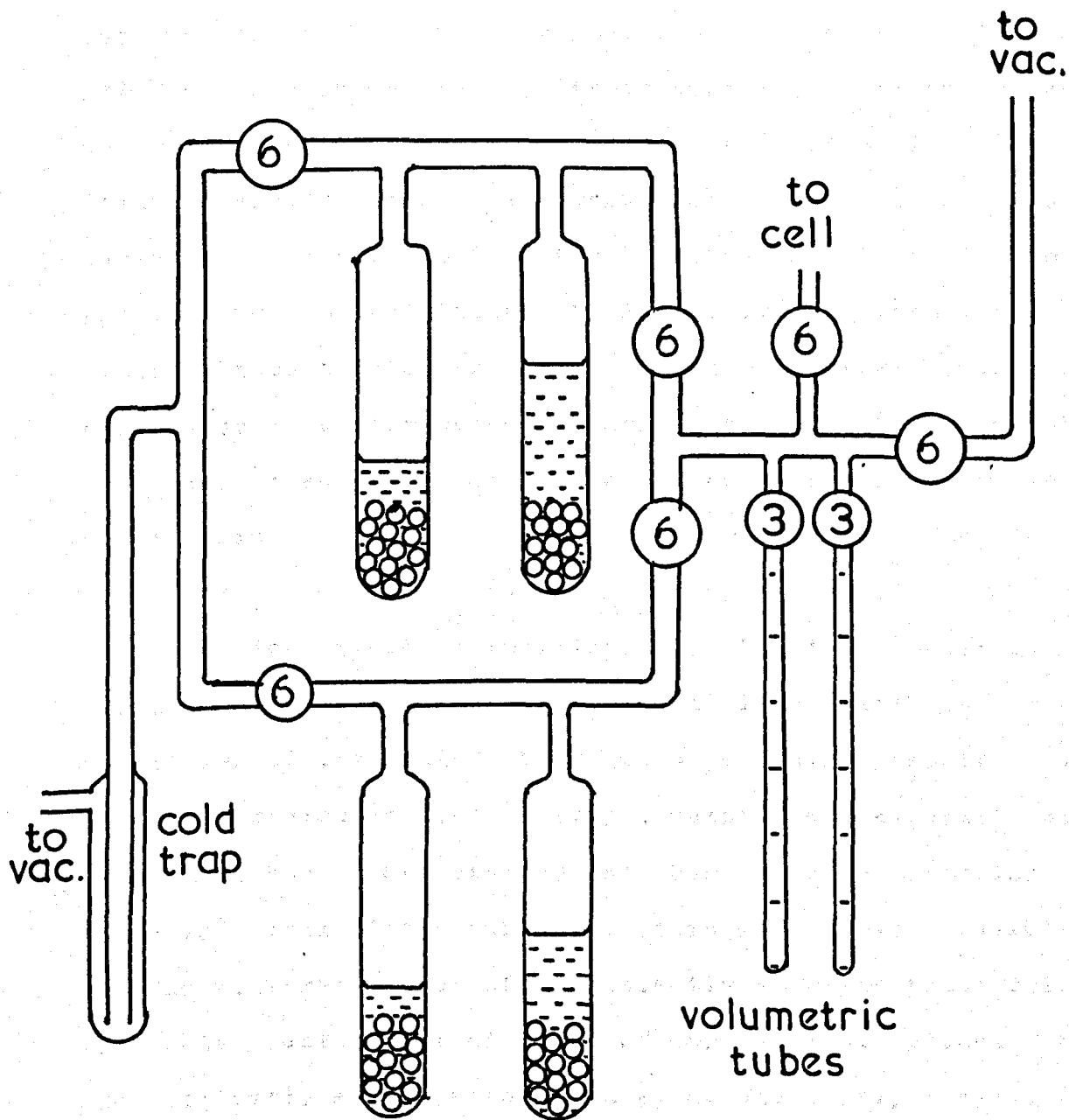
THE EXPERIMENTAL MEASUREMENT OF BUBBLE- AND DEW-POINTS

The experimental work involved attempts to measure the bubble and dew pressures of liquid mixtures of approximately known composition to the maximum accuracy attainable with the pressure measuring systems. All the pressure measurements in this work were made with thermostatted mercury manometers, using a Precision Tool And Instrument Company 100 cm cathetometer, capable of being read to 0.01 mm, representing a limiting pressure accuracy of circa 1.5 Pa. There were three successive versions of this apparatus, which will be referred to as the Marks 1, 2 and 3 respectively, and although the manometer systems differed, all Marks shared a common sample preparation and metering system, which will be described first.

The liquids were first obtained in Analar grade, and further purified, in the same manner as those used in the calorimetry section. The final portion of the liquid, for this work, was distilled once more, under very stringent conditions: the thermostat of the Fenske column was set to only 0.03 K below the pressure corrected boiling point of the liquid, and the liquid again distilled, only the fraction boiling within 0.01 K of the boiling point being collected, at a reflux ratio of greater than 100:1. The liquids were then transferred to the reservoirs in the vacuum system for degassing (diagram 2.9). The initial degassing was carried out by repeated freeze-pump-thaw cycles, after which the liquids were finally totally degassed by vacuum sublimation

DIAGRAM 2.9

the reservoirs and metering tubes



③ 3mm "Rotaflo" tap

⑥ 6mm "Rotaflo" tap

between the two tubes of the reservoirs three or four times. The reservoirs were isolated from the system by a liquid nitrogen trap, in order to avoid cold-trapping any impurities from the system into the liquids during the sublimation. The liquids were finally further purified by repeatedly pumping off the vapour above the liquid surface, in order to remove any more-volatile impurity, and, after distillation of the liquids slowly across a temperature gradient of some two degrees, the pumping off of the final few cm of the liquid, to reduce the concentration of less-volatile impurity. The liquids thus treated were only accepted for further work when the change in vapour-pressure between bubble- and dew-points was less than 0.1% of the absolute vapour pressure at the bubble-point. The small quantities of liquid required for measurement were metered by distilling slightly greater quantities of the liquids than were actually required into tubes graduated in 0.01 cm steps, pumping any excess to waste with the tubes thermostatted at 298 K, then closing the "Rotaflo" taps of the tubes. In this way, it was possible to make up mixture samples of sufficiently accurate total volume, with mole fractions within 0.02 of any nominal value, which was perfectly adequate for this work, where only a reasonably accurate estimate of composition is required.

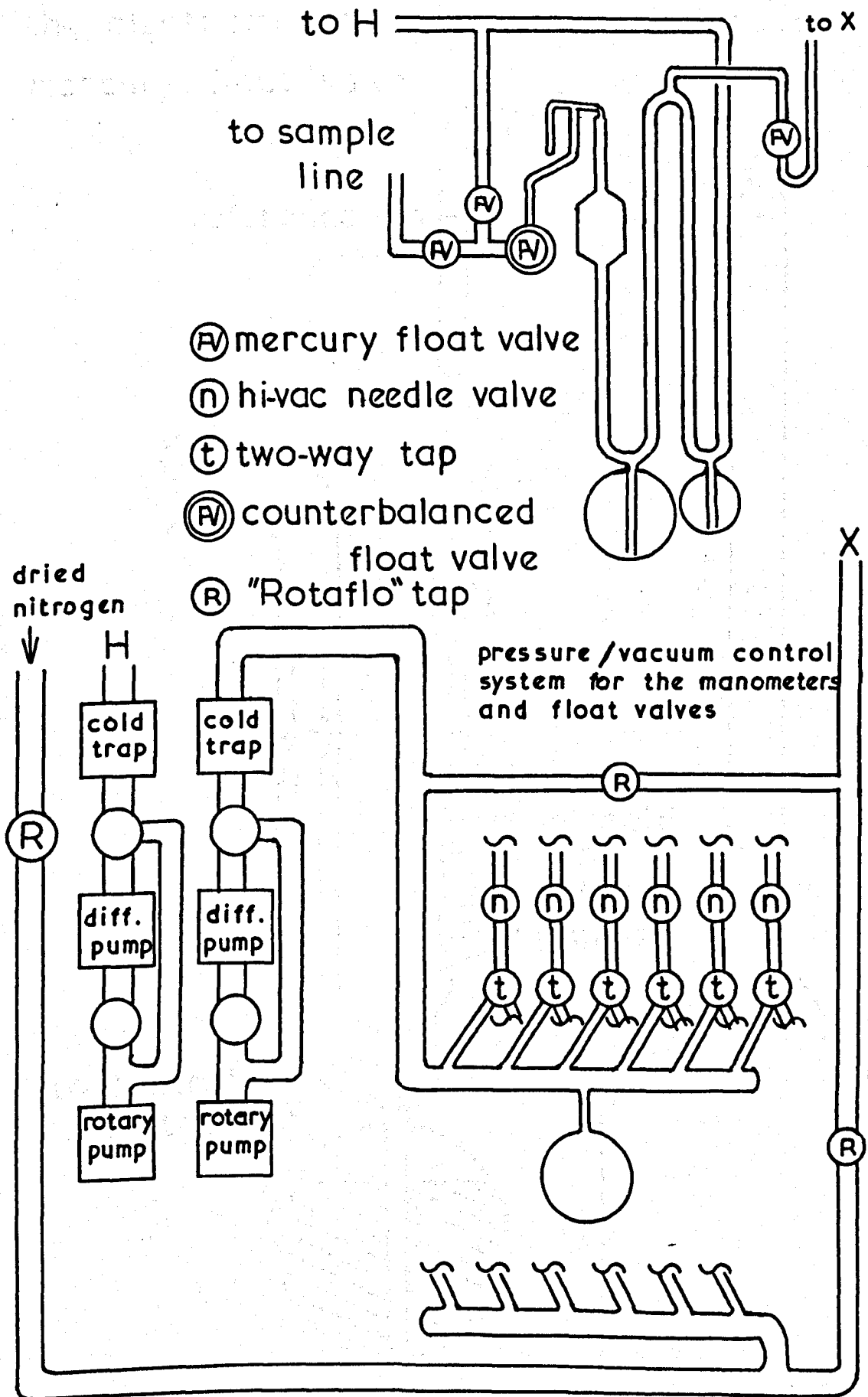
The Mark 1 Apparatus

This apparatus consisted of two, 1 cm bore, mercury manometers, the first of which was fitted with a liquid cell and expansion bulb, as shown in diagram 2.10. The system as a whole was highly complex, with the cell being shut off by an electromagnetically counterbalanced mercury float valve (diagram 2.11) which allowed mercury to flow up almost to the cell before closure, thus ensuring minimal dead volume. There were three further float valves of standard type associated with the gas ballast manometer and the sample transfer system.

The net result of the complexity of the whole system was that it became almost impossible to operate it without assistance, and it was extremely difficult to avoid pressure gradients sufficient to jam one or more of the float valves. The valves themselves were a further source of trouble, in that they frequently failed to seat properly, leading to the flooding of parts of the system with mercury; additionally, the pressure/vacuum control system required to control the valves remotely became very complex, greatly increasing the possibility of failure somewhere in the system.

In view of the difficulty of operating this system, it was therefore decided that a simpler version would be produced, using "Rotaflo" Teflon taps in place of the mercury float valves, thus removing many of the difficulties of operating the system previously caused by pressure gradients.

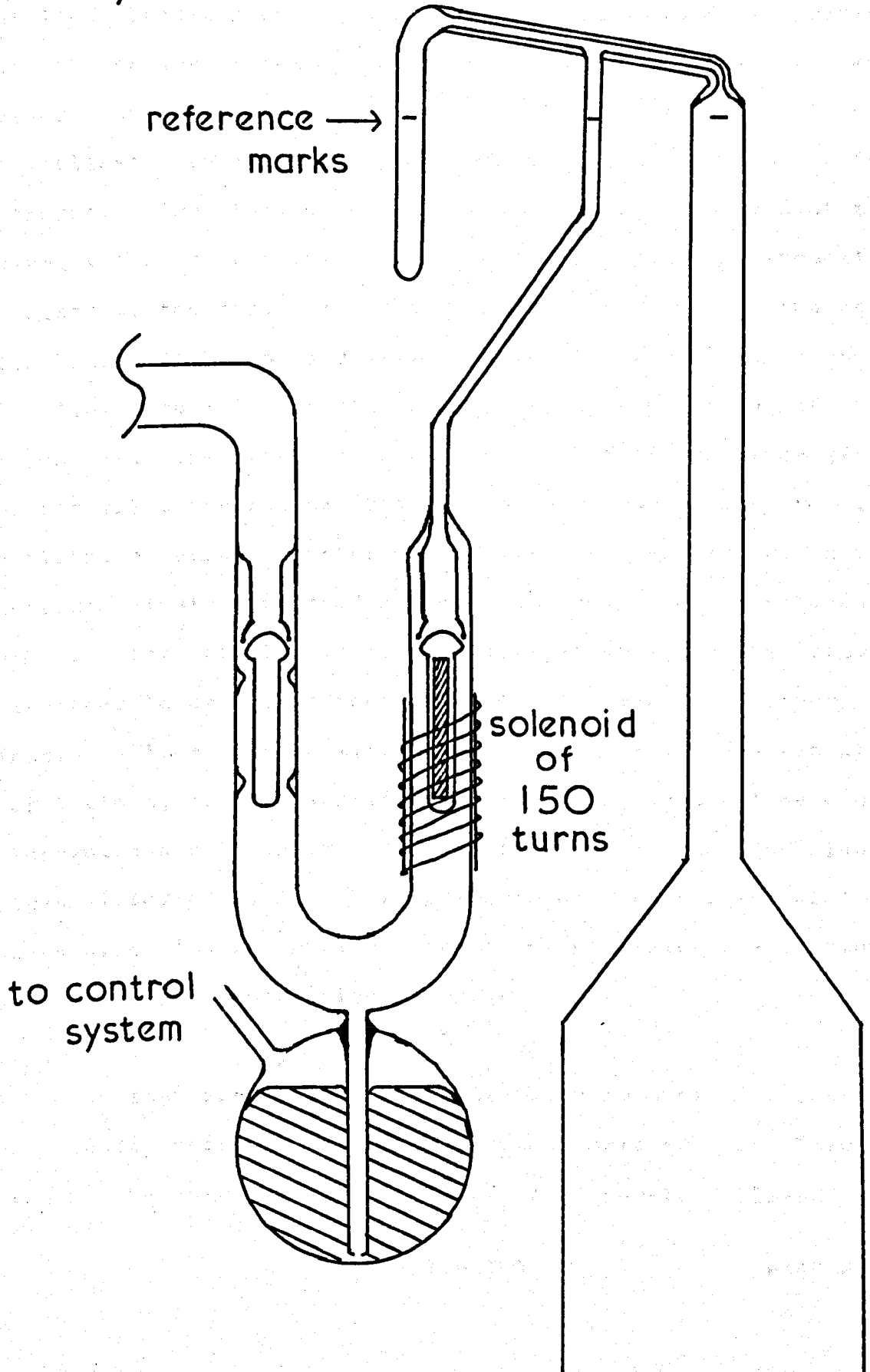
DIAGRAM 2.10



the Mark I apparatus

DIAGRAM 2.11

the electromechanically counterbalanced mercury float valve



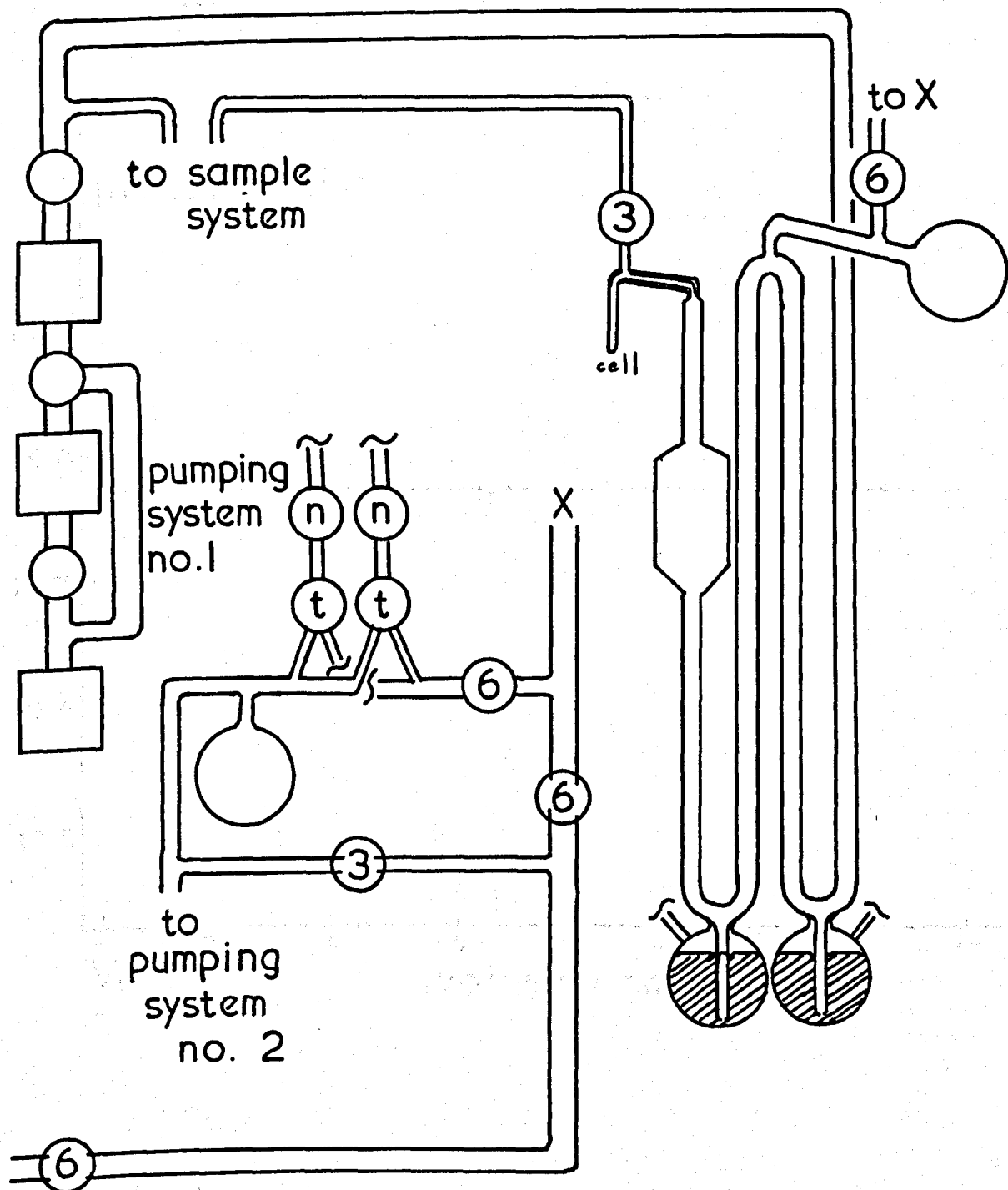
The Mark 2 Apparatus

The first of the meaningful results were obtained with this apparatus, which, in spite of faults which will be detailed later, proved reasonably straightforward to operate. With the entire system at optimum vacuum, the mercury was raised halfway up manometers 1 and 2, and a suitable gas-ballast pressure applied through tap 1 with dried nitrogen. The tap, which was below the water surface of the thermostat bath, was then closed, and the mercury in manometer 1 raised to the top. The sample was transferred into the cell with liquid nitrogen, and after the tap (number 2) was closed, was allowed to melt, and to warm to the temperature of the thermostat, the mercury level being maintained by increasing the control pressure, as the vapour pressure rose to its equilibrium value. After 15 minutes, the mercury column and meniscus heights were read and also the height of a reference mark on the first manometer tube, after which the mercury column was lowered 2 cm down manometer 1, and a further 15 minutes allowed for equilibration. This process was repeated 6 or 7 times, so that a graph of pressure against volume could be drawn, and extrapolated the small distance to the liquid volume (diagram 2.13). This pressure was the bubble point of the sample. The internal volume of the apparatus was obtained by the nitrogen compression method.

When sufficient points had been obtained to define the bubble pressure adequately, the mercury was lowered through the expansion bulb, and the sample allowed to

DIAGRAM 2.12

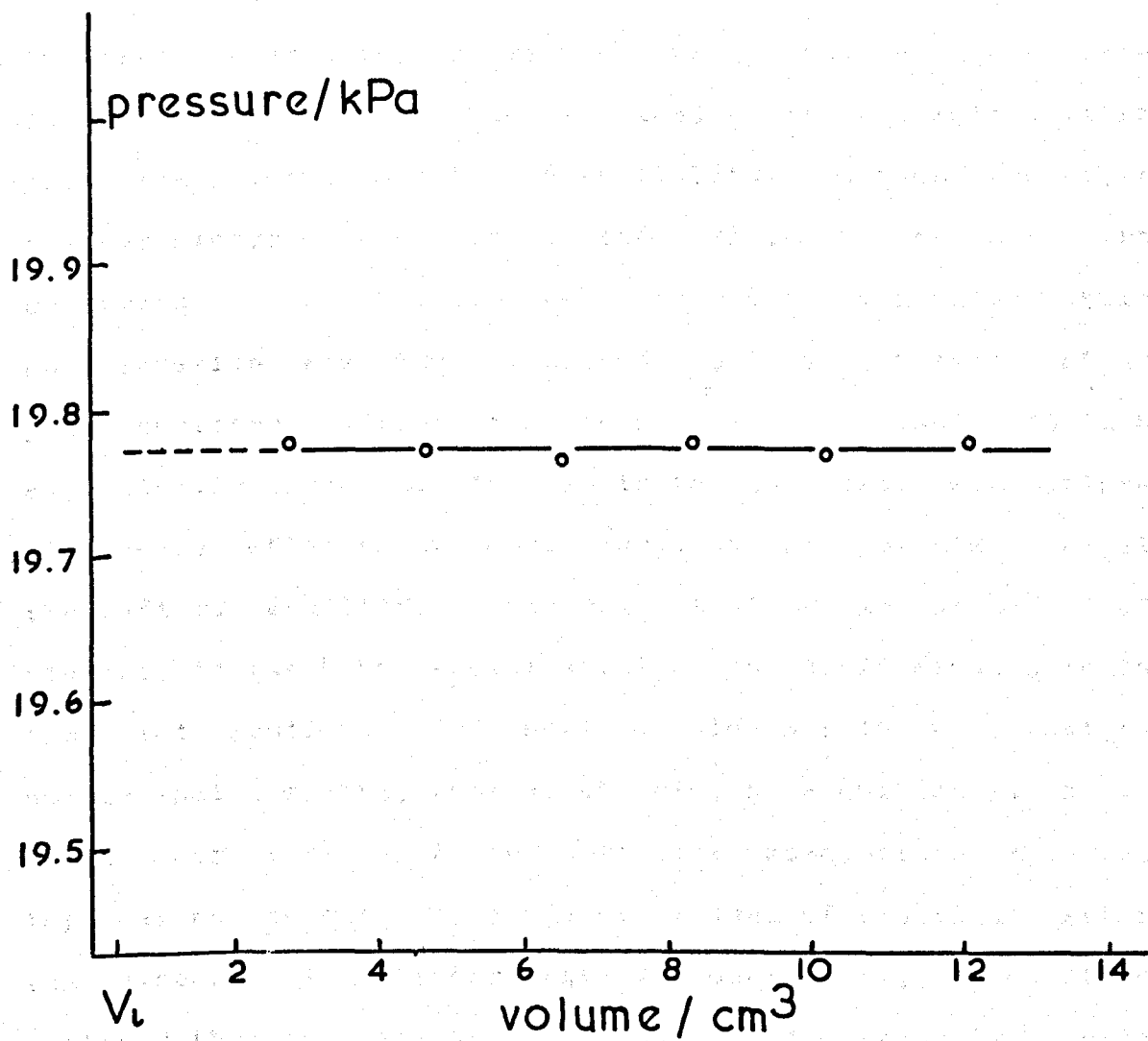
the Mark 2 apparatus



- ③ 3mm 'Rotaflo' tap
- ⑥ 6mm 'Rotaflo' tap
- ① Edwards needle valve
- ② two way tap

DIAGRAM 2.13

the Mark 2 apparatus: bubble-point

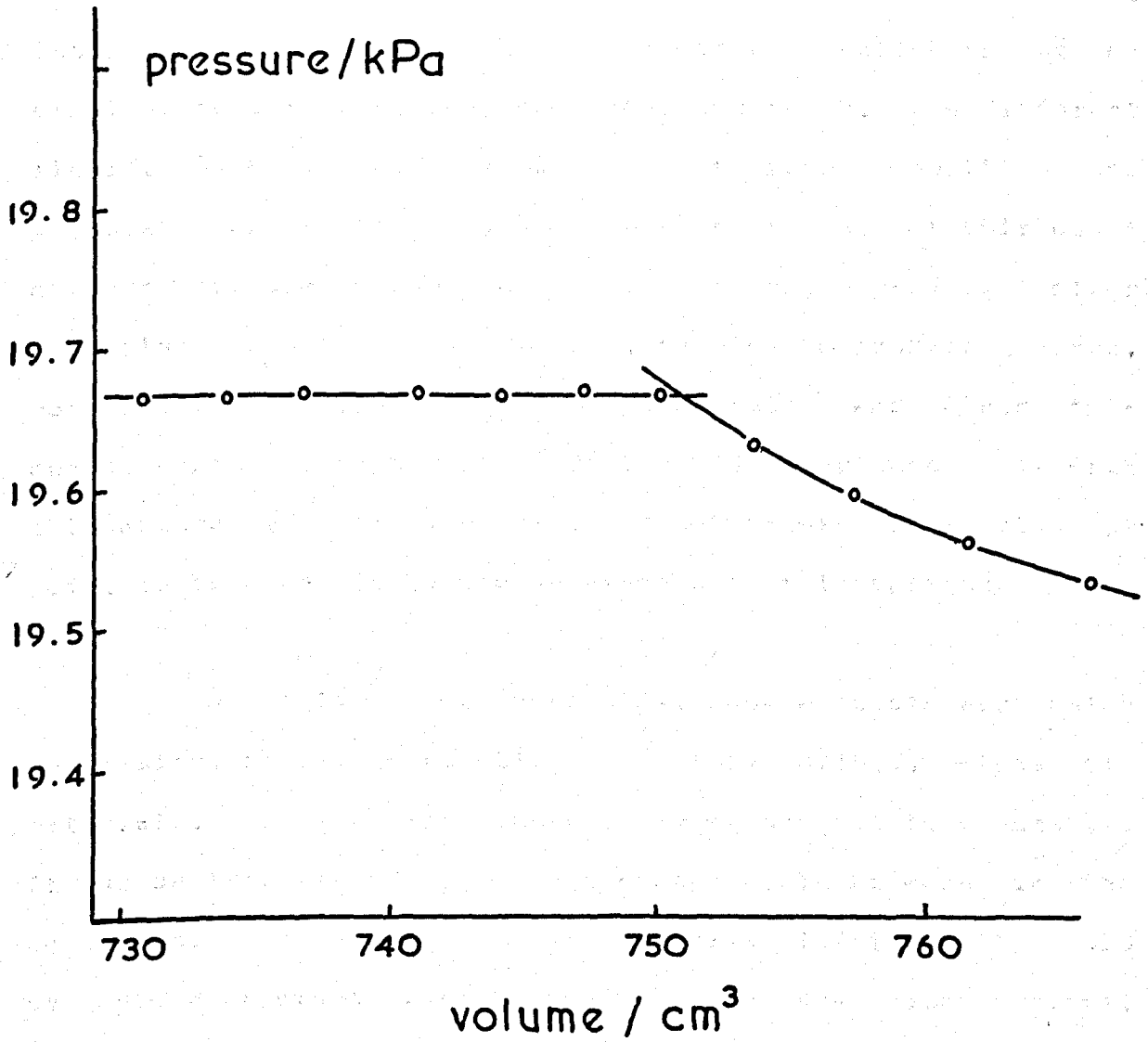


vapourise into the bulb. A further series of measurements was then carried out, in the same way as the first, in order to determine the dew pressure of the mixture, by successively lowering the mercury down the lower tube (diagram 2.14).

The main problems arising were as follows: firstly the trend to equilibrium seemed very slow, and was often incomplete even after 20 minutes, an effect, which, it was felt, was probably due to the small liquid surface exposed, to the narrowness of the tube to the cell, and to the large unstirred volume (750 cm^3) of the expansion bulb. Equilibration was much improved by the fitting of a glass-enclosed stirrer rod into the cell, which could be magnetically operated. The liquid in the cell was stirred vigorously after volume adjustment, and at 5 minute intervals thereafter. Equilibrium was now attained in around 10-15 minutes, in the bubble-point section, and 15-20 minutes in the dew-point section. The next problem was the fact that the bubble-point graphs, instead of being straight lines, showed marked curvature, appearing much like gas-compression curves. This was not acceptable, and a great deal of fruitless effort was expended in further degassing operations, before it was realised that this was not the cause of the trouble. After considerable experimentation, it was found that the problem did not arise with refrigerants which were not as cold as liquid nitrogen, and it was assumed that the nitrogen had caused any gas present in the system to be trapped in the cell, with the sample.

DIAGRAM 2.14

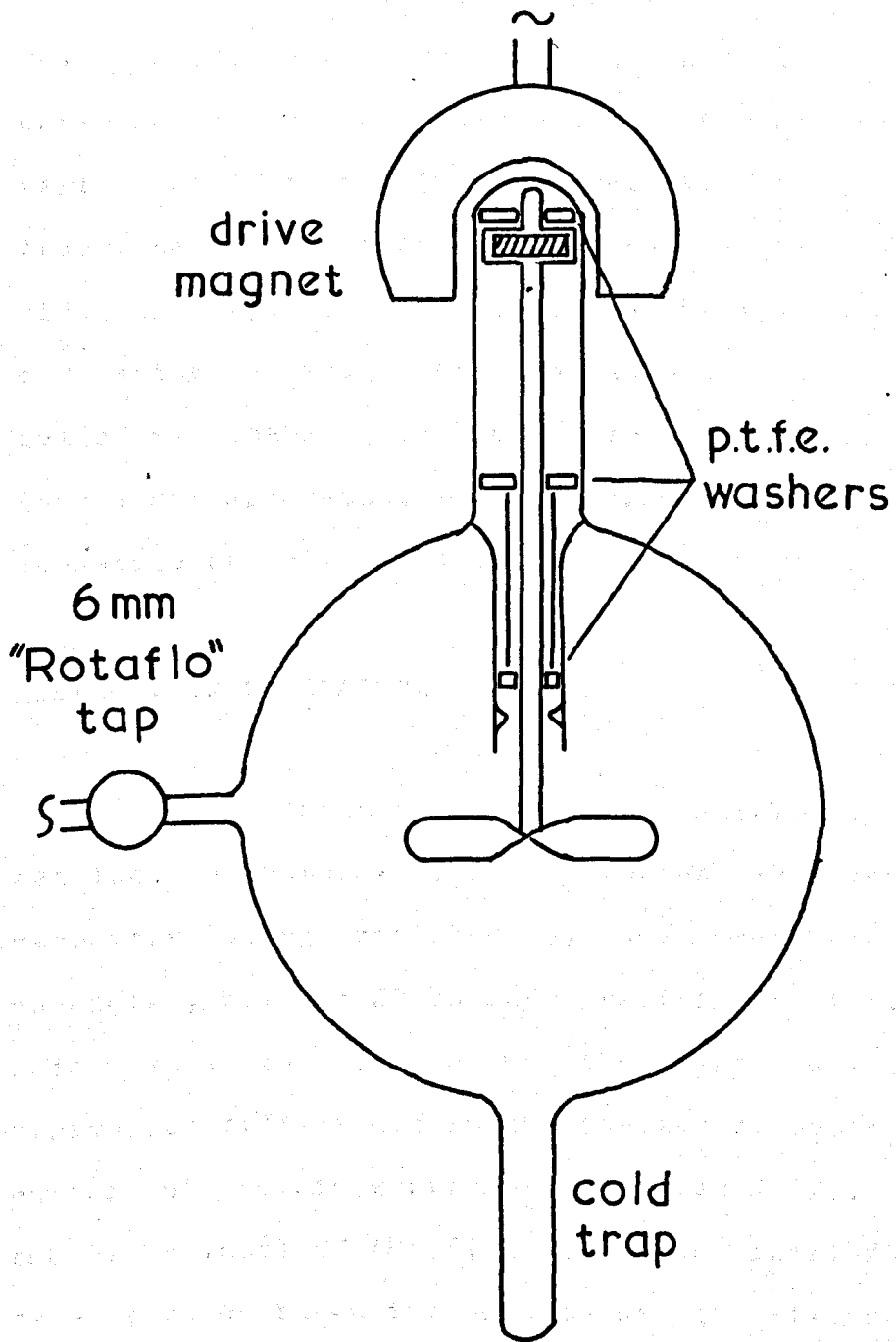
the Mark 2 apparatus: dew-point



The final problem was a good deal more severe, and was a result of the equilibrium behaviour of the liquids used. The first system tested was benzene/cyclohexane, and it was found extremely difficult to obtain a linear bubble point graph with cyclohexane present, although no such problems arose with the benzene alone. The cause of this behaviour was later resolved, but at the time it was decided to put the problem, temporarily, into abeyance, and to choose a different liquid. A sample of n-hexane was therefore purified and degassed for use in benzene/n-hexane mixtures. At this point another problem arose: n-hexane did not produce clear dew-point results like benzene, tending to produce a curve, rather than the required sharp discontinuity, and since this curve spread over the whole of the P/V range accessible with this apparatus in the dew-point region, it was obviously not going to be possible to use n-hexane with this apparatus.

By this time, obviously, severe doubts were being entertained about the viability of this method, since two materials, out of three tested, had proved not to be usable. It was decided therefore, that a change would be made in the apparatus, such that the volume change:sample size ratio could be made much greater, in both bubble- and dew- point regions. This was done by replacing the large expansion bulb by a larger external gas-mixing vessel (diagram 2.15), equipped with a large, magnetically driven propeller stirrer. The bubble-point measurement was carried out as before, after which the sample was transferred with solid/liquid acetone to a finger of the mixing bulb. The bulb was then closed off,

DIAGRAM 2.15



Gas Mixing Vessel

and the liquids allowed to vapourise, after which the resulting gas mixture was stirred for about one hour. The tap of the bulb was then opened, and a sample of the mixed gases trapped in the bubble-point section of the manometer system. This sample was condensed into the cell with the aid of cold water and the mercury raised to the top of the section, and a series of P/V readings taken. It was found that the large fractional volume change produced a very clear dew point discontinuity, (diagram 2.16), in the system benzene/n-hexane, and after a trial series of such experiments had produced a set of reasonably good bubble- and dew-points, it was decided that a new apparatus, the Mark 3, would be constructed to take advantage of this approach.

The Mark 3 Apparatus

The changes made were solely in the manometer section, the complex first manometer and the plain second manometer being replaced by one small and one large plain manometer, both in 20 mm bore precision tubing, this increase being made to dispose of the large effect of capillary depression differences in the smaller tubes, thus halving the number of readings required (diagram 2.17). The lowering of the upper level of the first tube was carried out to allow dew- and bubble-point pressures of mixtures with absolute pressures of less than 22 kPa to be carried out simply by three readings: first and second meniscus and reference line, this latter being scratched with a diamond at the top of the first tube.

DIAGRAM 2.16

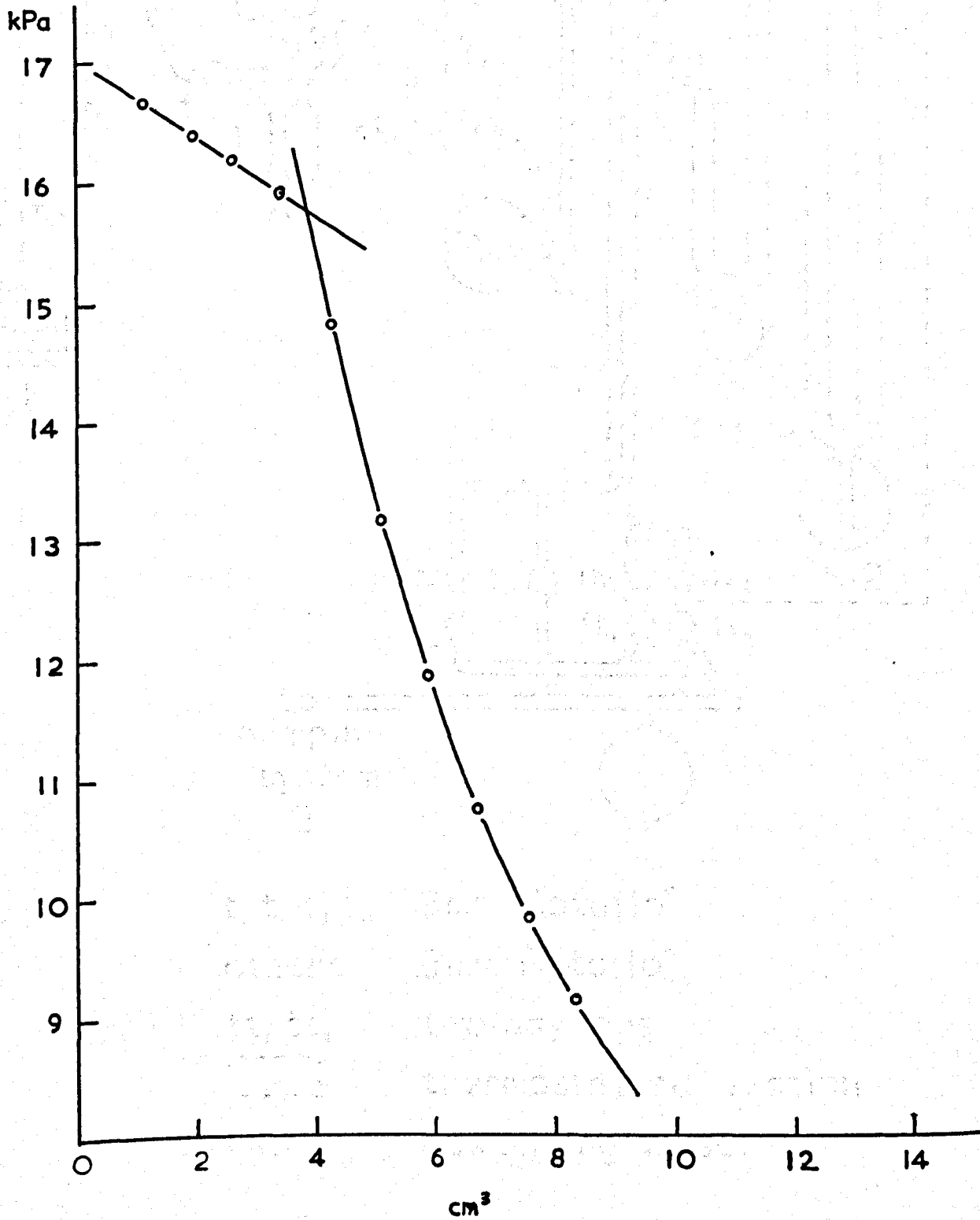
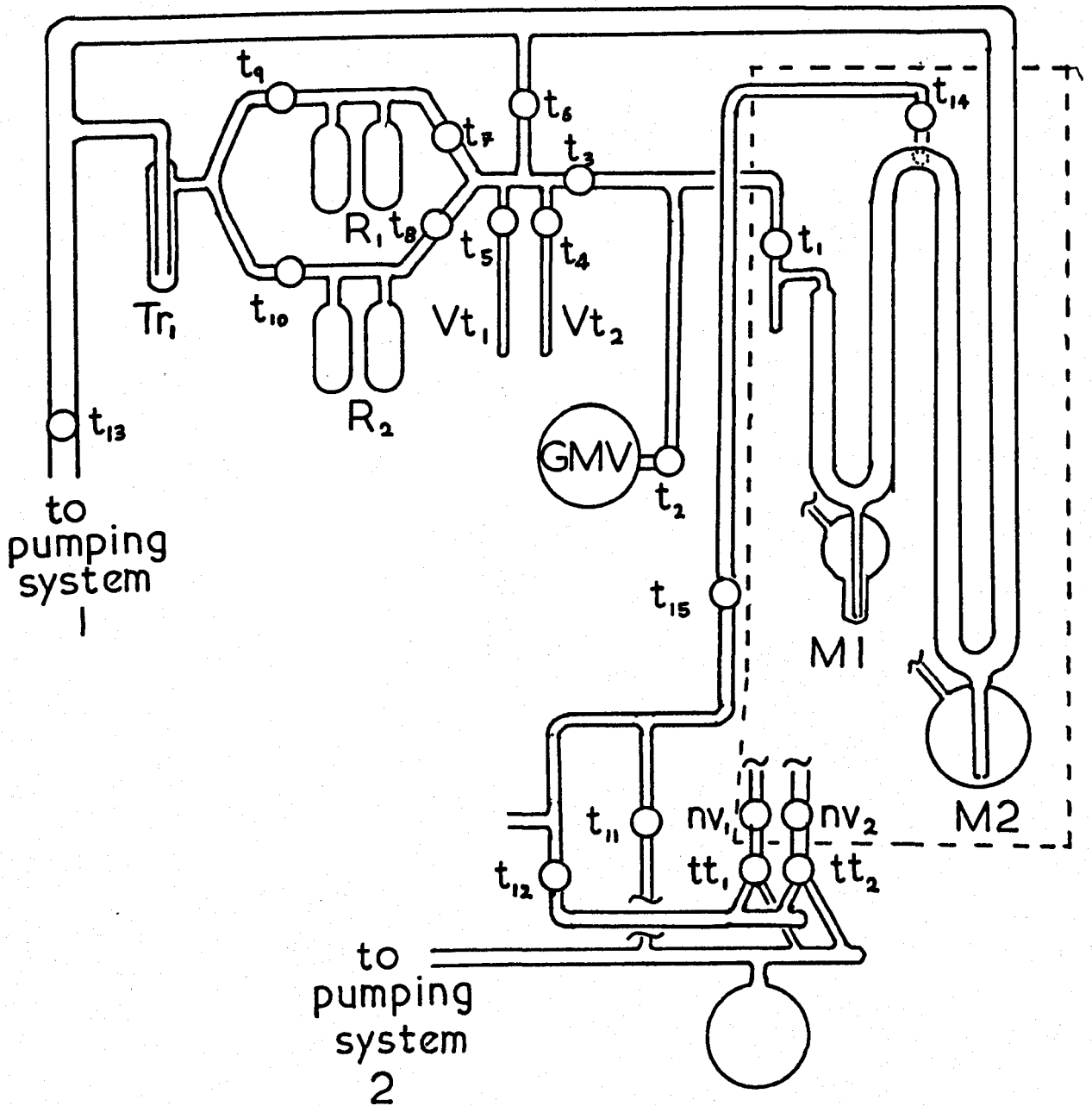


DIAGRAM 2.17

the Mark 3 apparatus



- | | |
|-------------------------|-----------------------|
| t_1, t_4, t_5, t_{11} | 3mm "Rotaflo" |
| others | 6mm "Rotaflo" |
| tt_1, tt_2 | two-way taps |
| [dashed box] | thermostatted section |
| GMV | gas mixing vessel |

This final model proved highly effective in practice, the standard deviation of the bubble-point lines and the linear portion of the dew-point lines being reduced to 2-3 Pa, or only slightly greater than the limiting accuracy of the cathetometer. The temperature control of the thermostat tank, as will be seen in the next section, was easily good enough to prevent apparent pressure errors due to temperature changes from being measurable. The thermostat tank, which was 100 mm in diameter, was filled with water and equipped with a circular heater in a vertical plane, to insure a uniformity of temperature throughout the tank.

Temperature Control

This was by means of a large temperature-sensitive resistor, utilizing a Wheatstone bridge, placed on a specially designed glass lamp, combined with an adjustable resistance power source, to provide a constant temperature. The heater and a resistance of 100 ohms, enclosed in a large glass bulb, was at the bottom. The regulator tank is shown in diagram 2.10 and the control circuit of the power stabilizer in diagram 2.11. The volume of the tank was approximately 200 cc, that of mercury approximately 70 cc, leaving a volume of the vapour surface in the cylinder of 130 cc/cm². The resistor lead was shielded, reducing the errors which could be caused by electrostatic pressure changes; and control to 0.1 ohm was possible. The tank was surrounded by a 2 inch thick layer of expanded polystyrene.

THE MECHANICAL AND ELECTRONIC CONTROL APPARATUS

The Thermostat Tank

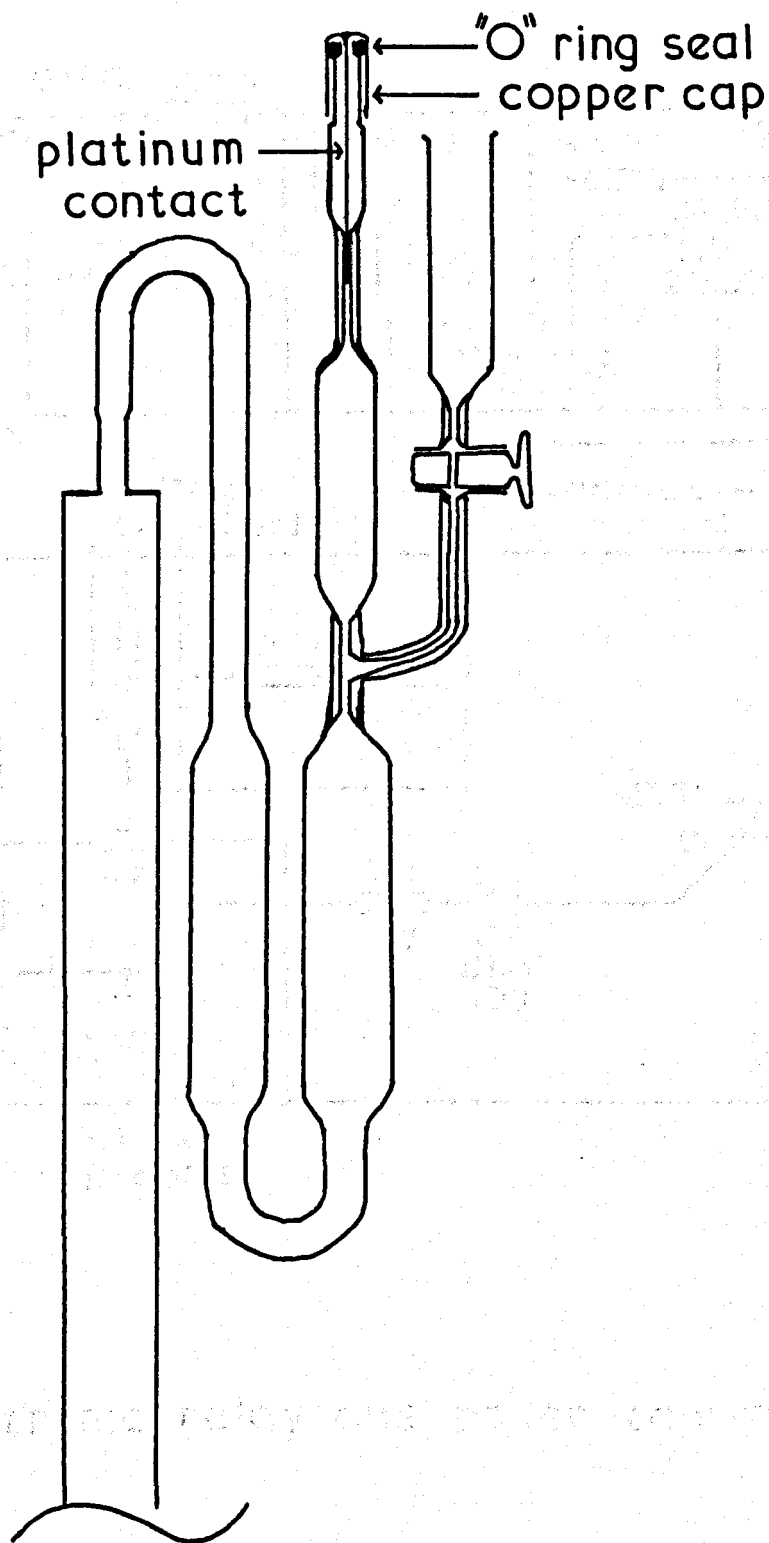
This was 1.2 metres tall, 0.6 metres square, with an angle-iron frame and bracing, iron plating, and a 9.5 mm plate-glass front window. The tank was stirred by four stirrer shafts at the corners, running the full depth of the tank, each with four, four bladed propellers, of 10 cm diameter, rotated at 300 rpm. The blades were set to cause a circulatory motion in a vertical plane, to improve homogeneity of temperature throughout the bath.

Temperature Control

This was by means of a large mercury-toluene regulator, switching a diac-triac device, giving an adjustable constant power input, combined with an adjustable switched power input, to a maximum of 3 kW. The heater was a kettle-type element, soldered to a large heat sink beside one of the stirrers. The regulator head is shown in diagram 2.18, and the circuit diagram of the power controller in diagram 2.19. The volume of toluene was approximately 250 cm³, that of mercury approximately 70 cm³, leading to a movement of the mercury surface in the capillary of 0.03 cm/mK. The regulator head was sealed, removing the errors which could be caused by atmospheric pressure changes, and control to 2 mK or better was easily achieved, once the tank had been carefully insulated with a 2 inch thick layer of expanded polystyrene.

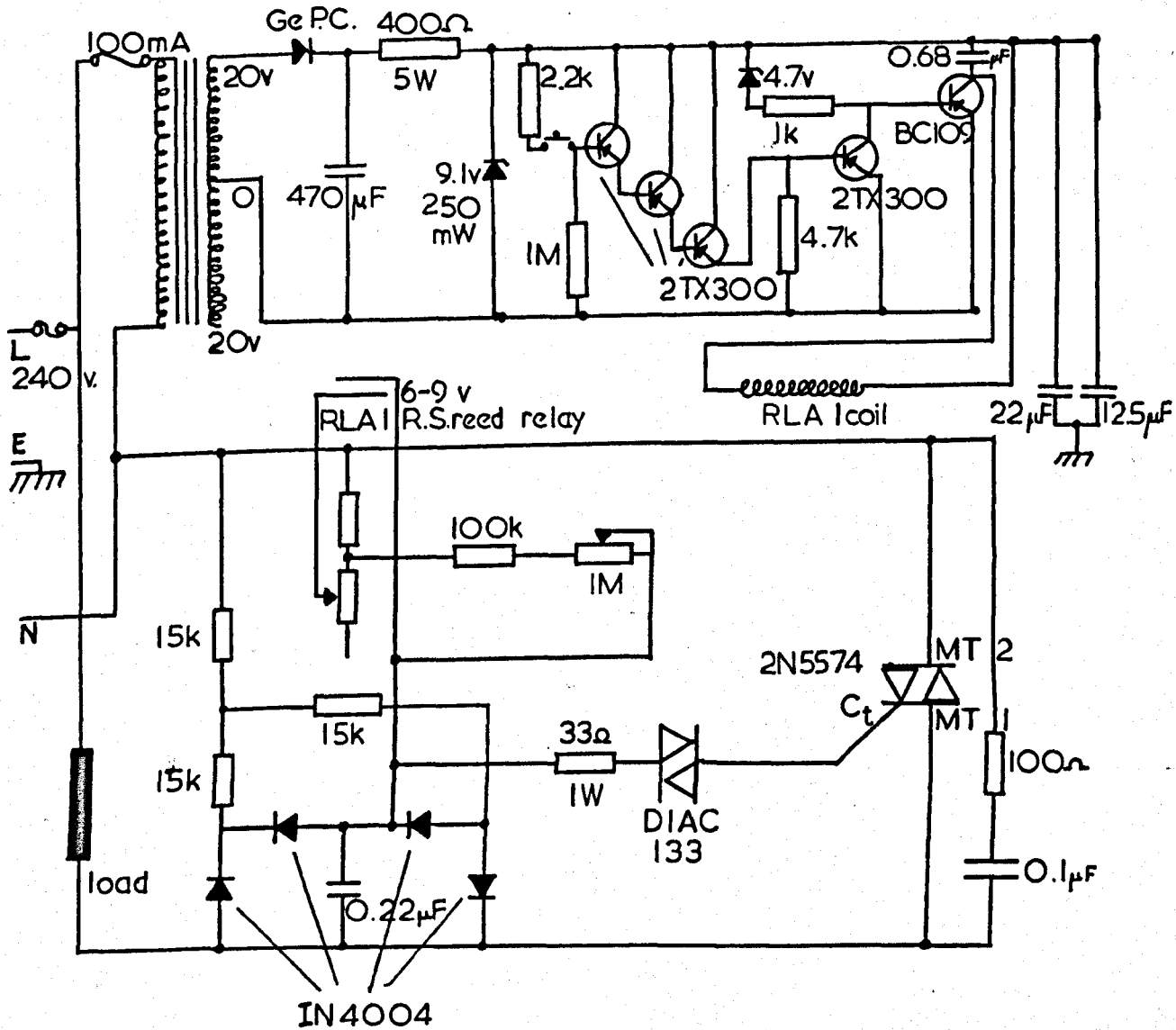
the regulator head

DIAGRAM 2.18



the regulator head

DIAGRAM 2.19



the electronic relay and power controller

For operation at or near room temperature, it was necessary to provide cooling for the thermostat, to remove the heat generated by the stirring. This was achieved by placing a cooling element in the tank, the flow of cold water in which could be adjusted to provide sufficient cooling such that the heating system would control the temperature adequately. There was also an external, pumped circuit, to allow filtration of the water, and the fitting of a flow-cooler if required.

Table 2, 4, 5, 6 give the results, and the correct related quantities of the various runs. The values of η_{sp}/c are given at the bottom of the table, and are calculated from the observed values of η_{sp}/c at the various concentrations, and the values of η_{sp}/c at the various concentrations, and the values of η_{sp}/c at the various concentrations.

THE EXPERIMENTAL PROCEDURE WITH THE MARK 3 APPARATUS

The Degassing And Purification Of Liquid Samples

The purified samples were loaded into reservoirs R1 and R2, the apparatus having first been maintained at a vacuum of better than 10^{-3} Pa for three days to remove as much adsorbed gas as possible. The reservoirs were "flamed out" under vacuum before the liquids were loaded, to regenerate the molecular sieve which they contained, and remove adsorbed water from the walls of the apparatus. Trap Tr1 was then immersed in liquid nitrogen and the samples subjected, alternately, to ten freeze-pump-thaw cycles, the reservoirs being evacuated through taps T9 and T10. The samples were then further degassed by vacuum sublimation between the two tubes of the reservoirs, and further purified as previously described.

Taps 2, 4, 5, 6 were then closed, and the mercury raised one-third of the way up the left-hand tube of Manometer M1, the ballast pressure having previously, if necessary, been adjusted via T14 to some suitable value. One of the taps T7 and T8 was then opened, and the vapour pressure allowed to come to its equilibrium value in the section M1-T1-T3-T7, the mercury level being carefully maintained by use of two-way tap TT1 and needle valve NV1. Tap T1 was then closed, the temperature of the thermostat corrected, if necessary, to some suitable exact value, and the vapour pressure in the closed section of the first manometer M1 measured, the volume of

which could also be calculated. A series of pressure/ volume readings was then taken, between the dew- and bubble-points of the sample by raising the mercury in the manometer through successive increments. If the change in vapour pressure between dew- and bubble-points was less than 0.1% of the bubble point pressure, then the sample was accepted for further work, and the process repeated for the second liquid. Should the sample not have been completely degassed by this stage, then the liquid in the reservoir was subjected to further vacuum sublimation until the desired standard was achieved. This failure completely to degass was the cause of the initial difficulty with cyclohexane. If, as was the case with the initial sample of n-hexane, the purity of the material was shown to be inadequate, then the sample was pumped out of the reservoir, and further purification work undertaken on a new liquid sample.

The Calculation Of Mixture Quantities

Once pure samples had been obtained, the quantities could be calculated for the mixtures. In the first mixture studied, n-hexane/ benzene, these quantities were calculated for the volume of the gas- mixing vessel and a pressure of 85% of the estimated dew-pressure of the sample. Calculation was done on the basis of the second virial equation

$$PV = n(RT + B_p)$$

where B_p the second virial coefficient of the mixture, was calculated from

$$B_x = x_1^2 B_{11} + 2x_1 x_2 B_{12} + x_2^2 B_{22}$$

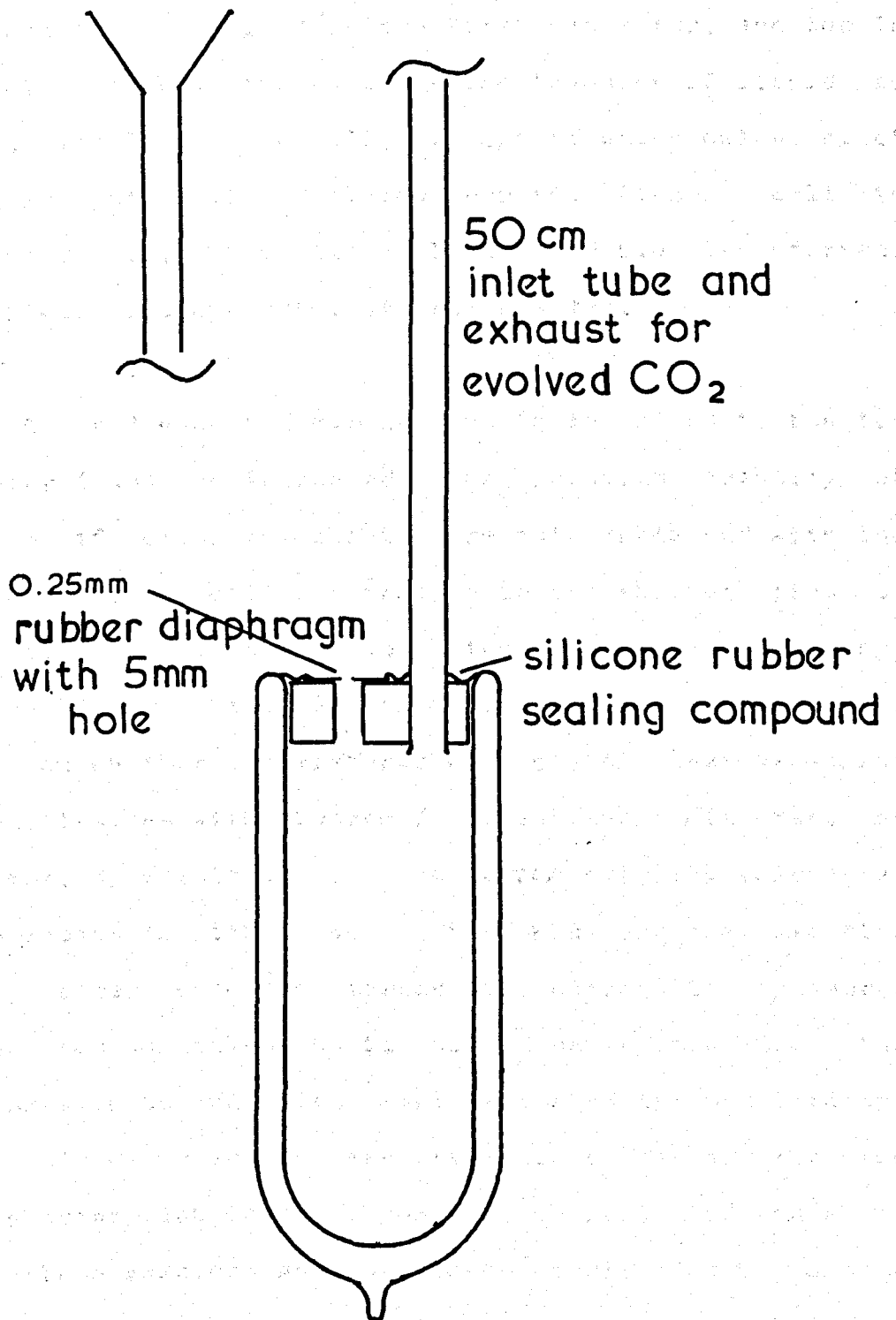
where B_{12} was either taken from the literature, or estimated by a corresponding states method (Cruickshank, Windsor and Young, 1966). This second virial correction, for the mixtures studied, i.e. benzene/n-hexane and benzene/cyclohexane, was not really necessary, since at the temperatures concerned, it produced a difference in n of only about 1% from the value calculated from the ideal gas equation. The estimation of dew-pressure in a system of unknown phase behaviour would obviously pose some problems, but these could be dealt with simply by taking quantities for four samples to yield, say, one-third of the ideal dew-pressure, mixing in the mixing vessel, and determining the dew-pressure, then drawing a rough dew-point line through the measured points, which could then be used for calculation of the required mixture quantities. Since the samples were being metered, not by weight, but by volume, a knowledge of the density of the liquids at the temperature of metering was required. The accuracy required however was not great, and although for this work, the necessary data were available from the literature, a simple specific gravity measurement would have sufficed. The mixtures were made by evacuating the system with all taps, other than those of the liquid reservoirs, open, then closing taps T6 and T3. T7 was opened, and a Dewar vessel containing very cold water placed on VT2. When slightly more of the liquid had been transferred than was

actually required, taps T7 and T5 were closed, and the section bounded by T3, T6, T7, and T8 again evacuated. The process was repeated with VT1 for the other liquid. The cold water in the Dewar was replaced by water at 298.15 K, and this (clear) Dewar was raised to cover both VT1 and VT2. T6 was opened, and any excess liquid was pumped away, slowly, in order to avoid excessive temperature changes whilst adjusting the quantities. T5 and T4 were then closed, T3 and T2 opened, and when the mercury had been raised to the top of Manometer 1, the system was again thoroughly evacuated. An acetone/solid carbon dioxide refrigerant mixture was then made up and poured into the special cold-trap Dewar (diagram 2.20). Tap T1 was then closed and the cold trap immersed in the thermostat and slipped over the "finger" cell. Tap T6 was then closed and taps T4 and T5 opened, after which tap T1 was opened and the sample transferred to the cell. When this process was complete, T1 was closed, and the cold-trap slowly removed, the mercury level being maintained by the use of TT1 and NV1 with the dry nitrogen pressure supply.

The Measurement Of Bubble And Dew Points

The sample was stirred some 30 times with the magnetic stirrer, splashing the liquid well up the walls of the cell, and then a further 10 times, at intervals of 5 minutes. After about 30 minutes the first of the bubble-point pressure/volume readings was taken. The mercury was then lowered about 1 cm down the tube, the liquid again stirred 30 times, and after 15 minutes, with two further stirrings, the

DIAGRAM 2.20



the submersible cold trap

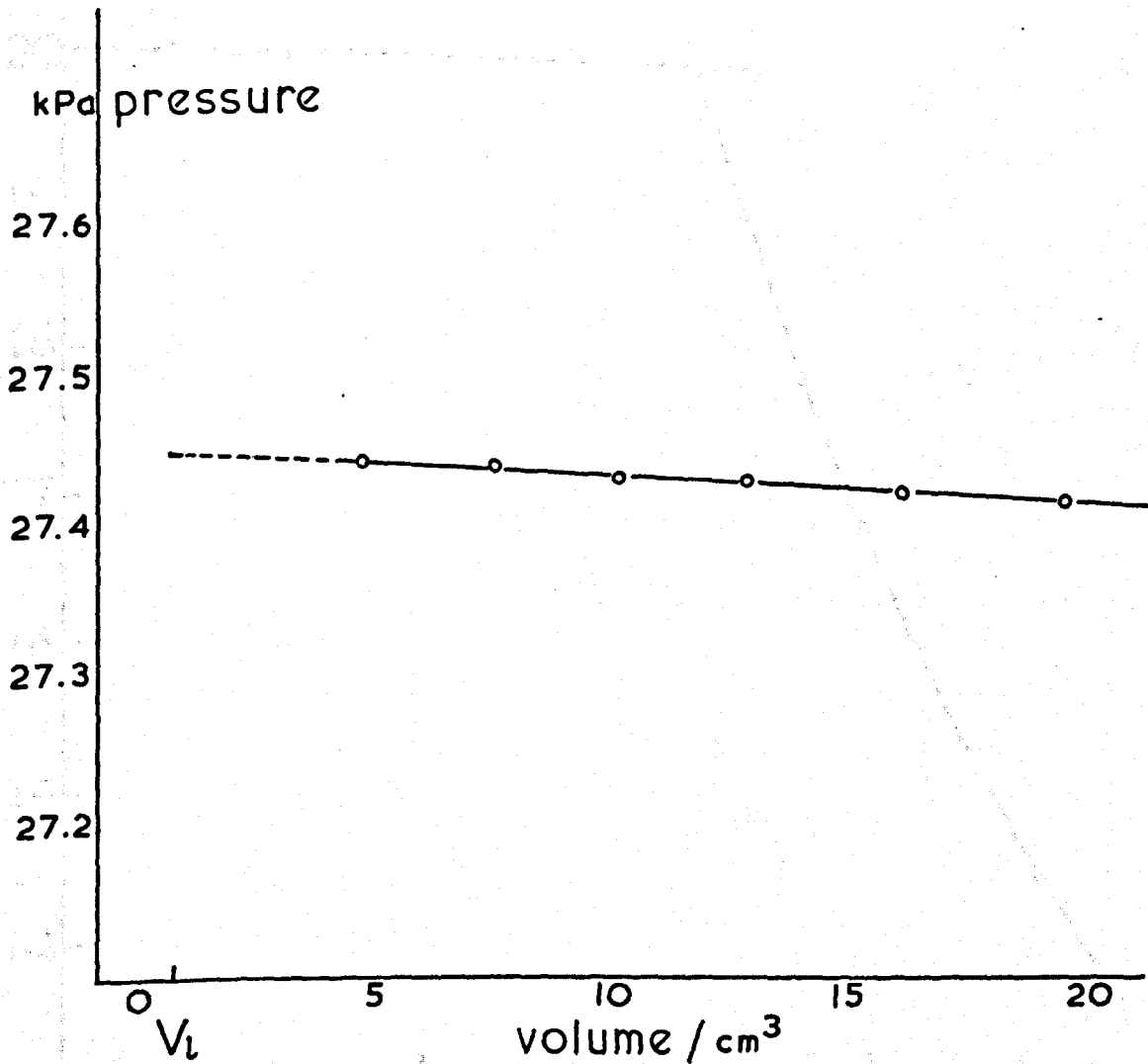
second of the readings was taken (diagram 2.21). This process was repeated 4 or 5 times more, and then the liquid was removed to the gas-mixing vessel. To do this the mercury was lowered about half-way down the first manometer, and tap T6 closed, which had been opened after the transfer of liquid to the cell. Tap T1 was then slightly opened and a cold-trap of solid/liquid acetone placed over the "finger" cell in the mixing vessel. Once all the liquid had been transferred, the tap T2 was closed and the stirrer started.

After 1 hour the mercury was again raised to the top of Manometer 1 and tap T2 opened. The required quantity of gas (large if clear dew-points were being obtained with the liquids, otherwise small) was trapped in the shorter limb of the manometer by suitably adjusting the mercury level, and closing tap T1. At this stage procedures differed slightly, depending on whether the mixtures were giving clear dew-point discontinuities, as with benzene/ cyclohexane mixtures, or unclear curved results. In the latter case the volume was slowly decreased to within about 5-6 kPa of the expected dew-point, after which a series of compression pressure/ volume readings was taken, until clear divergence from the virial curve occurred. The sample was then trapped into the cell with cold water and the mercury again raised to the top of the shorter limb of the manometer. A series of expansion pressure/volume readings was then taken, consisting of some 5 or 6 points, producing a line to intercept the virial curve at the dew-point, avoiding the central region of connecting curvature (diagram 2.22).

DIAGRAM 2.21

bubble point measurement

Mark 3 apparatus



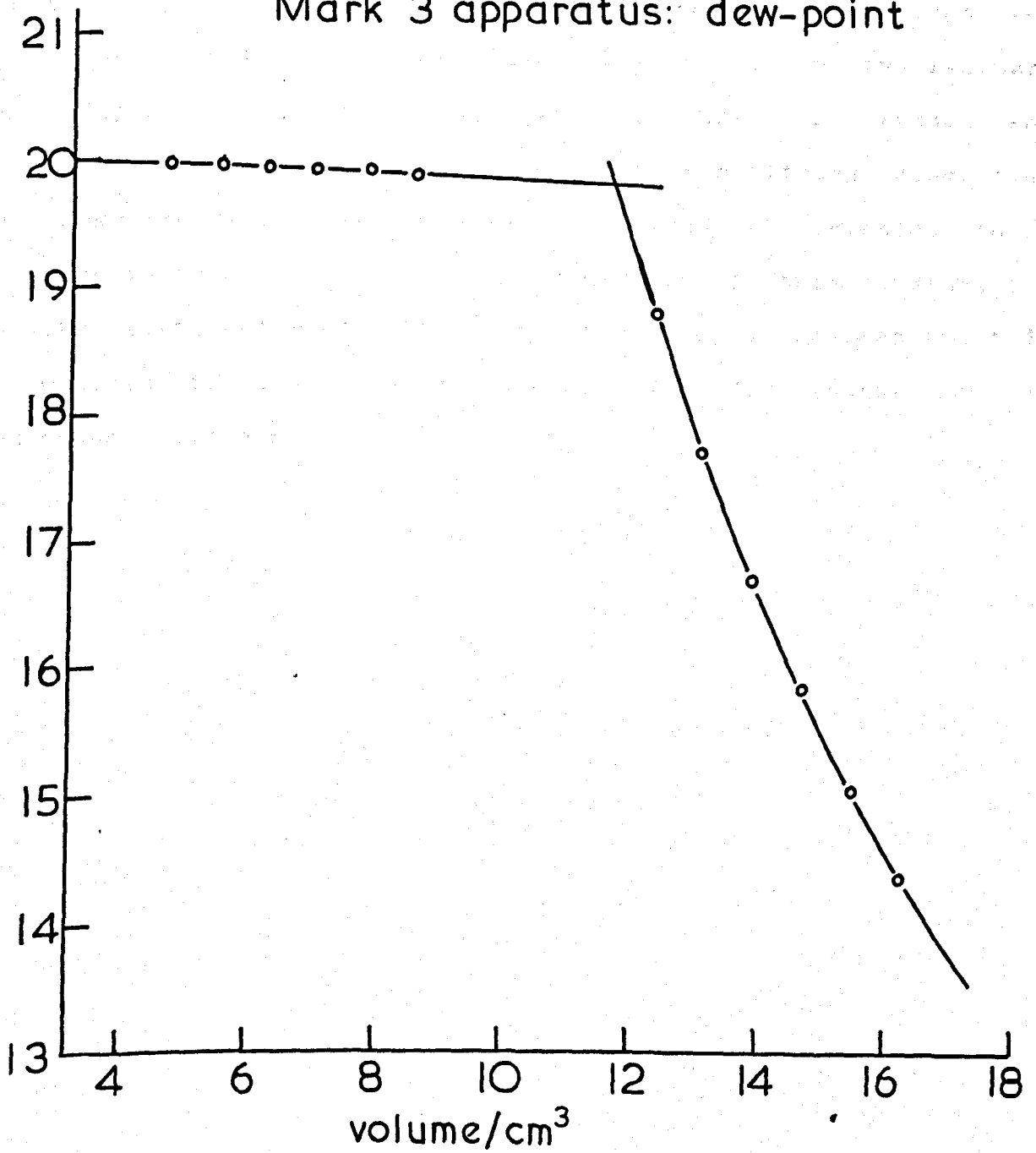
a benzene+cyclohexane mixture at 313.15 K

$x_2 \sim 0.40$

DIAGRAM 2.22

pressure / kPa

Mark 3 apparatus: dew-point



a benzene+n-hexane mixture at 298.15K

$x_2 \sim 0.70$

In the case of mixtures giving clear dew-points the mercury was raised until the pressure was about 1 kPa below the expected dew-point and then, with very small decrements of volume, a series of compression pressure/ volume readings was taken for both one- and two-phase portions of the isotherm (diagram 2.23). The virial section, when this method was employed, appeared linear, and computer fitting showed that lower standard deviations were obtained by treating these results as linear. There was no stirring in this section, and the time interval after adjustment of volume was about 10 minutes in the one-phase region and 15 minutes in the two-phase region.

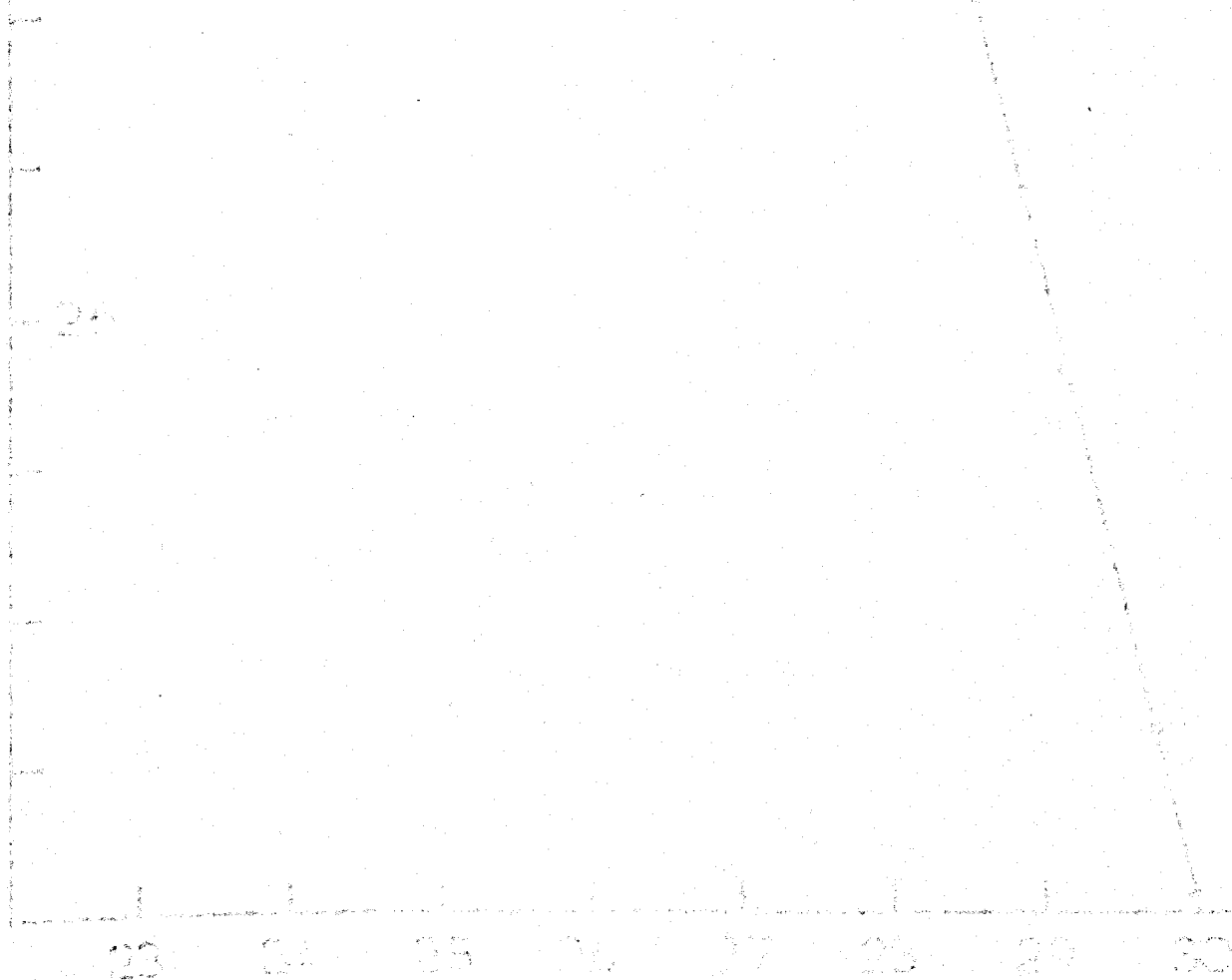
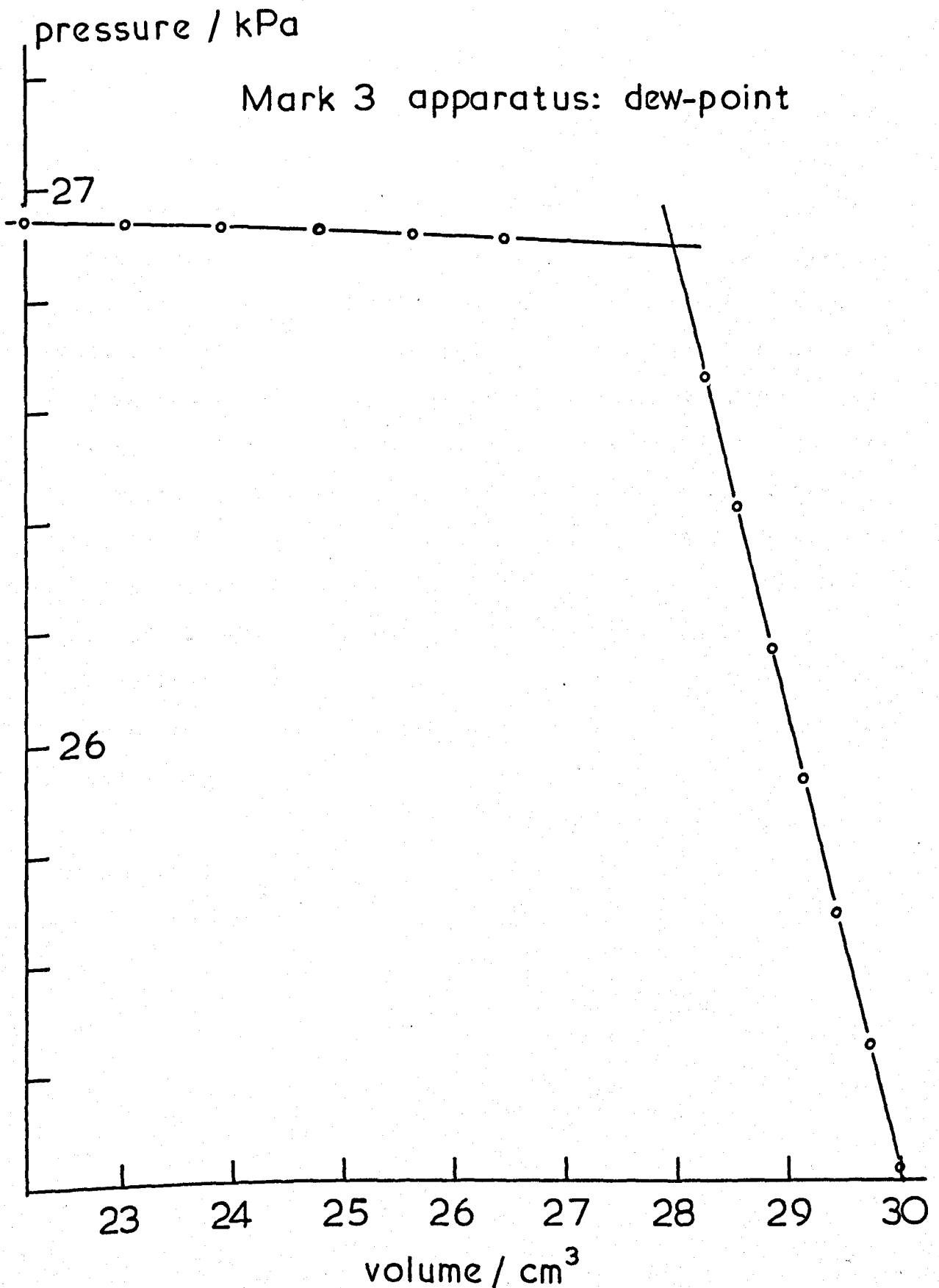


DIAGRAM 2.23



a benzene+cyclohexane mixture at 313.15K
 $x_2 \sim 0.70$

THE RESULTS OBTAINED

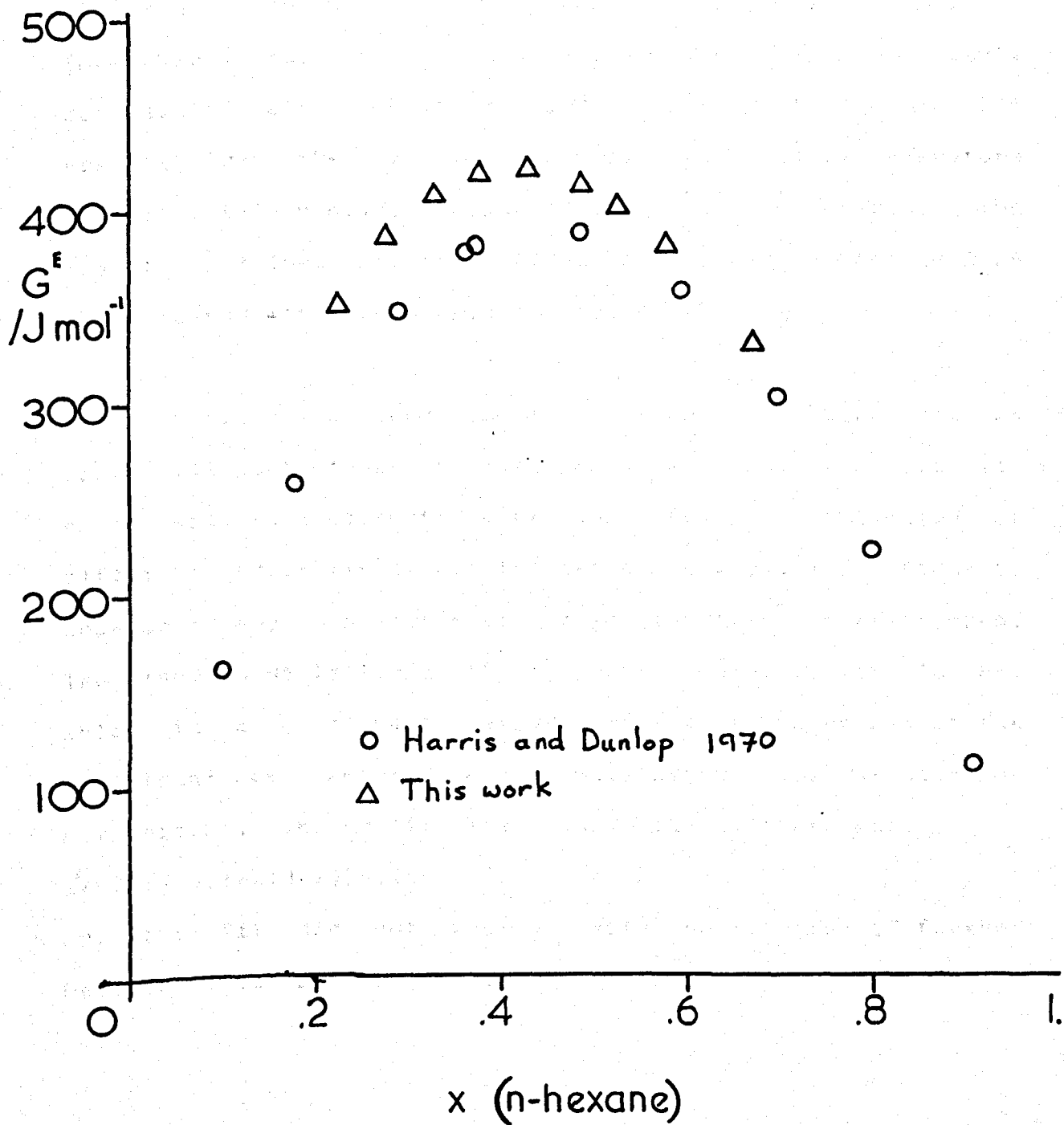
The System Benzene + n-Hexane At 298.15 K

This system was the first to be studied in detail with the Mark 3 apparatus, and the results are slightly suspect, because of the relatively high gas pressure in the gas mixing vessel. The system was chosen because two previous studies of vapour pressure against composition had been carried out, with two different apparatus, yielding results which agreed very closely (Harris and Dunlop 1970, and Murray and Martin 1975). The results obtained are shown in diagram 2.24, plotted against those of Harris and Dunlop, and in tabular form, in Table 2.1, where the corrected value for overall composition is listed, with the corresponding measured values of bubble and dew pressures and the calculated values of excess free energy. The standard deviation of the measured pressures was 14.5 Pa, and the Redlich-Kister equation obtained was:

$$G^E/RT \text{ /J mol}^{-1} = x(1-x)[0.65907 + 0.20084(1-2x) + 0.11888(1-2x)^2 + 0.03236(1-2x)^3]$$

DIAGRAM 2.24

benzene + n-hexane at 298.15 K



The System Benzene + Cyclohexane At 313.15 K

This system was used as a further test of the limiting capability of the Mark 3 apparatus, since much clearer dew-points are obtained than for the previous system; also there are two different measurements of this system by different methods, one a recirculatory still method (Scatchard, Wood and Mochel 1939), and the other a dew-point, composition method (Brewster and McGlashan 1973) and the results from the two methods agree well. It was therefore felt that this provided a good test for the apparatus. The results obtained are shown in Table 2.2, and in diagram 2.25 are compared with those from the two references.

It may be seen from the diagram that agreement is good, although these results are, perhaps, very slightly skewed with respect to the others, possibly a reflection of different adsorbitivity of the two components, which tends to show up in any apparatus having a large internal surface area. The standard deviation of the measured pressures is 16 Pa, which is a good deal larger than any of the errors of the individual measurements, again suggesting some problem of composition. The Redlich-Kister equation obtained was:

$$G^E/RT / J \text{ mol}^{-1} = x(1-x)[0.460102]$$

and the fit did not improve with the addition of further Redlich-Kister coefficients.

DIAGRAM 2.25

benzene + cyclohexane at 313.15 K

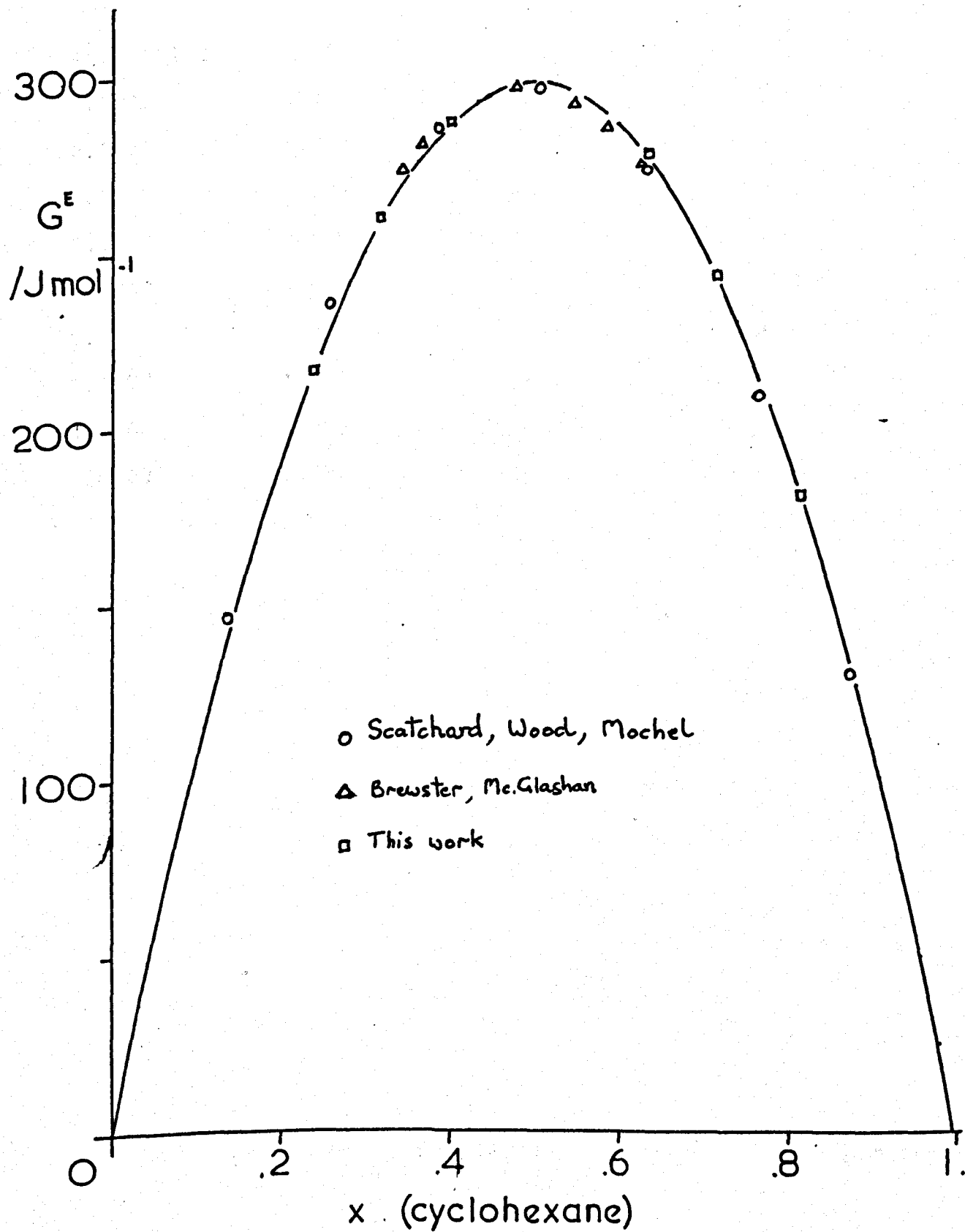


TABLE 2.1The System Benzene + n-Hexane At 298.15 K

<u>x(overall)</u>	<u>P_{bub} /Pa</u>	<u>P_{dew} /Pa</u>	<u>G^E /J mol⁻¹</u>
0.2245	17305	15218	350.1
0.2773	17799	15892	385.0
0.3300	18232	16562	406.9
0.3784	18569	17177	417.1
0.4317	18909	17808	418.9
0.4896	19258	18412	410.9
0.5287	19433	18795	400.2
0.5804	19673	19221	380.1
0.6722	20024	19811	329.2

TABLE 2.2

The System Benzene + Cyclohexane At 313.15 K

<u>x(overall)</u>	<u>P_{bub} /Pa</u>	<u>P_{dew} /Pa</u>	<u>G^E /J mol⁻¹</u>
0.2372	26758	26402	216.7
0.3179	27146	26955	259.8
0.3997	27411	27336	287.4
0.6338	27393	27296	278.0
0.7156	27118	26888	243.8
0.8145	26550	26216	181.0

The first part of the chapter is devoted to a discussion of the various methods used in the study of the properties of the system. The second part is devoted to a discussion of the results of the study. The third part is devoted to a discussion of the conclusions of the study.

The first part of the chapter is devoted to a discussion of the various methods used in the study of the properties of the system. The second part is devoted to a discussion of the results of the study. The third part is devoted to a discussion of the conclusions of the study.

CHAPTER THREE

The first part of the chapter is devoted to a discussion of the various methods used in the study of the properties of the system. The second part is devoted to a discussion of the results of the study. The third part is devoted to a discussion of the conclusions of the study.

The first part of the chapter is devoted to a discussion of the various methods used in the study of the properties of the system. The second part is devoted to a discussion of the results of the study. The third part is devoted to a discussion of the conclusions of the study.

FURTHER DEVELOPMENT OF THE METHOD

It might, at this stage, be interesting to consider the further development of the bubble-point, dew-point method. In the Mark 3 apparatus, we have an efficient and accurate method for obtaining excess Gibbs free energies for mixtures, and also, incidentally, the phase behaviour of the mixtures (since corrected composition values are produced during the solution), but there are still certain areas where improvement would be desirable. The most obvious of these possible improvements are, perhaps, the reduction of the overall size and complexity of the system, and the measurement, and possibly the recording of pressure by some less arduous and tedious method. These desired improvements are, in fact, complementary, in that the replacement of the manometers as a means of measuring pressure would, in itself, lead to a considerable simplification and reduction in size of the system, in particular of the thermostatted section. The system which will now be described seems, on the basis of the experience with the preceding systems, probably the most straightforward solution of the above problem. The main constraints placed upon the design were, firstly, that the product be as simple to construct as possible, even at the expense of requiring some specialist engineering work, secondly, that the product be as simple to operate as possible, finally, that the operation of the system require as little direct attention from the operator as possible. The

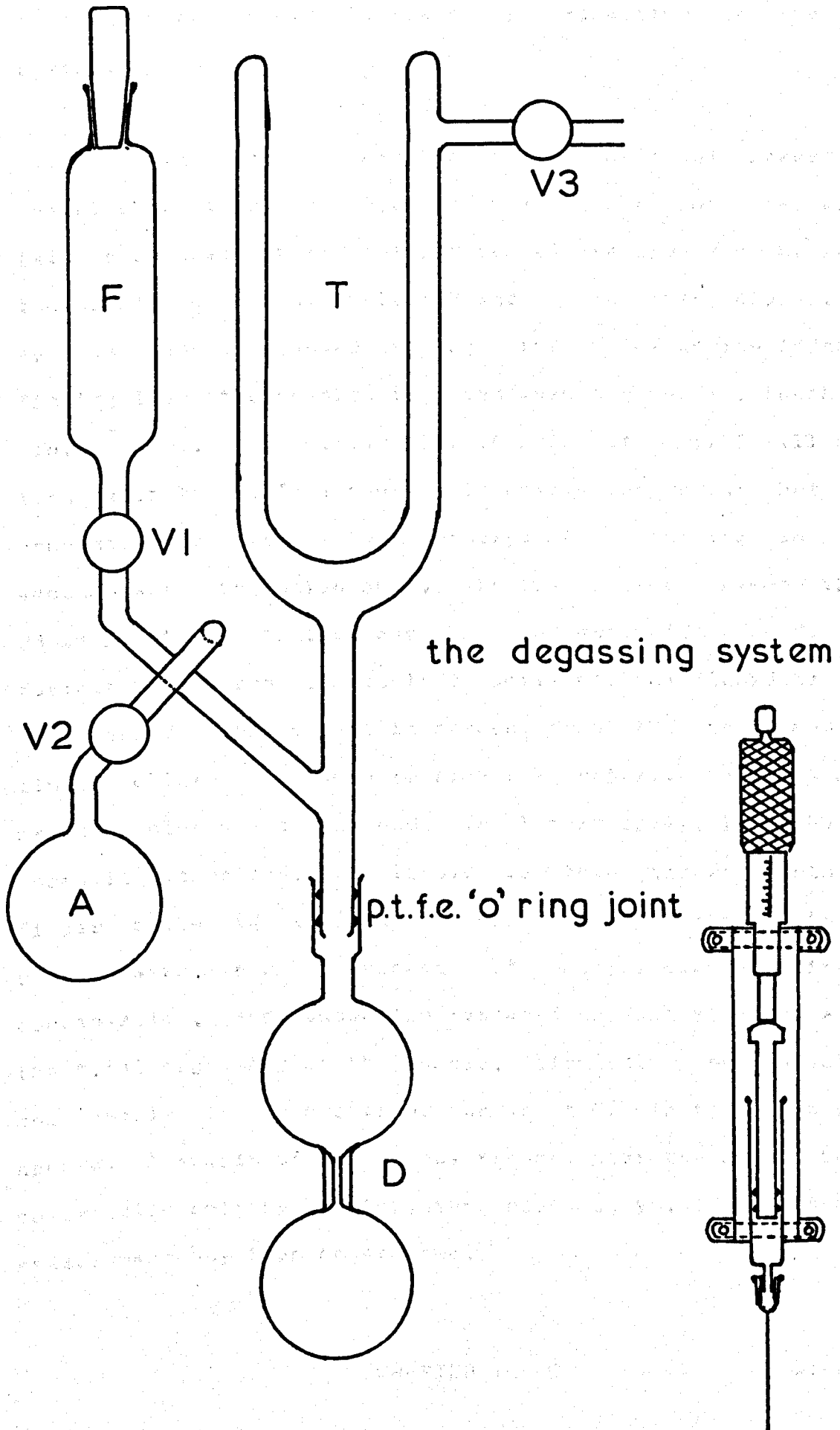
estimated cost of the system, which is largely the cost of the electronic equipment, is around 2500 Pounds Sterling at the time of writing (July 1976), but this is not too unreasonable, in view of the results which might be obtained and of the pressure and temperature range over which the system could be operated.

The operation of the system is based upon the stepwise compression of a gaseous sample, through the two-phase region, almost to the liquid region. The apparatus is of piston and cylinder form, where the seal is obtained by the use of p.t.f.e. sealing rings between piston and cylinder, both of which are constructed in stainless steel and highly polished. The sample preparation and metering system is much simplified and depends upon the use of storage flasks similar to those used in the calorimetry work, and modified micrometer syringes having p.t.f.e. sealed pistons. The vacuum demanded is higher than that for the Mark 3 system, but with so small and simple a system the Edwards F203A diffusion pumps used in this work should be adequate, as, with suitable working fluid, the limiting vacuum attainable is of the order of 10^{-5} Pa. The pressure is measured with an electronic pressure transducer, for example one of the National Semiconductor models, by means of a Solartron Master Series digital voltmeter, on-line calculator and thermal printer or punched paper tape output device. The operation of the system, once the sample is sealed into the compression cylinder, is entirely automatic, with the compression steps and read/print pressure commands being controlled by a synchronous drum timer. This means that

the system could be loaded (a relatively brief task with this apparatus), and then left to run the bubble-point, dew-point measurement unattended, e.g. overnight.

We now consider the detailed construction of the equipment. The thermostat may be small, since the powered compression vessel is itself small, but should be controllable to better than 0.005 K, and be capable of operating over a wide range of temperature. The liquids are pre-purified as for the current dew-point, bubble-point work and loaded into the double flasks after degassing in the apparatus shown in diagram 3.1. The valves are all stainless steel bellows-sealed types having extremely low leak rates. The apparatus is connected to high vacuum, thoroughly degassed, and "flamed out" to remove adsorbed gas and water, after which the liquid is loaded into flask A from funnel F, with the aid of a solid/liquid acetone cold trap. The frozen solid is then sublimed with continuous pumping onto the cold-finger T, V3 is closed and the liquid is transferred back to flask A. This process is twice repeated, which should be sufficient to ensure complete degassing (Murray and Martin 1975), then the sample is allowed to melt, and run into the double flask D, and is sealed by mercury which is run in from funnel F. The flask is then removed and the process repeated for the second liquid. The modified micrometer syringes are also shown in diagram 3.1: these consist of standard "Aglas" (Wellcome) units, in which the ground syringes are replaced by Youngs or Hamilton p.t.f.e. sealed units of considerably greater capacity, which must of course be calibrated. The filling

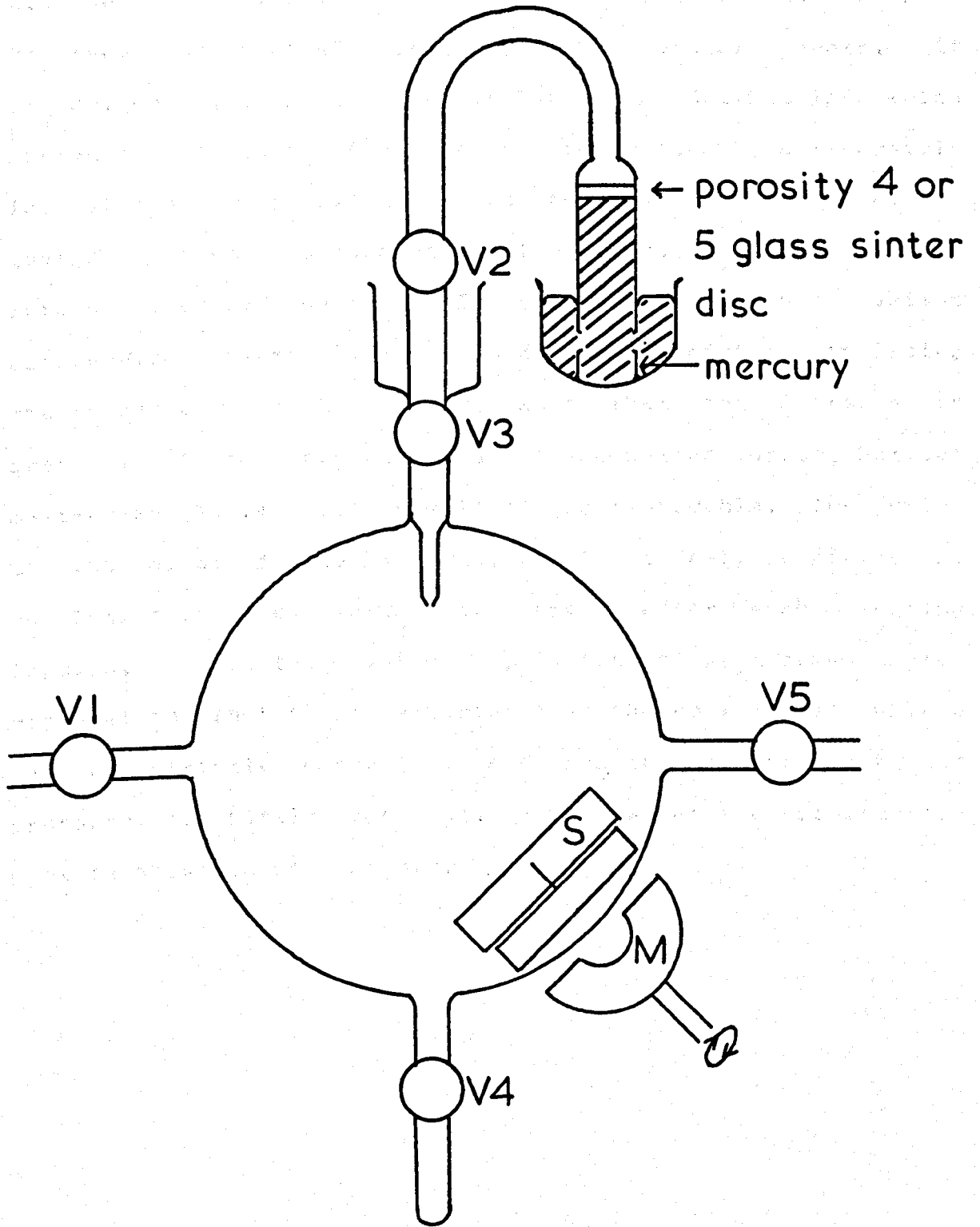
DIAGRAM 3.1



procedure involves the flushing of the syringes with two small samples to remove air, followed by extraction of the main sample.

The liquids are then fed to the sample preparation vessel shown in diagram 3.2: at this stage all of the valves (all stainless steel bellows types) are open and the system thoroughly evacuated. Valves 2 and 3 are then closed, the syringe needles passed through the holes in the injection fitting I and the samples injected when the needles touch the sinter disc. This sinter disc of porosity 4 or 5 will allow liquids of low surface tension to pass under vacuum, but will prevent the passage of mercury, thus forming an ideal vacuum-sealed injection port. The trap between between V2 and V3 is partially filled and V2 progressively opened, with further additions of coolant until all the liquid has been transferred. The coolant is removed from the trap and the liquid allowed to warm to room temperature. Valves 1 and 5 are then closed and 3 opened. The liquid sprays into the bulb where it vapourises. The liquid is then trapped into the finger below V4 and V4 is closed. The system is then re-evacuated, and a process of evaporation, stirring, condensation, and evacuation repeated several times to ensure the final degassing of the sample. With V1, V3 and V5 closed the sample is then stirred for about 30 minutes, then V5 is opened. A sample of gas is now trapped over the piston in the compression unit by opening, then closing, V6. The automatic measurement may then be started.

DIAGRAM 3.2



sample preparation vessel

The drive screw of the piston is machined from rod with opposed flats, and passes through a shaped block designed to prevent movement of the piston in the rotatory sense. It is driven by a captive nut in the end of a tube, into which passes the screw, the tube itself being driven by a reversible induction motor geared down, preferably with a planetary gearing system, to turn at about 3 r.p.m., and fitted with a ratchet overload device. In this design the maximum compression volume is about 50 cm and the minimum, including the transducer, about 1-2 cm, such that the increase in pressure of the residual gas, at the design vacuum, between maximum and minimum volume will not be measurable. The drive of the motor is so arranged that it only completes one revolution of the final drive shaft after each starting impulse, before the power supply is cut off by a cam-operated microswitch, in this way ensuring that the decremental volume can be strictly controlled and related to the recorded pressure, for fitting purposes. A diagram of the compression unit is shown in diagram 3.3.

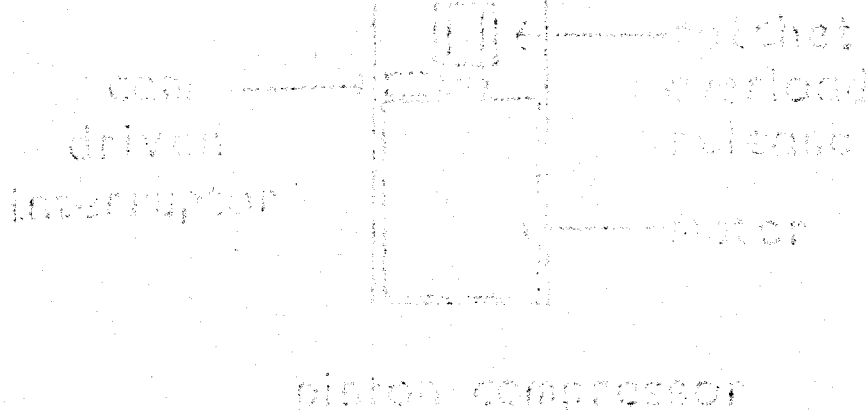
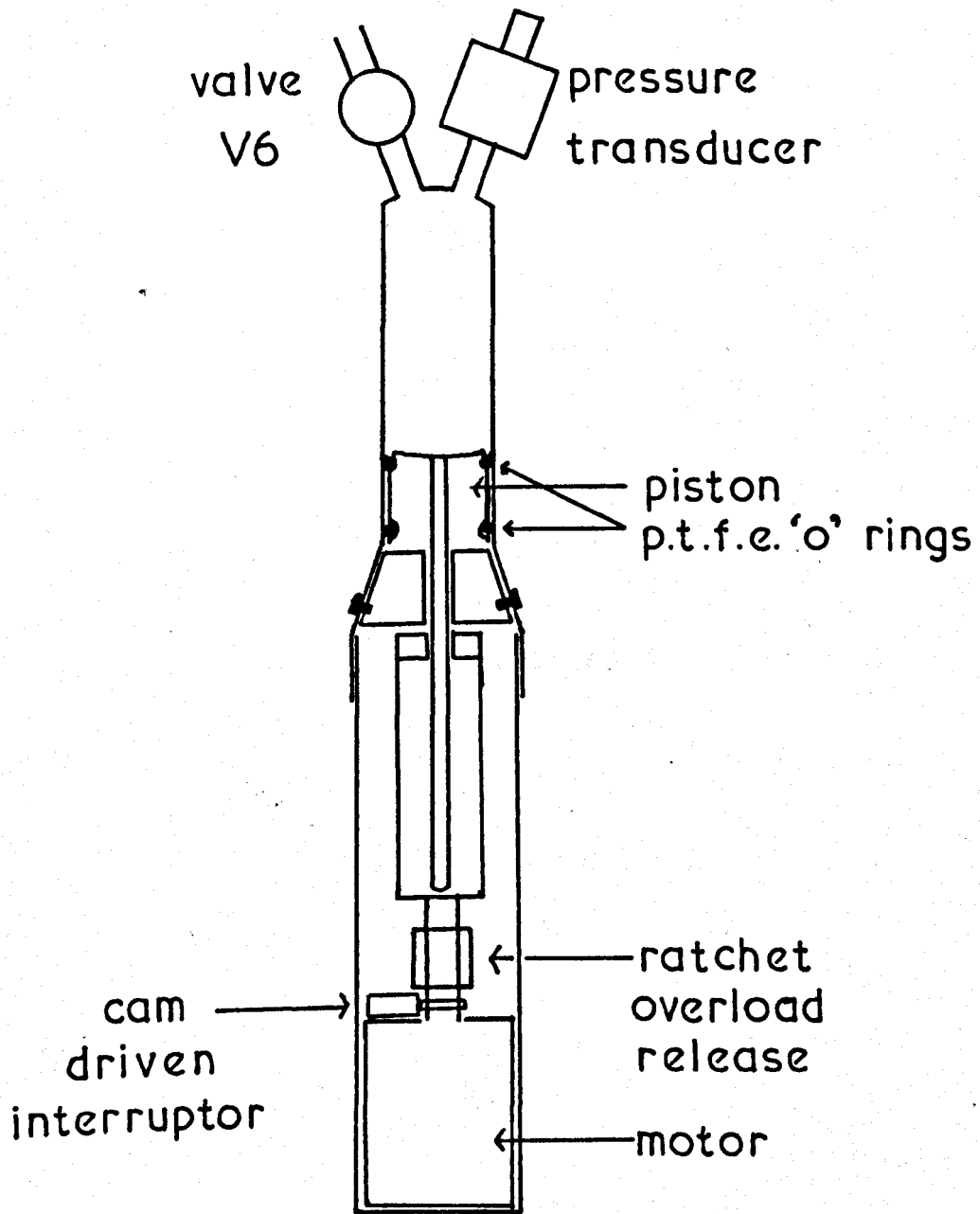


DIAGRAM 3.3



piston compressor

THE MEASUREMENT OF THE EXCESS VOLUMES OF MIXING

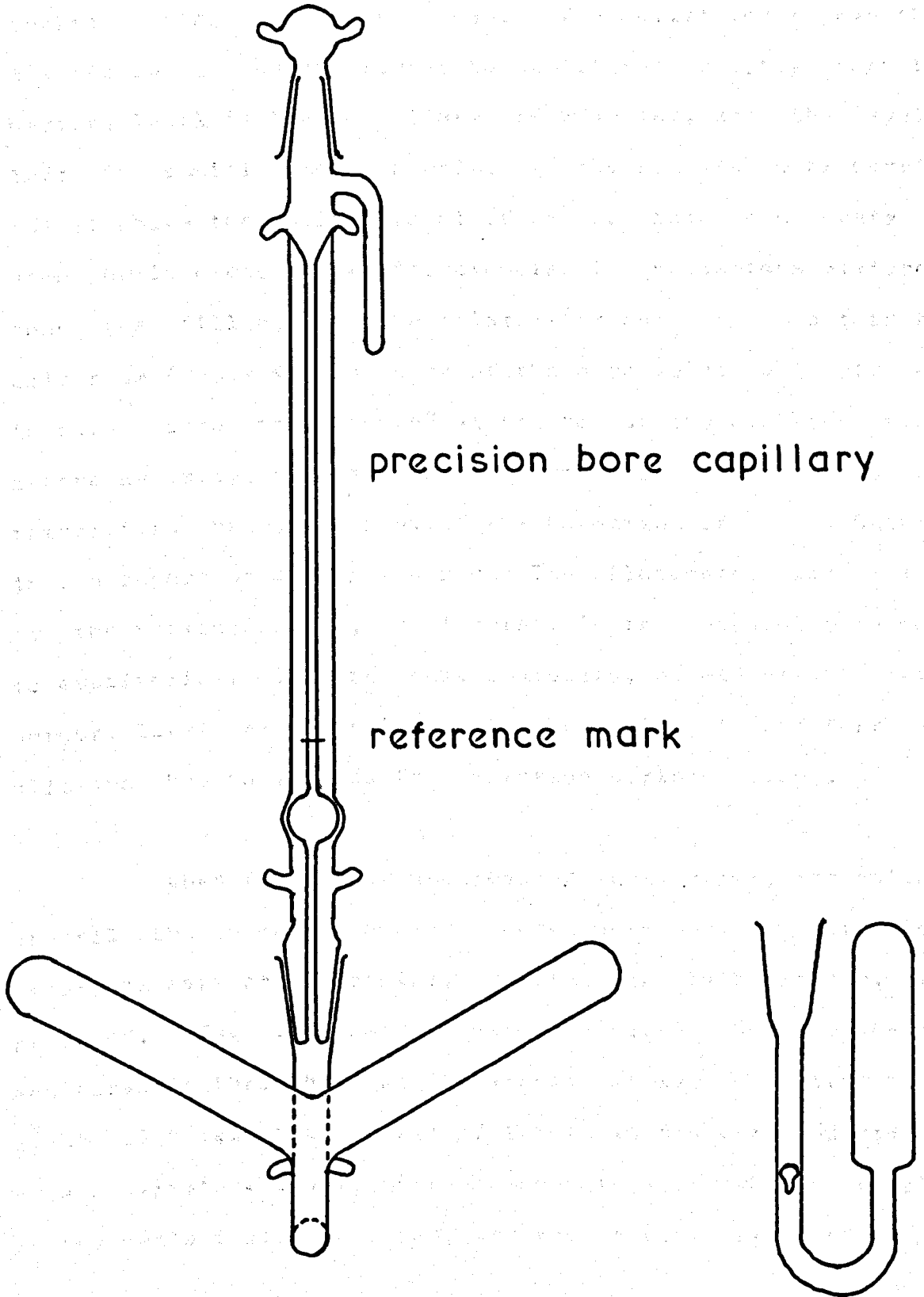
The excess volumes were measured with a small batch-type dilatometer, illustrated in diagram 4.1. The same thermostat was used as in the measurement of excess enthalpies, but the pump was replaced by a more powerful, glandless, magnetically driven type, as the original one was becoming badly worn.

The precision bore capillary tubing of the dilatometer, specified to be 0.86 mm in diameter, was calibrated by filling different sections with mercury, thermostating, measuring the thread length, and weighing the mercury. The bore was found to be constant to within the limits of experimental accuracy, and to be 0.8520 mm with an uncertainty, expressed by the standard error of several measurements, of 0.0002 mm.

The procedure for an excess volume measurement commenced with the calculation of the volumes of the two liquids required, these being scaled so that the larger was 2 cm³, the largest quantity of liquid which could be delivered with sufficient accuracy by the micrometer syringes, and contained safely in one arm of the dilatometer. The B.10 joint was lightly greased at the top, and fitted to the same mercury-filling attachment on the bubble-point, dew-point system as had been used for the filling of the calorimeter, and the dilatometer body was filled with mercury. It was then transferred to a clamp on a stand, where the liquids were

DIAGRAM 4.1

the dilatometer

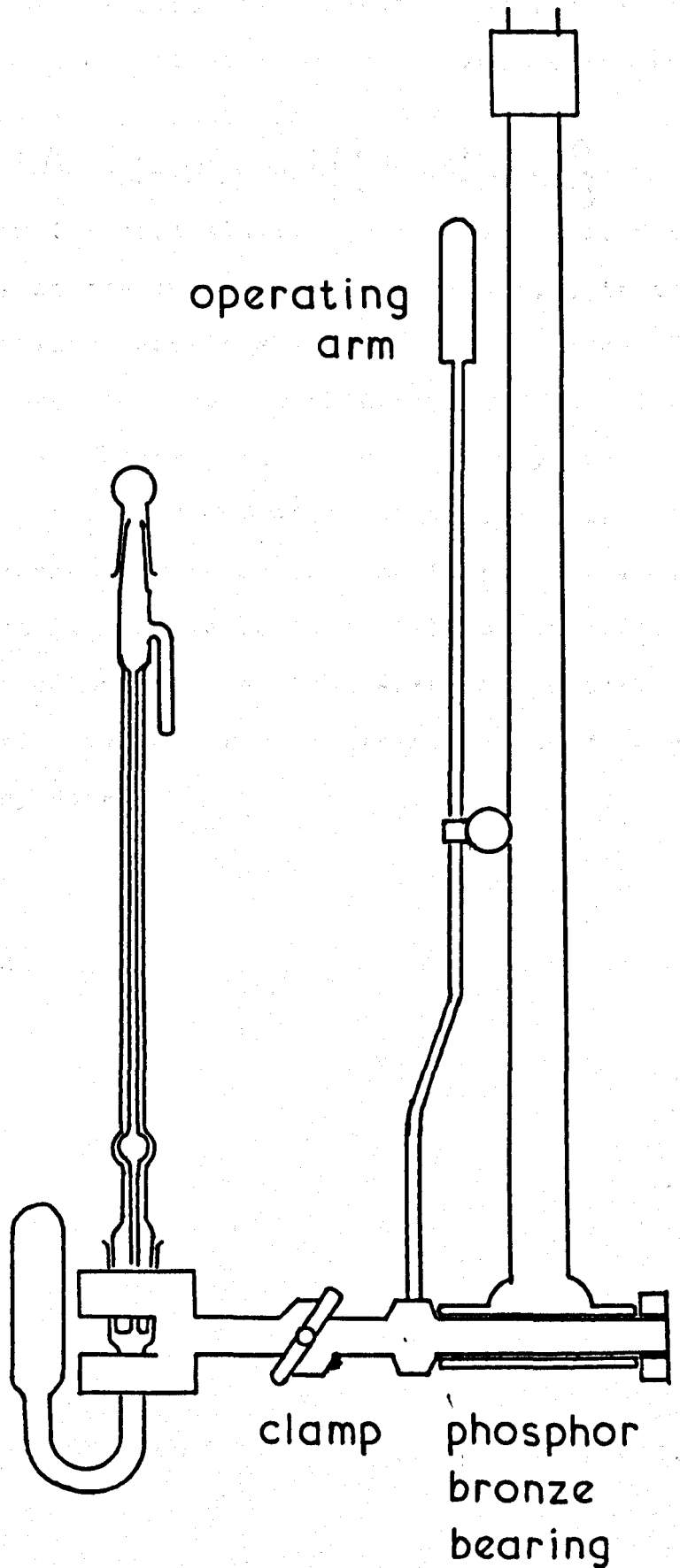


injected through bent syringe needles, after removal of the grease. Mercury was then added to bring the level to about half-way up the 8.10 joint, and the capillary cone and tube fitted tightly, without grease, and clamped in place with springs using the lugs shown. The dilatometer was then transferred to the thermostat to equilibrate roughly, then the mercury level in the capillary was adjusted, and the system left to equilibrate properly. If the run was to be carried out at above the boiling point of one or both components at atmospheric pressure, as for example with neopentane mixtures, then the filling of the dilatometer was carried out in the cold room (273.7 K), and some of the more volatile liquid was injected into the "finger" at the top of the capillary tube, before assembly, to balance the pressure increase as the temperature rose, and prevent the formation of vapour bubbles in the apparatus during the run. The dilatometer was fitted to the rocking device, and immersed in the thermostat to come to equilibrium. In this case, obviously, no adjustment of the mercury level was possible at thermostat temperature and allowance had to be made for expansion during filling.

When the system had reached equilibrium, the heights of all the mercury menisci were measured, relative to a reference mark on the capillary, with the cathetometer, and recorded. The dilatometer was then rocked gently backwards and forwards through about 70 degrees between positive stops about 10 times, and the liquid levels in the arms adjusted to be approximately level: after re-equilibration the new heights of the menisci were measured, and recorded. For changes in

DIAGRAM 4.2

the dilatometer support



mercury levels of greater than about 1 cm the change in volume had to be corrected for compressibility changes, and the formula below was arrived at after two assumptions had been made, one, that the isothermal compressibility of a mixture was the sum of volume fraction isothermal compressibility products for the pure liquids; and two, that the compressibility of the mercury could be ignored.

$$\Delta V_{comp} = (dg/10) \left\{ [v_1 k_1 (h_1 - h_{c1}) + v_2 k_2 (h_1 - h_{c2})] - [(v_1 k_1 + v_2 k_2)(h_2 - h_m)] \right\}$$

where k_i is the isothermal compressibility of component i , d is the density of mercury at the thermostat temperature, g is the local value of gravitational acceleration, h_1 and h_2 are the heights of the mercury in the capillary before and after mixing, h_{c1} , h_{c2} and h_m are the heights of the mercury in the arms of the dilatometer before and after mixing, measured in cm, relative to the reference mark on the capillary, and V_i is the volume of component i . The calculated values, corrected also for cathetometer column expansivity, were then fitted to a Redlich-Kister equation by the same programme as that used for the excess enthalpy data.

the fraction of hydroxyl

and the constant

$V_1 k_1 (h_1 - h_{c1}) + V_2 k_2 (h_1 - h_{c2}) - [(V_1 k_1 + V_2 k_2)(h_2 - h_m)]$

with a standard deviation of 0.002 cm³.

the fraction of hydroxyl

THE RESULTS OBTAINED

A test of the dilatometer was carried out on the system benzene + cyclohexane at 298.15 K, the excess volume of which has been measured many times. A summary of these results has been made by Dickinson, Hunt, and McLure (1975), and the results from this dilatometer lay very close to their own results, all within one standard deviation of their fitted curve ($0.003 \text{ cm}^3 \text{ mol}^{-1}$). The results were fitted to the Redlich-Kister equation

$$V^E / \text{cm}^3 \text{ mol}^{-1} = x(1-x)[2.5722 - 0.1105(1-2x) + 0.0110(1-2x)^2]$$

This agreement was considered perfectly good enough to justify further work in measuring the excess volumes of the systems for which the excess enthalpies had already been obtained. The results obtained are shown in Table 4.1, and were fitted to Redlich-Kister equations, as follows:

Cyclohexane + tetramethyl silane:

$$V^E / \text{cm}^3 \text{ mol}^{-1} = x(1-x)[-4.3653 - 0.5509(1-2x) - 0.1612(1-2x)^2]$$

with a standard deviation of $0.002 \text{ cm}^3 \text{ mol}^{-1}$, where x was the mole fraction of cyclohexane

Cyclohexane + neopentane:

$$V^E / \text{cm}^3 \text{ mol}^{-1} = x(1-x)[-5.3209 - 1.0251(1-2x) - 0.0220(1-2x)^2]$$

with a standard deviation of $0.002 \text{ cm}^3 \text{ mol}^{-1}$, where x was the mole fraction of cyclohexane.

DIAGRAM 4.3

benzene + cyclohexane at 298.15 K

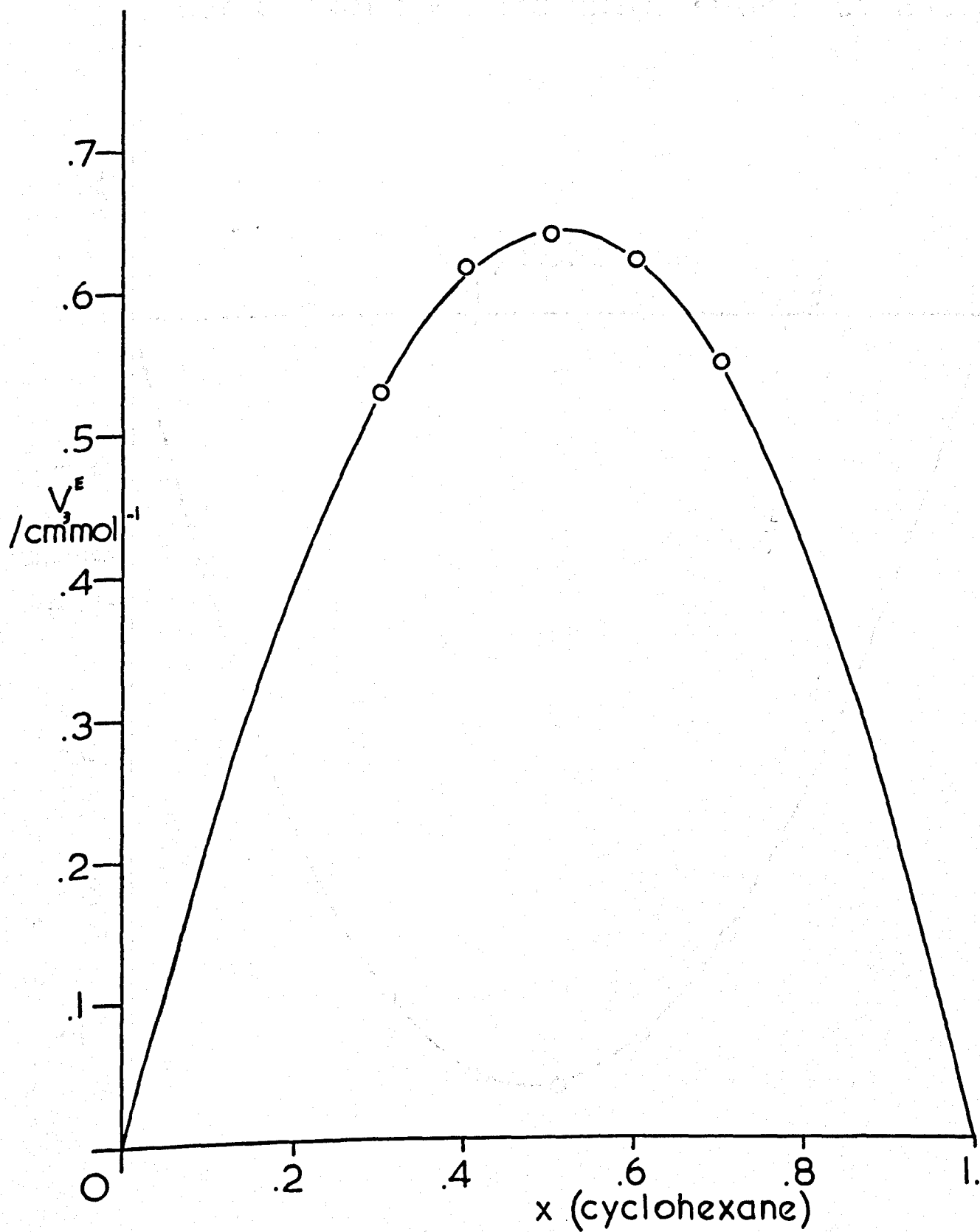


DIAGRAM 4.4

cyclohexane + tetramethyl silane at 298.15K

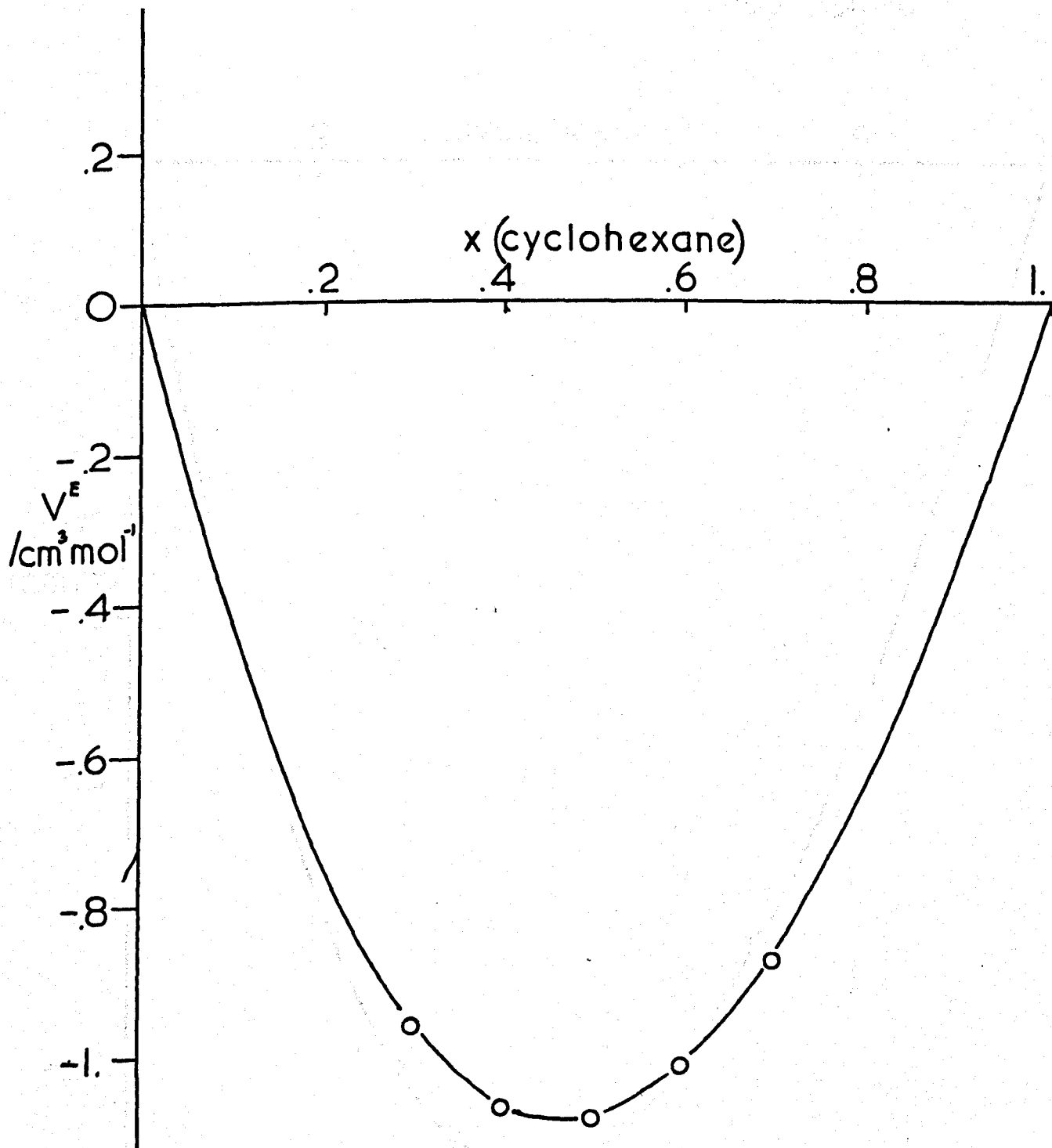


DIAGRAM 4.5

cyclohexane + neopentane at 298.15 K
and 200kPa

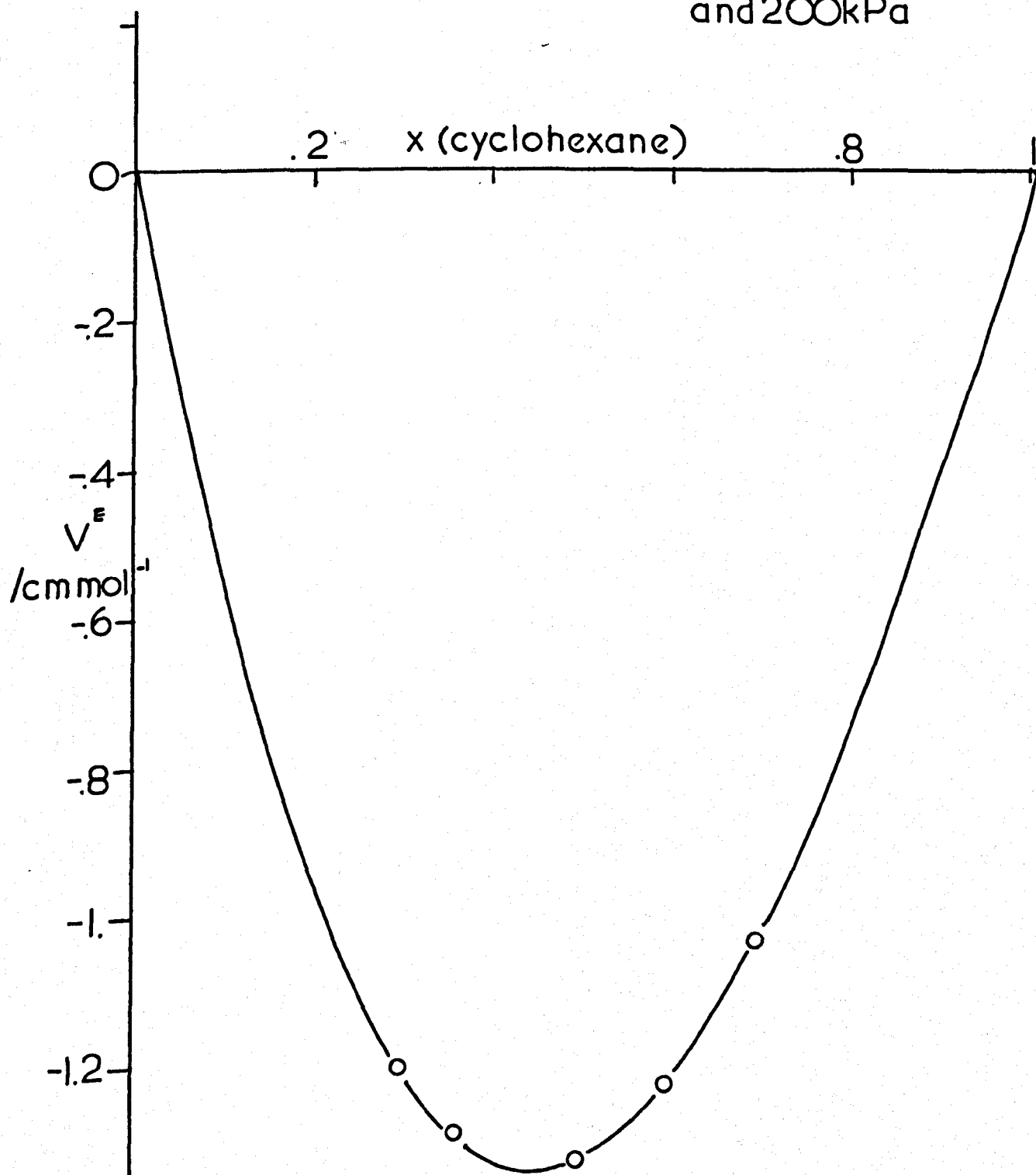


TABLE 4.1

The System Cyclohexane + Tetramethylsilane At 298.15 K

<u>x (cyclohexane)</u>	<u>$V^E / \text{cm}^3 \text{mol}^{-1}$</u>	<u>$V^E_{\text{exp}} - V^E_{\text{calc}} \text{cm}^3 \text{mol}^{-1}$</u>
0.6990	-0.8788	+0.0011
0.5997	-1.0206	-0.0025
0.4996	-1.0930	+0.0016
0.3996	-1.0757	+0.0003
0.2998	-0.9676	-0.0005

TABLE 4.2

The System Cyclohexane + Neopentane At 298.15 K

<u>x (cyclohexane)</u>	<u>$V^E / \text{cm}^3 \text{mol}^{-1}$</u>	<u>$V_{\text{exp}}^E - V_{\text{calc}}^E / \text{cm}^3 \text{mol}^{-1}$</u>
0.6987	-1.0345	-0.0005
0.5989	-1.2309	+0.0007
0.4997	-1.3301	+0.0003
0.3621	-1.2935	-0.0017
0.2996	-1.2044	+0.0012

CHAPTER FIVE

CHAPTER FIVE
[Faint text block containing the beginning of Chapter Five]

CHAPTER FIVE

[Faint text block containing the main body of Chapter Five]

THE PREDICTION OF THE EXCESS FUNCTIONS

At the beginning of this work it was decided that efforts would be made to predict the values measured, developing in the process a general method for the quantitative prediction of non-ideal behaviour in at least the quasi-spherical group of liquid mixtures. It was hoped that this method could then be extended to mixtures of this group with other non-electrolytes, forming a fairly general predictive method.

The first requirement was a choice of the general approach to be used, i.e. whether specific equations of state would be used, or experimental equations of state derived from fitting of state data of the compounds of interest, or a less direct method, working from some assumed form of intermolecular potential, or a statistical approach. A survey of some of the recent publications^(18,19,20,22,23,24,30) in this field suggested that the most accurate of the statistically based approaches yielded results only slightly better than those obtained by the relatively simple state-equation methods, and it was therefore decided that the first attempts at the prediction of the mixing functions would be made using a similar approach to that employed by Marsh, McGlashan, and Warr (1970). Two state equations would be chosen: the simple van der Waals⁽³³⁾ equation, and the rather more complex Guggenheim⁽¹²⁾ equation (Guggenheim 1965).

These equations may be expressed in a common form:

$$PV/RT = F(y) - a/RTV$$

where $F(y)$ is a function approximating the compression factor, PV/RT , of a hard-sphere gas, where sphere volume is $b/4L = yV/L$, where L is the Avogadro constant. For the van der Waals equation

$$F(y) = (1 - 4y)^{-1},$$

and for the Guggenheim equation

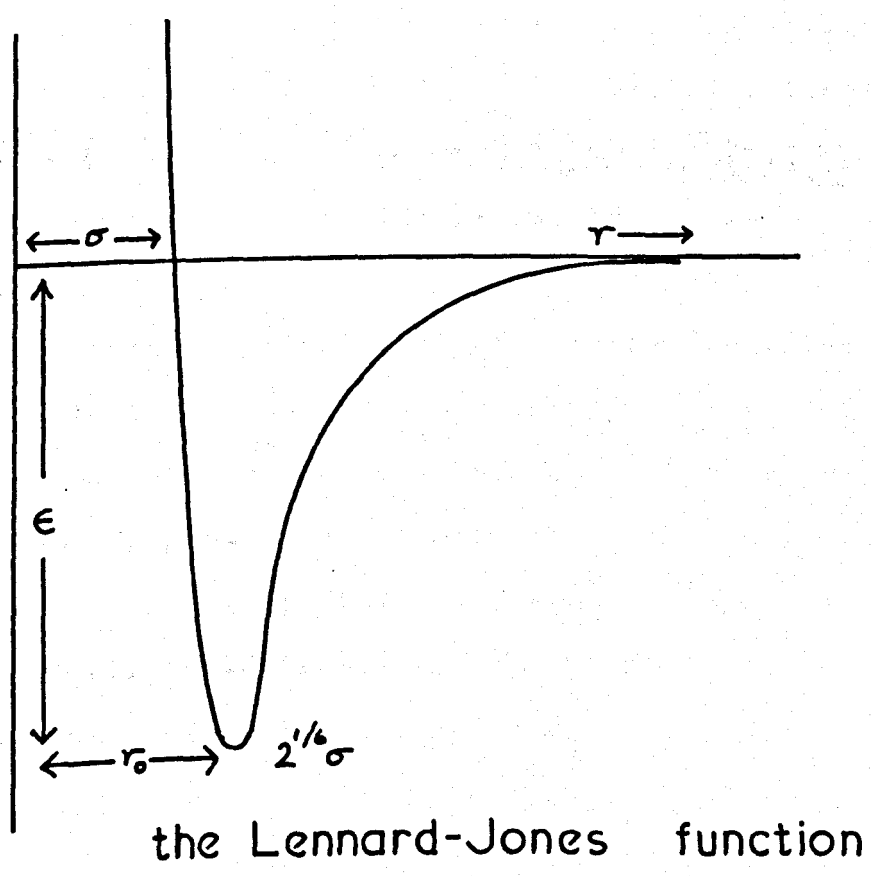
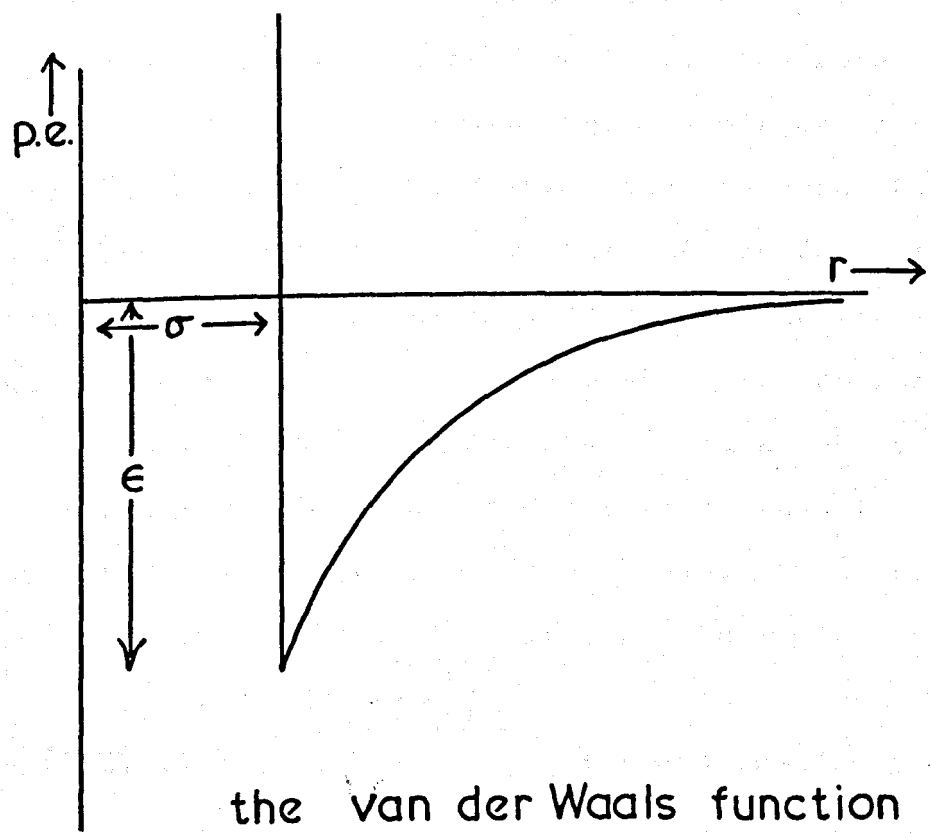
$$F(y) = (1 - y)^{-4}.$$

For any such equation the values of a and b for the pure components may be calculated by equating the first and second differentials of P w.r.t. V at constant T , with zero, for the critical values of the pure components. The resulting equations are then solved for a and b . In the case of the van der Waals equation $a = 9(RT_c V_c)/8$ and $b = V_c/3$ and in the case of the Guggenheim equation $a = 1.350833 (RT_c V_c)$ and $b = V_c/7.89898$. In order that the state equations may be used for mixtures, two further steps are required: firstly, a relationship between the interaction parameters a and b for like interactions, and those for unlike interactions; secondly, a relationship defining the relative importance of the like and unlike interactions in the overall interaction at a given composition. In order that such relationships may be derived it is necessary, first, to examine the nature of the equations of state more closely. The equations of state may, if we wish, be expressed in a "reduced" form, where pressure, volume, and temperature are replaced by the reduced terms, that is, the state functions divided by their corresponding

critical values. The use of these reduced functions produces a general equation, without variable parameters. For any equation of state involving two adjustable parameters, such a reduced equation may be obtained, and the only difference between such equations is in the relationship of the numerical values of the reduced terms. The result of this feature is that for any such equation, any substances having the same reduced pressures at a given reduced temperature will have the same reduced volume. Under such conditions, such substances are said to be in "corresponding states", or "conformal", and the above relationship is one statement of the "corresponding states law". If we consider mixtures of substances obeying these requirements, it should be possible to apply such two-parameter equations to the prediction of the properties of the mixtures, and this possibility is the source of the suggestion, at the beginning of this chapter, that an experimental two-parameter state equation might be derived for compounds and mixtures of interest from suitable reduced data.

In the method employed here, we have not produced a fitted state equation, but, as previously stated, have chosen two state equations of predetermined form, which avoids the fitting process, and the need for suitable data. This process is, essentially, a presetting of the form of the intermolecular potential function, which is then considered to apply to the conformal liquids, and their mixtures. The form of the van der Waals potential function is illustrated in diagram 5.1, and represents the behaviour of a pair of hard spheres of the volume already defined.

DIAGRAM 5.1



The extension of the corresponding states principle to mixtures requires some model for the behaviour of the mixture, and the two most commonly employed are the one-, and two-fluid models. In the former it is assumed that the mixture is a single fluid, conformal with the pure components. In the latter, it is assumed that the mixture comprises two fluids, each of which is conformal with the pure fluids, and in the same molar ratio. Since both of the foregoing require critical values for the unlike interactions in the liquid, an expression must also be derived to produce such critical values, from which may be calculated the a and b constants for the unlike interactions, which may then be used in the model chosen for the mixture. Hudson and McCoubrey (1960), employing a potential function of the form

$$\phi(r) = 4\epsilon \left[\left(\frac{\sigma}{r} \right)^{12} - \left(\frac{\sigma}{r} \right)^6 \right]$$

where σ is the collision diameter and epsilon the depth of the potential well (commonly known as the Lennard-Jones 12-6 potential), and the London theory of dispersion forces, arrived at an expression for the mixed critical temperature of

$$T_{12}^c = (T_1 T_2)^{1/2} \left[\frac{(\sigma_1^3 \sigma_2^3)}{(\sigma_1 + \sigma_2)^6} \right]^{1/2} \cdot \left[\frac{\chi(I_1 I_2)^{1/2}}{(I_1 + I_2)} \right]$$

which reduces to the Berthelot⁽³⁾ expression:

$$T_{12}^c = (T_1^c T_2^c)^{1/2}$$

if the ionisation potentials and collision diameters are equal. Both the Berthelot approximation and the more precise Hudson-McCoubrey equation have been used in this work. From the values of T_{12}^c and V_{12}^c may be calculated the mixed terms a_{12} and b_{12} . The second requirement, that of obtaining the a_x and b_x parameters for solutions at given compositions, is dependent on the choice of some model for the solution, e.g. one, two,

or three fluid, and as it had been shown (Leland, Rowlinson, and Sather 1968) that the van der Waals "one-fluid relations" and the equivalent two-fluid relations (van der Waals, (1900) - extension of his equation of state to mixtures) produced better agreement with experiment than the random mixing approximation employed by Prigogine (1957) and others, these were employed in this work.

$$\begin{array}{l}
 a_x = x_1^2 a_{11} + 2x_1 x_2 a_{12} + x_2^2 a_{22} \\
 b_x = x_1^2 b_{11} + 2x_1 x_2 b_{12} + x_2^2 b_{22} \\
 a_{12} = x_1 a_{11} + x_2 a_{12} \\
 a_{22} = x_2 a_{22} + x_1 a_{12} \\
 \text{similarly for } b_{12}, b_{22}
 \end{array}
 \left| \begin{array}{l}
 \text{one-fluid} \\
 \text{two-fluid}
 \end{array} \right.$$

The final requirement is for the calculation of the excess functions from the equations of state. In this work this was done by first calculating the "residual" functions, defined as

$$X^R = \int_{\infty}^V \left[\left(\frac{\partial X}{\partial V} \right)_T - \left(\frac{\partial X}{\partial V} \right)_{\text{perfect gas}} \right] dV$$

then combining these as below, to obtain the excess functions for one- and two fluid theories

$$X^E = X^R(T, a_x, b_x) - x_1 X^R(T, a_{11}, b_{11}) - x_2 X^R(T, a_{22}, b_{22}) \quad \text{one fluid}$$

$$\begin{aligned}
 X^E = & x_1 [X^R(T, a_{1x}, b_{1x}) - X^R(T, a_{11}, b_{11})] \\
 & + x_2 [X^R(T, a_{2x}, b_{2x}) - X^R(T, a_{22}, b_{22})] \quad \text{two fluid}
 \end{aligned}$$

the residual functions for the van der Waals equation were:

$$G^R = -RT \log_e (V_m - b) - a/V_m$$

$$H^R = -a/V_m$$

$$V^R = +V_m + \text{const.}$$

and for the Guggenheim equation:

$$G^R = -RT \log_e(V_m - b) + 3bRT/(V_m - b) + 3b^2RT/[2(V_m - b)^2] + b^3RT/[3(V_m - b)^3] - a/V_m$$

$$H^R = -a/V_m$$

$$V^R = V_m + \text{const.}$$

where the term V_m is obtained by solution of the state equation concerned, as P tends to zero, selecting the root corresponding to a rational isotherm, rather than one of the spurious, mathematically induced values. The required a and b terms for the liquid model and combining rules in question are used in this solution.

The methods of computing excess functions, given above, were written into computer programmes in Fortran 4, which are listed in Appendix one. These programmes were tested on the mixtures previously used by McGlashan (1969), and Marsh, McGlashan and Warr (1970), using their data, with the addition of ionisation potentials^(16,17) taken from the literature, with the results shown in Table 5.1. From this it may be seen, firstly, that the two fluid models generally gave better results than the one fluid models, especially for excess volumes, though less reliably for excess enthalpies; secondly, that the Guggenheim equation generally gave better results than the van der Waals; thirdly, that the Hudson-McCoubrey combining rules almost invariably produced much more accurate predictions of the values than the Lorentz-Berthelot⁽²¹⁾ versions. The next step was to use the methods so far developed to predict the excess functions for the systems

TABLE 5.1

Species	V _E (cm ³ mol ⁻¹)				G			
	1fl	2fl	1fl	2fl	1fl	2fl	1fl	2fl
Ar ⁺	-1.27	-0.94	-0.88	-0.88	-1.10	-0.83	-0.76	-0.76
Ar ⁺	-1.22	-0.94	-0.88	-0.88	-1.10	-0.83	-0.76	-0.76
O ₂ ⁺	-1.27	-0.94	-0.88	-0.88	-1.10	-0.83	-0.76	-0.76
O ₂ ⁺	-1.27	-0.94	-0.88	-0.88	-1.10	-0.83	-0.76	-0.76
Ar ⁺	-1.27	-0.94	-0.88	-0.88	-1.10	-0.83	-0.76	-0.76
Ar ⁺	-1.27	-0.94	-0.88	-0.88	-1.10	-0.83	-0.76	-0.76
CH ₄ ⁺	-1.27	-0.94	-0.88	-0.88	-1.10	-0.83	-0.76	-0.76
CH ₄ ⁺	-1.27	-0.94	-0.88	-0.88	-1.10	-0.83	-0.76	-0.76
N ₂ ⁺	-1.27	-0.94	-0.88	-0.88	-1.10	-0.83	-0.76	-0.76
N ₂ ⁺	-1.27	-0.94	-0.88	-0.88	-1.10	-0.83	-0.76	-0.76
CO ⁺	-1.27	-0.94	-0.88	-0.88	-1.10	-0.83	-0.76	-0.76
CO ⁺	-1.27	-0.94	-0.88	-0.88	-1.10	-0.83	-0.76	-0.76
CH ₄ ⁺	-1.27	-0.94	-0.88	-0.88	-1.10	-0.83	-0.76	-0.76
CH ₄ ⁺	-1.27	-0.94	-0.88	-0.88	-1.10	-0.83	-0.76	-0.76

Species	H _E				G			
	1fl	2fl	1fl	2fl	1fl	2fl	1fl	2fl
L-B	-64	-13	-55	-55	-28	-5	-5	-5
H-M	-49	-13	-55	-55	-28	-5	-5	-5
L-B	-28	-28	-55	-55	-28	-5	-5	-5
H-M	-49	-13	-55	-55	-28	-5	-5	-5
L-B	-19	+6	+44	+44	+54	+11	+12	+12
H-M	-13	+6	+44	+44	+54	+11	+12	+12
L-B	-28	+6	+44	+44	+54	+11	+12	+12
H-M	-49	+6	+44	+44	+54	+11	+12	+12
L-B	-21	+21	+50	+50	+37	+5	+5	+5
H-M	-29	+21	+50	+50	+37	+5	+5	+5
L-B	-21	+21	+50	+50	+37	+5	+5	+5
H-M	-29	+21	+50	+50	+37	+5	+5	+5

Species	G _E				G			
	1fl	2fl	1fl	2fl	1fl	2fl	1fl	2fl
L-B	+18	+38	+84	+84	+50	+5	+5	+5
H-M	+28	+38	+84	+84	+50	+5	+5	+5
L-B	+29	+38	+84	+84	+50	+5	+5	+5
H-M	+28	+38	+84	+84	+50	+5	+5	+5
L-B	+21	+19	+37	+37	+24	+16	+16	+16
H-M	+25	+19	+37	+37	+24	+16	+16	+16
L-B	+21	+19	+37	+37	+24	+16	+16	+16
H-M	+25	+19	+37	+37	+24	+16	+16	+16
L-B	+13	+20	+57	+57	+24	+2	+2	+2
H-M	+21	+20	+57	+57	+24	+2	+2	+2
L-B	+13	+20	+57	+57	+24	+2	+2	+2
H-M	+21	+20	+57	+57	+24	+2	+2	+2
L-B	+21	+23	+43	+43	+46	+9	+9	+9
H-M	+25	+23	+43	+43	+46	+9	+9	+9
L-B	+21	+23	+43	+43	+46	+9	+9	+9
H-M	+25	+23	+43	+43	+46	+9	+9	+9
L-B	+18	+38	+84	+84	+50	+5	+5	+5
H-M	+28	+38	+84	+84	+50	+5	+5	+5
L-B	+29	+38	+84	+84	+50	+5	+5	+5
H-M	+28	+38	+84	+84	+50	+5	+5	+5
L-B	+21	+19	+37	+37	+24	+16	+16	+16
H-M	+25	+19	+37	+37	+24	+16	+16	+16
L-B	+21	+19	+37	+37	+24	+16	+16	+16
H-M	+25	+19	+37	+37	+24	+16	+16	+16

being measured, and also any similar systems of interest. The results of these predictions are given in Table 5.2.

Once again, the Hudson- McCoubrey combining rules appear to produce the better predictions, when combined with the Guggenheim equation, although the most accurate predictions no longer seem to be produced consistently by the two-fluid models, and the excess volumes are, in one or two cases, better predicted by the van der Waals equation.

Clearly, in the transition from the simple mixtures, such as Ar/Kr, to the more complex molecules involved here, there has been some loss of predictive capability (see Table 5.4). What is more surprising, perhaps, is that this is just as marked in the cases where good agreement might have been expected, e.g. neopentane + tetramethylsilane, where the molar volumes and ionisation potentials are similar, and where the rotation of the molecules might be expected to lead to their behaving as approximately spherical entities, as in the cyclohexane mixtures, where the slight difference in reduced volumes might have been expected to lead to some inaccuracy.

A study of the reduced vapour pressure, volume, and temperature, plotted against reduced temperature, (diagrams 5.2-5.4) suggests that the behaviour is reasonably conformal, except in the previously mentioned case of volumes where the tetramethyls appear to form a separate group. This might, as suggested before, be expected to lead to some loss of accuracy in a corresponding-states method, where substances from the

TABLE 5.2

Chemical	VE (cm ³ mol ⁻¹)		H _F (J mol ⁻¹)		G (J mol ⁻¹)	
	1ft	2ft	1ft	2ft	1ft	2ft
C ₆ H ₁₂ ⁺	-1.19	-1.68	58	2	73	69
C ₆ H ₁₂ ⁺ 5?	-1.13	-1.66	74	6	84	72
C ₅ H ₁₂ ⁺	-0.94	-1.22	40	17	53	63
C ₄ H ₁₂ ⁺ 5?	-0.88	-1.20	56	21	64	66
C ₆ H ₁₂ ⁺	-1.10	-1.33	191	98	135	139
C ₅ H ₁₂ ⁺	-1.26	-1.74	142	67	153	143
C ₄ H ₁₂ ⁺	-1.19	-1.72	172	75	98	121
C ₃ H ₁₂ ⁺	-0.99	-1.24	100	80	121	126
C ₂ H ₁₂ ⁺	-0.91	-1.22	130	87	116	126
C ₆ H ₁₂ ⁺	-1.19	-1.68	71	1	73	69
C ₅ H ₁₂ ⁺	-1.25	+0.12	83	33	112	112
C ₄ H ₁₂ ⁺	-1.00	-0.64	57	1	80	80
C ₃ H ₁₂ ⁺	-0.90	+0.12	69	32	89	89
C ₂ H ₁₂ ⁺	-0.50	+0.16	310	168	320	320
C ₆ H ₁₂ ⁺	-0.14	-0.05	189	2	199	199
C ₅ H ₁₂ ⁺	-0.06	+0.05	212	62	213	213
C ₄ H ₁₂ ⁺	-0.10	-0.05	148	1	153	153
C ₃ H ₁₂ ⁺	-0.02	+0.05	171	61	168	168

exp (G_F)

VPW

exp (H_F)

VPW

exp (V_F)

VPW

DIAGRAM 5.2

○ benzene
□ carbon tetrachloride
△ cyclohexane
▽ neopentane
◇ tetramethylsilane

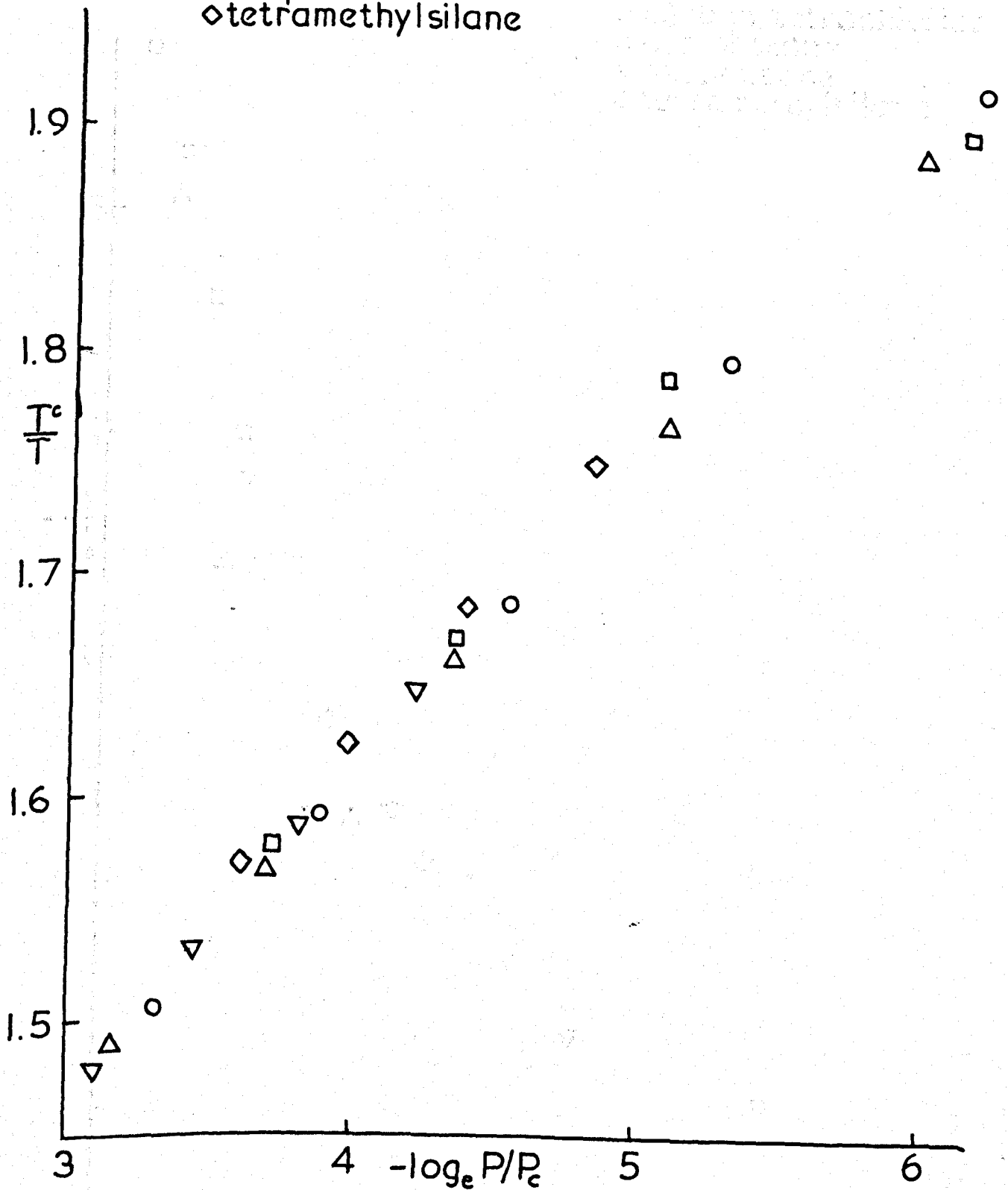


DIAGRAM 5.3

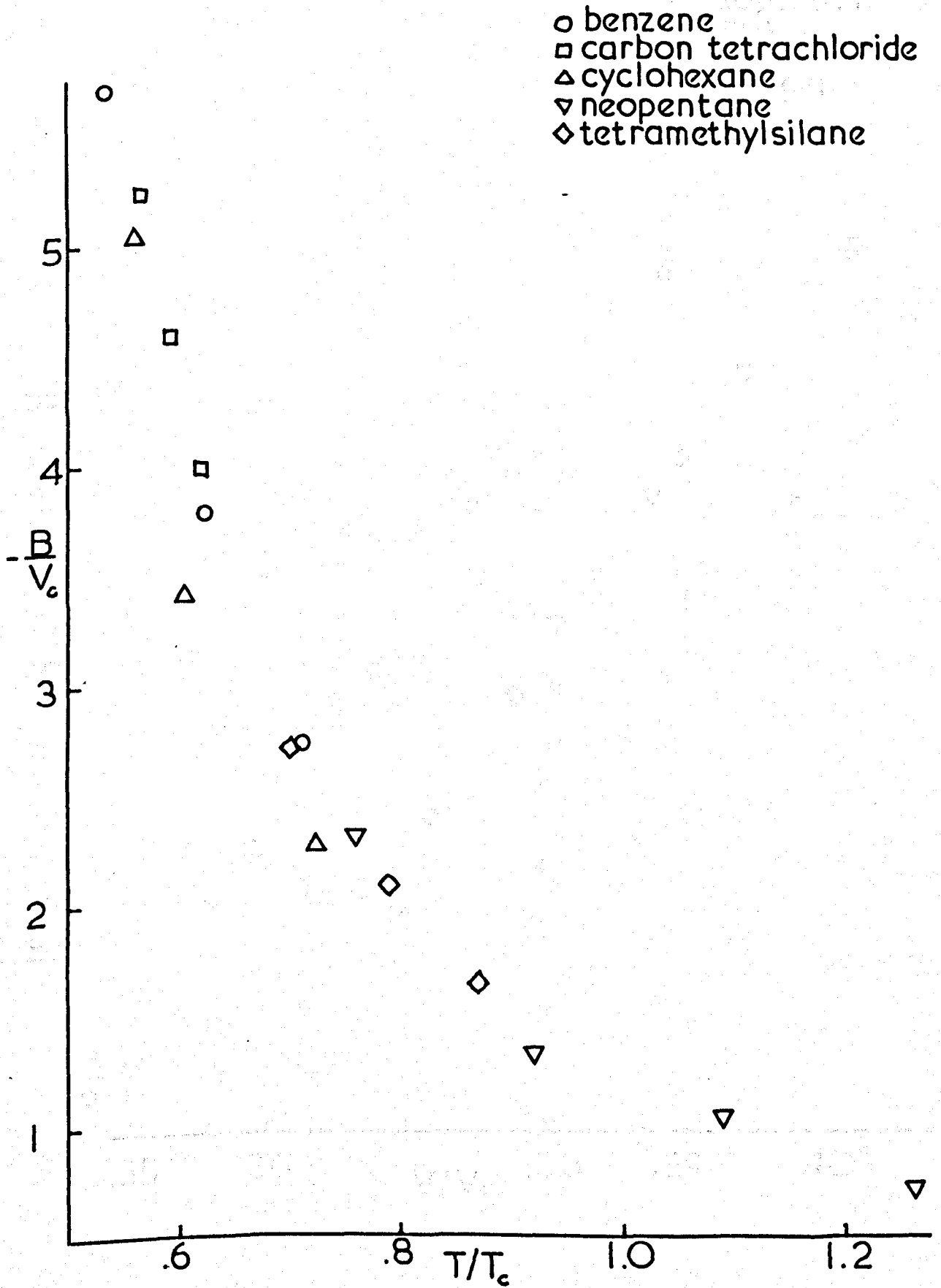
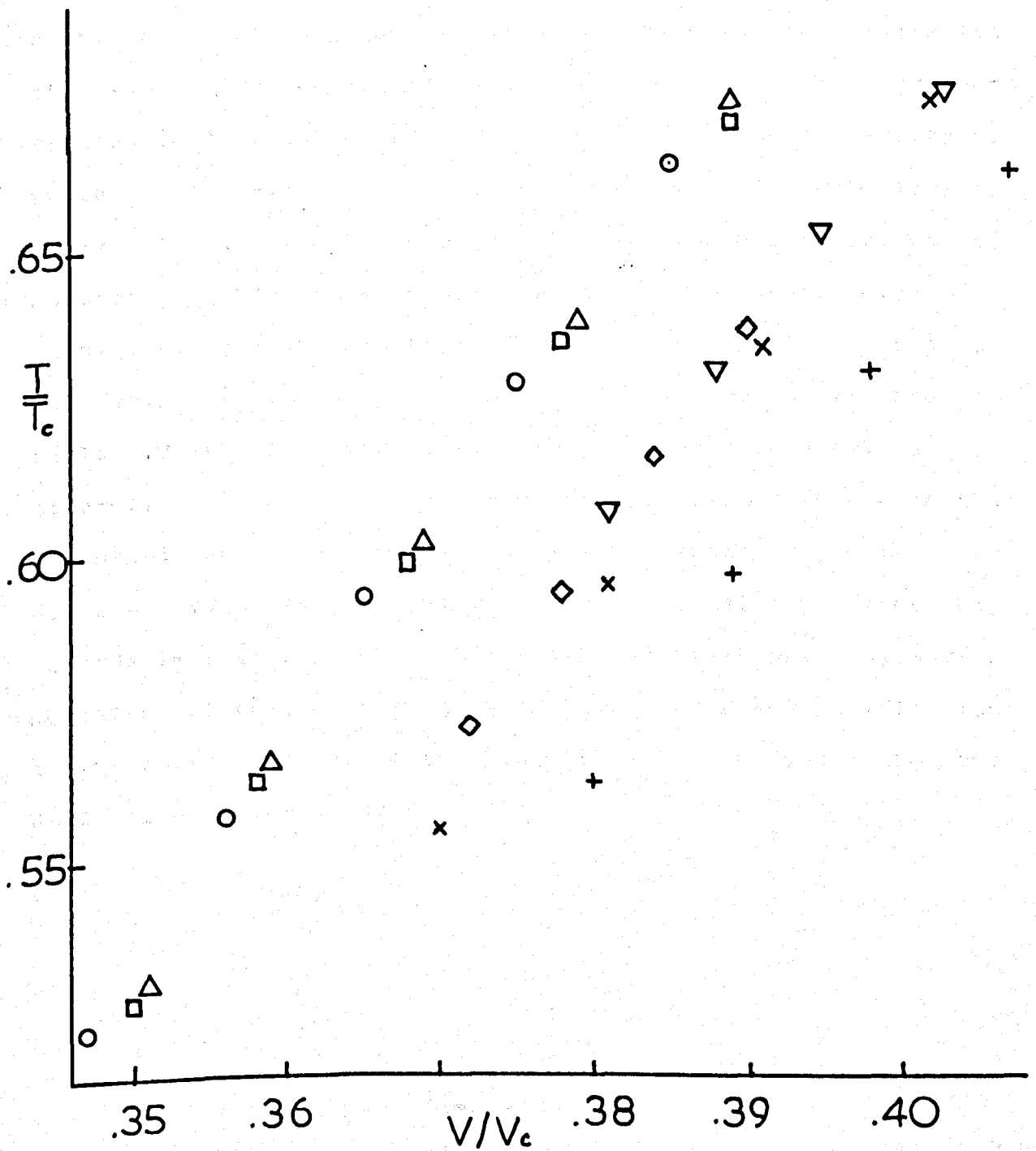


DIAGRAM 5.4

- benzene
- CCl₄
- △ cyclohexane
- ▽ neopentane
- ◇ t.m.s
- + argon
- x nitrogen



different volume groups were considered, but we see that, in fact, the agreement here is no worse than that for intra-group mixtures. This perhaps suggests that the difference observed is not of an order to generate major inaccuracies, but that some other factor is clearly doing so. Rowlinson (1969, page 244), concludes that the Lorentz-Berthelot combining rules produce values for intermolecular potential energy and collision diameter with an accuracy of about 2 per cent, but points out that this causes major inaccuracies in prediction of excess functions. A numerical test of such 2 per cent errors, in the system Ar/Kr, for the van der Waals equation, showed the extreme sensitivity of the excess functions to these values, with a maximum change in predicted values occurring when both errors were of the same sign and magnitude, this change being of the order of 200 per cent of the original value. The results of these tests are shown in table 5.3, where it can be seen that the predicted values are generally closer to the experimental values when both the potential and distance terms are somewhat reduced. The Hudson-McCoubrey combining rules obviously go some way towards improving matters, but are by no means perfect, and a possible direction for improvement would be the modification of the Lorentz rule, which is taken as accurate in the derivation of the rules.

TABLE 5.3

variation of predicted excess functions
with ϵ_{12} and σ_{12}

van der Waals' equation
system Ar + Kr at 116K $x = 0.5$

	ϵ_{12}	L-B	$\epsilon_{12}-2\%$	ϵ_{12} L-B	$\epsilon_{12}+2\%$	$\epsilon_{12}-2\%$	$\epsilon_{12}-2\%$	exp	
	σ_{12}	L-B	σ_{12} L-B	$\sigma_{12}-2\%$	$\sigma_{12}-2\%$	$\sigma_{12}+2\%$	$\sigma_{12}-2\%$		
	V_{cm}^E	mol^{-1}	-1.3	-1.1	-2.4	-2.5	+0.1	-2.2	-0.5
one fluid	H_J^E	mol^{-1}	-64	-8	-66	-121	-4	-13	
	G_J^E	mol^{-1}	+18	+55	+45	+9	+28	+80	+84
	V_{cm}^E	mol^{-1}	-0.9	-0.7	-2.0	-2.2	+0.4	-1.8	-0.5
two fluid	H_J^E	mol^{-1}	-28	+29	-29	-85	+31	+27	
	G_J^E	mol^{-1}	+29	+64	+56	+20	+38	+90	+84

TABLE 5.4

[predicted/experimental] x 100 averaged over rows of
Tables 5.1 and 5.2

5.1	5.2	5.1	5.2	5.1	5.2		
55	18	11	-3	23	22	LB	1fl
61	53	24	17	36	35	HM	van der Waals
38	11	12	25	23	19	LB	2fl
44	40	25	24	34	32	HM	
57	43	39	19	49	46	LB	1fl
68	85	63	53	68	66	HM	Guggenheim
41	33	37	27	43	38	LB	2fl
51	74	62	62	63	58	HM	
V^E		H^E		G^E			

The program is designed to calculate the standard deviation of a set of data.

THE COMPUTER PROGRAMS

where the standard deviation is calculated with a series of coefficients increasing from 1 to 7, which is the number of points, or 7, whichever is the smaller. For each specified the standard deviation is calculated as the overall standard deviation. The standard deviation is calculated with allowance for the dispersion caused by errors of frequency the number of coefficients increasing etc. This needs the calculation of the standard deviation against standard deviation as that of "less fit". The standard deviation is carried out by a series of steps. The set of coefficients is calculated from the data available in the program, and the resulting matrix is formed. The matrix is then partitioned by the main lines left-hand side, to give the coefficient vector. The first coefficient "vector" is a given degree routine, and to produce the ability to proceed to the next step.

The Redlich-Kister Curve-Fitting Programmes

This programme fits excess function/composition data to a polynomial equation of the form:

$$H^E = x(1-x)(a + b(1-2x) + c(1-2x)^2 + \dots)$$

where the excess function is fitted to equations with numbers of coefficients increasing from 1 (a), to n-1, where n is the number of points, or 7, whichever is the smaller. For each equation the deviations of each point are calculated, as is the overall standard deviation. The standard deviation is calculated with allowance for the decreasing number of degrees of freedom as the number of coefficients increases, and this permits the selection of the equation which gives the smallest standard deviation as that of "best fit". The fitting is carried out by a matrix method. The set of equations resulting from the individual H^E, x values is normalised, and the resulting square matrix inverted. The inverse is then postmultiplied by the normalised left-hand sides, to yield the coefficient vector. The final subroutine "Tester" is a graph drawing routine, used to produce the fitting diagrams shown in this thesis.

C REDLICH-KISTER CURVE FIT USING F.A.H. MATRIX SET SIMFON

DIMENSION W(30,17),W2(7,60)

MAXN=30

READ(7,30)N

IF(MAXN.LT.N) GO TO 1

CALL MAIN(W(1,1),W(1,8),W(1,9),W(1,10),W2(1,1),W2(1,31),W2(1,38),
1W2(1,39),W2(1,40),W2(1,47),W2(1,54),N)

GO TO 2

1 WRITE(2,40)

30 FORMAT(I2)

40 FORMAT(30HT00 MANY POINTS FOR DIMENSIONS)

2 STOP

END

```

SUBROUTINE MAIN(F,X,H,FUNC,TRNFNC,SQMT,PRODMT,COEF,C,R,D,N)
  DIMENSION F(N,7),X(N),H(N),FUNC(N,7),TRNFNC(7,N),SQMT(7,7),
  IPRODMT(7,1),COEF(7,1),C(7,7),R(7,7),D(7,7)
  INTEGER P
  DO 40 J=1,N
40  READ(7,50)H(J),X(J)
50  FORMAT(F8.3,F6.4)
  IF(N.GE.8)P=7
  IF(N.LE.7)P=N-1
  DO 60 J=1,P
  DO 60 I=1,N
  F(I,J)=X(I)*(1.0-X(I))
  IF(J.NE.1) F(I,J)=F(I,J)*((1.0-2.0*X(I))**(J-1))
60  CONTINUE
  WRITE(2,90)
  DO 85 K=1,P
  WRITE(2,120)
  CALL TRLEMC(F,FUNC,H,N,K,TRNFNC,PRODMT,SQMT,COEF,C,R)
  DO 80 J=1,K
  D(J,K)=COEF(J,1)
80  WRITE(2,100)D(J,K)
85  CONTINUE
  CALL FITEST(D,H,X,N)
  CALL TESTER(N,K,X,H,D)
90  FORMAT(1H1,18HCOEFFICIENT MATRIX)
100  FORMAT(1PF20.8)
120  FORMAT(/)
  RETURN
  END

```

```
1 SUBROUTINE TRFLM (F, FUNC, H, N, K, TRNFNC, PRODMT, SOMT, COFF, C, P)  
1 DIMENSION FCN(7), H(N), FUNC(N, K), TRNFNC(K, N), PRODMT(K, 1), SOMT(K, K),  
1 COFF(K, 1), CK(K, K), RK(K, K)  
DO 10 J=1, K  
DO 10 I=1, N  
FUNC(I, J)=F(I, J)  
10 CONTINUE  
CALL SIMON(FUNC, N, K, H, TRNFNC, PRODMT, SOMT, COFF, C, P)  
RETURN  
END
```

```

SUBROUTINE FITFST(C,H,X,N)
DIMENSION H(N),X(N),C(7,7)
DO 30 K=1,7
WRITE(2,100)
WRITE(2,200)K
SUMSQ=0.0
WRITE(2,300)
DO 20 I=1,N
HT=0.0
DO 10 J=1,K
U=C(J,K)*X(I)*(1.0-X(I))
IF(J.NE.1)U=U*(1.0-2.0*X(I))**(J-1)
10 HT=HT+U
DIFF=HT-H(I)
DIFFSQ=DIFF**2
WRITE(2,400)X(I),H(I),HT,DIFF
20 SUMSQ=SUMSQ+DIFFSQ
P=N-K
STDDEV=SQRT(SUMSQ/P)
WRITE(2,500)
30 WRITE(2,600)STDDEV
100 FORMAT(1H1,18H NO.OF COEFFS=)
200 FORMAT(20X,13//)
300 FORMAT(5X,55H MOLE FRACTION EXPT.EX.FUNC. CALC.EX.FUNC. DIFFRENC
1E, //)
400 FORMAT(9X,F6.4,8X,F7.3,8X,F7.3,8X,F8.4//)
500 FORMAT(/10X,10H STD.DEV.=)
600 FORMAT(22X,F6.3)
RETURN
END

```



```

SUBROUTINE TESTER(N,K,X,H,C)
  DIMENSION H(N),X(N),C(N,7),HCURVE(101),XCURVE(101),TITLE(2)
  DATA TITLE/8H      COEFF,8HFIENCIES/
  DO 50 L=1,K
  DO 40 M=1,101
  I=M-1
  IF (I.EQ.0) GO TO 10
  P=FLOAT(I)/100.0
  GO TO 20
10 P=FLOAT(I)
20 HT=0.0
  DO 30 J=1,L
  U=C(J,L)*P*(1.0-P)
  IF(J.NE.1)U=U*(1.0-2.0*P)**(J-1)
30 HT=HT+U
  HCURVE(M)=HT
40 XCURVE(M)=P
  CALL GSTART(0,0,11.)
  CALL GDARFA(1.0,1.0,7.0,8.0)
  XRANGE=1.0
  SCALEX=XRANGE/7.0
  CALL GXSCAL(SCALEX)
  CALL EXTICK(0.2,7.0/5.0)
  CALL GSCALY(HCURVE,101)
  CALL GAXES
  CALL GLINE(XCURVE,HCURVE,101,-1)
  CALL GDATA(X,H,N,1)
  CALL GINTL(L,3.0,10.0)
  CALL GTEXT(TITLE,2)
  CALL GCLOSE
50 CONTINUE
  RETURN
  END

```

Parabolic Fitting Programme

This programme was generally used in the fitting of near-linear experimental data, such as density/temperature results, or log (vapour pressure)/temperature. The fitting was to an equation of the form: $y=a+bx+cx^2$, and the matrix routines employed were the same as those of the previous programme. The programme was also used, in modified form, to fit the virial portions of dew-point measurements, if this was necessary, as in the case of benzene/n-hexane mixtures.

```
C PARABOLIC FIT USING F.A.H. MATRIX SET SIMFON
  MAXPTS=25
  READ(7,10)NOPTS
10  FORMAT(I3)
  IF(NOPTS.GT.MAXPTS)GO TO 20
  CALL MATSOL (W(1,1),W(1,4),W(1,5),Z(1,1),Z(1,26),Z(1,27),Z(1,30),
  1Z(1,31),Z(1,34),NOPTS)
  GO TO 30
20  WRITE(2,40)
30  STOP
40  FORMAT(55H NO.OF PTS.TOO BIG FOR CURRENT DIMENSIONS.EXEC.HALTED .)
  END
```

```

SUBROUTINE MATSOL (FUNCMT,RHSVAR,VARLHS,TRNFNC,PRODMT,SQMT,COEF,C,
IR,NOPTS)
DIMENSION FUNCMT(NOPTS,3),RHSVAR(NOPTS),VARLHS(NOPTS),
1TRNFNC(3,NOPTS),PRODMT(3,1),SQMT(3,3),COEF(3,1),C(3,3),B(3,3)
DO 10 I=1,NOPTS
10 READ(7,20)VARLHS(I),RHSVAR(I)
20 FORMAT(F13.6,5X,F13.6)
WRITE(2,26)
26 FORMAT(1H1)
DO 30 J=1,NOPTS
FUNCMT(J,1)=1.0
FUNCMT(J,2)=RHSVAR(J)
FUNCMT(J,3)=RHSVAR(J)**2
30 WRITE(2,40)VARLHS(J),FUNCMT(J,1),FUNCMT(J,2),FUNCMT(J,3)
40 FORMAT(      E13.6,5X,E13.6,2X,E13.6,2X,E13.6)
CALL SIMEQN(FUNCMT,NOPTS,3,VARLHS,TRNFNC,PRODMT,SQMT,COEF,C,B)
WRITE(2,80)
WRITE(2,70)(COEF(I,1),I=1,3)
70 FORMAT(10X,F13.6)
80 FORMAT(///7X,19H COEFFICIENT VECTOR//)
CALL DEVC(COEF,VARLHS,RHSVAR,NOPTS)
CALL GRAPH(RHSVAR,VARLHS,NOPTS,COEF)
RETURN
END

```

```

SUBROUTINE DEV(WK1,VARLNW,RHSVAR,NOPTS)
  DIMENSION WK1(NOPTS),VARLNW(NOPTS),RHSVAR(NOPTS)
  WRITE(2,10)
  SUMSQ=0.0
  DO 5 I=1,NOPTS
    CALVAL=WK1(1)+WK1(2)*RHSVAR(I)+WK1(3)*RHSVAR(I)**2
    DIFF=CALVAL-VARLNW(I)
    DIFFSQ=DIFF**2
    SUMSQ=SUMSQ+DIFFSQ
    WRITE(2,20)VARLNW(I),CALVAL,DIFF,DIFFSQ
  5 CONTINUE
  STDDDEV=SQRT(SUMSQ/FLOAT(NOPTS-2))
  STDERR=SQRT(SUMSQ/FLOAT(NOPTS*(NOPTS-2)))
  WRITE(2,30)STDDDEV
  WRITE(2,40)STDERR
  10 FORMAT(///3X,6HVARLNW,11X,6HCALVAL,11X,4HDIFF,11X,6HDIFFSQ //)
  20 FORMAT(E13.6,5X,E13.6,2X,E13.6,2X,E13.6 //)
  30 FORMAT(/10X,8HSTDDDEV=,E13.6)
  40 FORMAT( / 10X,8HSTD.ERR=,E13.6)
  RETURN
  END

```

D

```
SUBROUTINE GRAPH (X,Y,N,CV)
DIMENSION X(N),Y(N),CV(N),XEQ(100),YEQ(100)
SMTVAL=X(1)
GTSVAL=X(1)
DO 10 I=1,N
IF(X(I).GT.GTSVAL)GTSVAL=X(I)
IF(X(I).LT.SMTVAL)SMTVAL=X(I)
10 CONTINUE
RANGE=GTSVAL-SMTVAL
SRANGE=SMTVAL-RANGE/4.0
HRANGE=GTSVAL+RANGE/4.0
VALINC=(HRANGE-SRANGE)/100.0
XEQ(1)=SRANGE
YEQ(1)=CV(1)+CV(2)*SRANGE+C(3)*SRANGE**2
DO 20 J=2,100
XEQ(J)=XEQ(J-1)+VALINC
YEQ(J)=CV(1)+CV(2)*XEQ(J)+C(3)*XEQ(J)**2
20 CONTINUE
CALL GSTART(0,0,11.0)
CALL GDARFA(1.0,1.0,7.0,8.0)
CALL GSCALS(XEQ,YEQ,100)
CALL GAXES
CALL GLINE(XEQ,YEQ,100,-1)
CALL GDATA(X,Y,N,1)
CALL GCLOSE
RETURN
END
```

C P

The Matrix Set SIMEQN

This set of routines was written as a general, non-weighted, high precision solution for sets of simultaneous equations. It was the first programme set of this type which the Author had written, and the method employed, while quite accurate, is rather inefficient. This is no real problem for the programme in which they were normally employed, as the matrices involved were generally small, but where large matrices were involved, as in the bubble-point, dew-point programme, the faster routine SIMEQ4 was used.

```
SUBROUTINE SIMEGN (FUNC,N,K,H,TRNFNC,PRODMT,SOMT,COEF,C,B)
  DIMENSION FUNC(N,K),TRNFNC(K,N),PRODMT(K,1),SOMT(K,K),COEF(K,1),
  1 C(K,K),R(K,K),H(N)
  CALL TRANSPC(FUNC,TRNFNC,N,K)
  CALL MATMPY(TRNFNC,H,PRODMT,K,N,1)
  CALL MATMPY(TRNFNC,FUNC,SOMT,K,N,K)
  IF(K.EQ.1) GO TO 10
  CALL INVERT(SOMT,R,K,(K-1),C)
  CALL MATMPY(C,PRODMT,COEF,K,K,1)
  GO TO 20
10 COEF(1,1)=PRODMT(1,1) /SOMT(1,1)
20 RETURN
  END
```



```
SUBROUTINE TRNSPS (AMATRX, TRNMAT, NOROWS, NOCOLS)
DIMENSION AMATRX (NOROWS, NOCOLS), TRNMAT(NOCOLS, NOROWS)
DO 10 N=1, NOROWS
DO 10 M=1, NOCOLS
TRNMAT(M, N)=AMATRX(N, M)
10 CONTINUE
RETURN
END
```

```
SUBROUTINE MATMPY (A,B,C,I,J,K)
DOUBLE PRECISION DOUB
DIMENSION A(I,J),B(J,K),C(I,K)
DO 30 N=1,I
DO 30 M=1,K
DOUB=0.0
DO 20 L=1,J
DOUB=A(N,L)*B(L,M)+DOUB
20 CONTINUE
C(N,M)=DOUB
30 CONTINUE
RETURN
END
```

```

SUBROUTINE INVERT (A,B,N,N1,COFACT)
DIMENSION A(N,N),B(N1,N1),COFACT(N,N)
DO 40 L=1,N
  DO 30 K=1,N
    DO 20 J=1,N
      NO=J
      IF(J.GE.L)NO=J+1
      IF(NO.GT.N)GO TO 20
      DO 10 I=1,N
        M=I
        IF(I.GE.K)M=I+1
        IF(M.GT.N)GO TO 10
        B(I,J)=A(M,NO)
10      CONTINUE
20    CONTINUE
      CALL DETERM (B,(N-1),COFAC)
      COFACT(K,L)=COFAC*FLOAT((-1)**(K+L))
30    CONTINUE
40  CONTINUE
  DO 44 I=1,N
    DO 42 J=I,N
      HOLD=COFACT(J,I)
      COFACT(J,I)=COFACT(I,J)
      COFACT(I,J)=HOLD
42  CONTINUE
44  CONTINUE
  CALL DETERM (A,N,DET)
  DO 60 I=1,N
    DO 50 J=1,N
      COFACT(J,I)=COFACT(J,I)/DET
50  CONTINUE
60  CONTINUE
  RETURN
  ENN

```

```

SUBROUTINE DETERM(A,N,DET)
DIMENSION A(N,N)
DOUBLE PRECISION DETA
DETA=1.0
ISIGN=1
IF(N.EQ.1) DET=A(1,1)
IF(N.EQ.1) GO TO 60
IF(N.EQ.2) GO TO 50
DO 40 L=1,N
X=10**(-20)
DO 3 I=L,N
DO 1 J=L,N
IF((ABS(A(J,I))).GT.X)GO TO 5
1 CONTINUE
3 CONTINUE
WRITE(2,4)
4 FORMAT(32HNO ELEMENTS GREATER THAN 10**-20)
STOP
5 IF(I.EQ.L)GO TO 7
DO 6 K=L,N
HOLD=A(K,L)
A(K,L)=A(K,I)
A(K,I)=HOLD
6 CONTINUE
ISIGN=-ISIGN
7 IF(J.EQ.L)GO TO 9
DO 8 K=L,N
HOLD=A(L,K)
A(L,K)=A(J,K)
A(J,K)=HOLD
8 CONTINUE
ISIGN=-ISIGN
9 J=L+1
DO 10 M=J,N
A(M,L)=A(M,L)/A(L,L)
10 CONTINUE
DETA=DETA/A(L,L)
ICOUNT=L+1
DO 30 K=ICOUNT,N
DO 20 I=ICOUNT,N
A(I,K)=A(I,K)-(A(I,L)*A(L,K))
20 CONTINUE
30 CONTINUE
IF(L.EQ.N-2)GO TO 50
40 CONTINUE
50 D=A(N-1,N-1)*A(N,N)-A(N,N-1)*A(N-1,N)
DET=D*FLOAT(ISIGN)/DETA
60 RETURN
END

```

The Pressure-Volume Calculation And Fitting Programmes

The first of these programmes used thermostat temperature and room temperature to convert measured mercury column heights and reference mark positions into pressures and volumes, in Pa and cm^3 , corrected for mercury density and cathetometer column expansivity. The results were both printed and output to a disc file, where they could be accessed by the succeeding programmes. In some cases the data for both one- and two- phase regions of the dew-point sector, as well as the bubble-point sector, could be fitted by the straight line fitting programme, in others the gas region of the dew-point sector was fitted by the third programme, that derived from the previously described parabolic fitting programme, which solved the two equations produced, the one linear, the other parabolic, simultaneously, for the point of intersection, the dew-point.

```

PRESSURE AND VOLUME CALCULATION FOR MARK 3 D.P.R.P. APPARATUS
  DIMENSION P(30),V(30)
  READ(7,15) NUMRUN
  15 FORMAT (I3)
  READ(7,20) RMTEMP,TSTEMP
  20 FORMAT(F4.1,1X,F7.3)
  READ(7,30) NOPTS
  30 FORMAT(I2)
  A=1.723E-5
  PI=3.1415926
  HGDENS=14.2978-.267295E-2*TSTEMP+.372294E-6*TSTEMP**2
  GACCN=981.303
  WRITE(2,110)NUMRUN
  110 FORMAT(1H1,12H RUN NUMBER ,I3)
  WRITE(2,120) RMTEMP,TSTEMP
  120 FORMAT(//12H ROOM TEMP =,F4.1,5X,18H THERMOSTAT TEMP =,F7.3/)
  DO 150 N=1,NOPTS
  READ(7,130)H1,H2,HREF,H3,H4
  130 FORMAT(5(1X,F6.3))
  P(N)=(H2-H1+H4-H3)*(1.0-A*(RMTEMP-20.0))*HGDENS*GACCN/10.0
  V(N)=(HREF-H1)*PI+4.594
  WRITE(2,140)H1,H2,HREF,H3,H4
  140 FORMAT( 5X,5(1X,F6.3))
  150 CONTINUE
  WRITE(2,800)
  WRITE(2,850)
  WRITE( 2,900)(P(I),V(I),I=1,NOPTS)
  WRITE(50,900)(P(I),V(I),I=1,NOPTS)
  ENDFILE 50
  800 FORMAT(///20H PRESSURE      VOLUME/)
  850 FORMAT(23H      PA          CM**3 ///)
  900 FORMAT(2X,F8.1,4X,F7.3)
  STOP
  END

```

C STRAIGHT LINE FIT

```

    DIMENSION X(25),Y(25)
    DO 100 N=1,3
    READ(7,10)NPTS
10  FORMAT(I3)
    IF(NPTS.GT.25)GO TO 60
    SUMX=0.0
    SUMY=0.0
    SUMXY=0.0
    SUMXSQ=0.0
    SUMYSQ=0.0
    SUMDEV=0.0
    SUMDSQ=0.0
    DO 22 M=1,NPTS
    READ(50,900)Y(M),X(M)
900  FORMAT(2X,F8.1,4X,F7.3)
    SUMX=X(M)+SUMX
    SUMXSQ=X(M)*X(M)+SUMXSQ
    SUMY=Y(M)+SUMY
    SUMYSQ=Y(M)*Y(M)+SUMYSQ
    SUMXY=Y(M)*X(M)+SUMXY
22  CONTINUE
    DET=FLOAT(NPTS)*SUMXSQ-SUMX**2
    GRAD=FLOAT(NPTS)*SUMXY/DET-SUMX*SUMY/DET
    CONST=SUMXSQ*SUMY/DET-SUMX*SUMXY/DET
    R=(SUMYSQ-2.0*GRAD*SUMXY-2.0*CONST*SUMY+2.0*GRAD*CONST*SUMX
1   +GRAD**2*SUMXSQ+FLOAT(NPTS)*CONST**2)/FLOAT(NPTS-2)
    S=FLOAT(NPTS)*R/(FLOAT(NPTS)*SUMXSQ-SUMX**2)
    T=SUMXSQ*R/(FLOAT(NPTS)*SUMXSQ-SUMX**2)
    WRITE(2,25)GRAD,CONST
25  FORMAT (1H1,15H EQUATION IS Y=,G13.6,2H*X,2X,1H+,G13.6,///)
    WRITE(2,30)
30  FORMAT(9X,1HX,17X,1HY,15X,4HYNEW,15X,3HDEV,/)
    DO 40 M=1,NPTS
    YNEW=X(M)*GRAD+CONST
    DEV=Y(M)-YNEW
    SUMDEV=ABS(DEV)+SUMDEV
    SUMDSQ=DEV**2+SUMDSQ
    WRITE(2,35)X(M),Y(M),YNEW,DEV
35  FORMAT(4(E13.6,3X),/)
40  CONTINUE
    DVMFAN=SUMDEV/FLOAT(NPTS)
    DVSTD=SQRT(SUMDSQ/FLOAT(NPTS-1))
    ERRSTG=SQRT(S)
    ERRSTC=SQRT(T)
    WRITE(2,50)DVMFAN
    WRITE(2,55)DVSTD
    WRITE(2,57)ERRSTG
    WRITE(2,58)ERRSTC
50  FORMAT(/16H MEAN DEVIATION=,G13.6)
55  FORMAT(/16H STD. DEVIATION=,G13.6)
57  FORMAT(/25H STD. ERROR OF GRADIENT =,G13.6)
58  FORMAT(/25H STD. ERROR OF CONSTANT =,G13.6)
100 CONTINUE
    WRITE(60,80)GRAD,CONST
    REWIND 50
    REWIND 60
    STOP
60  WRITE(2,70)
70  FORMAT(30HTOO MANY POINTS FOR DIMENSIONS )
80  FORMAT(2E20.8)
    STOP
    END

```

```
C VIRIAL SECTION FIT USING F.A.H. MATRIX SET SIMEQN
  DIMENSION P(20),V(20),FUNC(20,3),TRNFNC(3,20),PRODMT(3,1),
  1  SMT(3,3),COEF(3,1),C(3,3),R(3,3)
  READ(7,10)NOLINE
  10  FORMAT(I3)
  READ(50,20)(A,A,N=1,NOLINE)
  20  FORMAT(2X,F8.1,4X,F7.3)
  READ(7,30)NOCURV
  30  FORMAT(I3)
  CALL SOLVE(P,V,FUNC,TRNFNC,PRODMT,SMT,COEF,C,R,NOCURV)
  STOP
  END
```



```

SUBROUTINE SOLVE(P, V, FUNC, TRNFNC, PRODMT, SQMT, COEF, C, B, NOCURV)
DIMENSION P(NOCURV), V(NOCURV), FUNC(NOCURV, 3), TRNFNC(3, NOCURV),
1 PRODMT(3, 1), SQMT(3, 3), COEF(3, 1), C(3, 3), B(3, 3)
READ(50, 40) (P(N), V(N), N=1, NOCURV)
40 FORMAT(2X, F8.1, 4X, F7.3)
DO 60 M=1, 3
    DO 50 N=1, NOCURV
        FUNC(N, M)=V(N)**(M-1)
50    CONTINUE
60 CONTINUE
WRITE(2, 70)
70 FORMAT(1H1)
WRITE(2, 80) (P(N), V(N), N=1, NOCURV)
80 FORMAT(10X, F8.1, 4X, F6.2)
CALL SIMEQN(FUNC, NOCURV, 3, P, TRNFNC, PRODMT, SQMT, COEF, C, B)
WRITE(2, 90)
90 FORMAT(///)
WRITE(2, 100) (N, COEF(N, 1), N=1, 3)
100 FORMAT(10X, 11HCOEFFICIENT, I2, 2H =, E20.8/)
WRITE(2, 90)
CALL DEVIAT(NOCURV, COEF, 3, P, V)
RETURN
END

```

```

SUBROUTINE DEVIAT(NPTS, COEF, NCOFS, P, V)
DIMENSION COEF(NCOFS, 1), P(NPTS), V(NPTS)
WRITE(2, 10)
10 FORMAT(13X, 1HP, 18X, 1HV, 17X, 4HPFIT, 15X, 3HDEV, //)
SDEVSO=0.0
DO 30 N=1, NPTS
PFIT=COEF(1, 1)+COEF(2, 1)*V(N)+COEF(3, 1)*V(N)**2
SDEVSO= (PFIT-P(N))**2+SDEVSO
A=P(N)-PFIT
WRITE(2, 20)(P(N), V(N), PFIT, A)
20 FORMAT(/4(5X, G14.7))
30 CONTINUE
STDDEV=SQRT(SDEVSO/(FLOAT(NPTS-2)))
WRITE(2, 40)STDDEV
40 FORMAT(/// 5X, 16HSTD. DEVIATION =, G14.7)
A=COEF(1, 1)
B=COEF(2, 1)
C=COEF(3, 1)
READ (60, 80)GRAD, CONST
G=GRAD
CL=CONST
V1=(G-B-SQRT((B-G)**2-4.0*C*(A-CL)))/(2.0*C)
V2=(G-B+SQRT((B-G)**2-4.0*C*(A-CL)))/(2.0*C)
IF(V1.GT.15.0)DV=V2
IF(V2.GT.15.0)DV=V1
PR=G*DV+CL
WRITE(2, 50) PR
50 FORMAT(/// 5X, 14HDEW PRESSURE =, G14.7)
80 FORMAT(2E20.8)
RETURN
END

```

The State Equation Programmes

These programmes were written to calculate thermodynamic excess functions according to various state equations, one- and two-fluid liquid models and various combining rules.

C THIS PROGRAM EVALUATES EXCESS FUNCTIONS, FROM VAN DER WAAL'S EQUATION
C EMPLOYING BOTH ONE-, AND TWO-FLUID LIQUID MODELS
C
C

C READ CRITICAL TEMPERATURES AND VOLUMES
READ(7,10) TCA, VCA, TCB, VCB

C READ EVALUATION TEMPERATURE

C READ(7,20) T

C
10 FORMAT(4(F6.0))
20 FORMAT(F6.0)
R=82.053

C
C CALCULATE COMMON FACTORS A11, B11, A22, B22, A12, B12; FOR BOTH MODELS

A11=TCA*VCA*R*1.125
A22=TCB*VCB*R*1.125
B11=VCA/3.0
B22=VCB/3.0
X=1.125*R*SQRT(TCA*TCB)
Y=(((VCA**(1.0/3.0))+(VCB**(1.0/3.0)))/2.0)**3
A12=X*Y
B12=Y/3.0
VMX0=(A11/(2.0*R*T))*(1.0-SQRT(1.0-4.0*B11*R*T/A11))
VMX1=(A22/(2.0*R*T))*(1.0-SQRT(1.0-4.0*B22*R*T/A22))

C
C ONE FLUID MODEL

C
BX=B11/4.0+B12/2.0+B22/4.0

C
C TWO FLUID MODEL

C
B1X=(B11+B12)/2.0
B2X=(B22+B12)/2.0

C
C CALCULATE EXCESS FUNCTIONS WITH VARYING XI FACTOR

WRITE(2,30)
WRITE(2,40)
WRITE(2,45)

30 FORMAT(1H1,20X,43HEXCESS FUNCTIONS FROM VAN DER WAAL EQUATION,///
40 FORMAT(5X,2HXI,18X,13HEXCESS VOLUME,18X,15HEXCESS ENTHALPY,18X,
118HEXCESS FREE ENERGY,///
45 FORMAT(16X,3(4X,9HONE FLUID,9X,9HTWO FLUID,1X),///
DO 60 I=90,100

XI=FLOAT(I)/100.0
AX=A11/4.0+A12*X I/2.0+A22/4.0
A1X=(A11+A12*X I)/2.0
A2X=(A22+A12*X I)/2.0
VMX05=(AX/(2.0*R*T))*(1.0-SQRT(1.0-4.0*B1X*R*T/AX))
VFX1FL=VMX05-VMX0/2.0-VMX1/2.0
HEX1FL=(-AX/VMX05+A11/(VMX0*2.0)+A22/(VMX1*2.0))/9.869
GEX1FL=((-R*T*ALOG(VMX05-B1X)+(R*T/2.0)*ALOG(VMX0-B11))+(R*(T/2.0)*
1ALOG(VMX1-B22)))/9.869+HEX1FL

C
C TWO-FLUID SECTION

C
VY=(A1X/(2.0*R*T))*(1.0-SQRT(1.0-4.0*R*T*B1X/A1X))

TWO-FLUID SECTION

VY=(A1X/2.0*R*(1.0-SORT(1.0-4.0*K*T*R1X/A1X))

VZ=(A2X/2.0*R*(1.0-SORT(1.0-4.0*K*T*R2X/A2X))

VEX2FL=(VY-VMX0)/2.0+(VZ-VMX1)/2.0

HY=-A1X/VY

HZ=-A2X/VZ

HEX2FL=((HY-(-A11/VMX0))/2.0)+((HZ-(-A22/VMX1))/2.0)/9.869

GW=-R*T*ALOG(VMX0-R11)-((A11/VMX0)

GX=-R*T*ALOG(VMX1-R22)-((A22/VMX1)

GY=-R*T*ALOG(VY-R1X)- (A1X/VY)

GZ=-R*T*ALOG(VZ-R2X)- (A2X/VZ)

GEH2FL=((GY-GW)/2.0+(GZ-CX)/2.0)/9.869

WRITE(2,50)X1,VEX1FL,VEX2FL,HFX1FL,HFX2FL,GEH1FL,GEH2FL

FORMAT(7X,F4.2,7X,6(E13.6,3X),/)

60 CONTINUE

STOP

END

C
C
C
C
C

C THIS PROGRAM EVALUATES EXCESS FUNCTIONS FROM GUGGENHEIMS EQUATION,
C EMPLOYING BOTH ONE AND TWO-FLUID LIQUID MODELS.

C
C
C
C READ CRITICAL TEMPERATURES AND VOLUMES

C READ(7,10) TCA, VCA, TCR, VCR

C READ EVALUATION TEMPERATURE

C READ(7,20) T

C
C 10 FORMAT(4(F6.0))

C 20 FORMAT(F6.0)

C R=82.053

C C1=1.0/0.74028397

C C2=7.8989796

C
C CALCULATE COMMON FACTORS A11, B11, A22, B22, A12, B12; FOR BOTH MODELS

C A11=TCA*VCA*R*C1

C A22=TCR*VCR*R*C1

C B11=VCA/C2

C B22=VCR/C2

C X=C1 *R*SQRT(TCA*TCR)

C Y=(((VCA**(1.0/3.0))+(VCR**(1.0/3.0)))/2.0)**3)

C A12=X*Y

C B12=Y/C2

C CALL VM(VMX0, A11, B11, T)

C CALL VM(VMX1, A22, B22, T)

C
C ONE FLUID MODEL

C
C RX=R11/4.0+R12/2.0+R22/4.0

C
C TWO FLUID MODEL

C R1X=(B11+B12)/2.0

C R2X=(B22+B12)/2.0

C
C CALCULATE EXCESS FUNCTIONS WITH VARYING XI FACTOR

C WRITE(2,30)

C WRITE(2,40)

C WRITE(2,45)

C 30 FORMAT(1H1,20X,43HEXCESS FUNCTIONS FROM GUGGENHEIMS EQUATION ,//)

C 40 FORMAT(5X,2HX1,18X,13HEXCESS VOLUME,18X,15HEXCESS ENTHALPY,18X,
C 118HEXCESS FREE ENERGY,//)

C 45 FORMAT(16X,3(4X,9HONE FLUID,9X,9HTWO FLUID,1X),//)

C DO 60 I=90,100

C XI=FLOAT(I)/100.0

C AX=A11/4.0+A12*XI/2.0+A22/4.0

C A1X=(A11+A12*XI)/2.0

C A2X=(A22+A12*XI)/2.0

C CALL VM(VMX05, AX, RX, T)

C VFX1FL=VMX05-VMX0/2.0-VMX1/2.0

C HFX1FL=(-AX/VMX05+A11/(VMX0*2.0)+A22/(VMX1*2.0))/9.869

C G1=-R*T*ALOG(VMX05-RX)+3.0*BX*R*T/(VMX05-RX)+3.0*RX**2*R*T/

C 1 (2.0*(VMX05-RX)**2)+RX**3*R*T/(3.0*(VMX05-RX)**3)-AX/VMX05

```

G2=-R*T*ALOG(VMX0-R11)+3.0*R11*R*T/(VMX0-R11)+3.0*R11**2*R*T/
1 (2.0*(VMX0-R11)**2)+R11**3*R*T/(3.0*(VMX0-R11)**3)-A11/VMX0
G3=-R*T*ALOG(VMX1-R22)+3.0*R22*R*T/(VMX1-R22)+3.0*R22**2*R*T/
1 (2.0*(VMX1-R22)**2)+R22**3*R*T/(3.0*(VMX1-R22)**3)-A22/VMX1
GEX1 FL=(G1-0.5*G2-0.5*G3)/9.869

```

TWO-FLUID SECTION

```
CALL VM(VY,A1X,R1X,T)
```

```
CALL VM(VZ,A2X,R2X,T)
```

```
VEX2 FL=(VY-VMX0)/2.0+(VZ-VMX1)/2.0
```

```
HY=-A1X/VY
```

```
HZ=-A2X/VZ
```

```
HEX2 FL=((HY-(-A11/VMX0))/2.0)+((HZ-(-A22/VMX1))/2.0)/9.869
```

```
GW=G2
```

```
GX=G3
```

```
CY=-R*T*ALOG(VY-R1X)+3.0*R1X*R*T/(VY-R1X)+3.0*R1X**2*R*T/
```

```
1 (2.0*(VY-R1X)**2)+R1X**3*R*T/(3.0*(VY-R1X)**3)-A1X/VY
```

```
CZ=-R*T*ALOG(VZ-R2X)+3.0*R2X*R*T/(VZ-R2X)+3.0*R2X**2*R*T/
```

```
1 (2.0*(VZ-R2X)**2)+R2X**3*R*T/(3.0*(VZ-R2X)**3)-A2X/VZ
```

```
GFX2 FL=((CY-GW)/2.0+(CZ-GX)/2.0)/9.869
```

```
WRITE(2,50)XI,VEX1 FL,VEX2 FL,HEX1 FL,HEX2 FL,GEX1 FL,GFX2 FL
```

```
50 FORMAT(7X,F4.2,7X,(F13.6,3X),/)
```

```
60 CONTINUE
```

```
STOP
```

```
END
```

```

SUBROUTINE VM (V,A,R,1)
R=R2.053
VTRIAL=R*3.0
10 V=(VTRIAL**5*R*1/A)**(0.25)+R
DIFF=(V-VTRIAL)**2/VTRIAL
IF(DIFF.LE.5.0E-8) GO TO 20
VTRIAL=V
GO TO 10
20 RETURN
END

```


The Bubble-Point, Dew-Point Programme

This programme first generates the Jacobian of a matrix of simultaneous exponential equations, consisting of blocks of four such equations per experimental bubble-point, dew-point pair. The general construction of such a Jacobian has been shown earlier (diagram 2.8). The differential elements are obtained, not by the normal algebraic method, but by a process of approximate numerical differentiation, since this is a good deal easier to programme, and sufficiently accurate.

The generation of the Jacobian is carried out by the subroutine ASEMBL, which, in turn, uses the function routines DIFFL and PCALC. The initial estimates of the coefficients are read in by the main subroutine MAINSB, as data, and these are used in generating the Jacobian for the first cycle. The assembled Jacobian and the delta P vector, also calculated by ASEMBL, are then transferred to the simultaneous equation solution routine, SIMEQ4. The weights given to each point are also required by this routine. The solution is carried out by first normalising and weighting both right- and left-hand sides, by premultiplication by the weighted transpose of the Jacobian. The weighted transpose is never actually assembled as a matrix, as this would simply waste space, the product elements being transferred directly to the matrix ANORM. The set is then reduced by pivotal condensation, which is effectively the elimination of one coefficient at a time, with the eliminated rows being stored in the workspace of the

Jacobian, which is no longer required. Once the final element is reached, and the relevant coefficient evaluated, the remaining coefficients can be evaluated by successive back-substitution into the stored rows. Should the matrix for any reason be singular, this shows up at the stage of the reduction to the final element, when the result $0=0$ is produced. If this should occur, the programme is automatically halted, and control returned to the main subroutine, MAINSB, which determines which point is causing the trouble, and identifies it. If the solution is successful, the coefficient vector is returned to MAINSB, and is handed to the routine COFCOR, which increments the initial estimates and checks the values of the coefficients for convergence to a solution. It also examines coefficients derived from virial coefficients, if these are being calculated, to ensure that the method is sufficiently determinate in these terms to allow of a successful solution. If all the coefficients are satisfactory, and convergence to the required accuracy has not been obtained, then the coefficients are handed back to the main subroutine MAINSB, and another cycle commences, the process continuing until convergence occurs, or a limiting number of cycles, read in as data, is reached. The programme is then halted, by the setting of the cycle counter NOCYCL to the limiting cycle number, and the excess Gibbs free energy is calculated for the corrected composition values, and also for a set series of composition values, from $x=0.1$ to $x=0.9$.

It should be pointed out ,in conclusion, that as a self-consistent set of units is required for such calculation, the pressure input to this programme should be in Joules per cubic centimetre and volumes and virial coefficients in units of cubic centimetres. The $J\text{ cm}^{-3}$ is one million (10^6) Pascals. The units of the Redlich-Kister coefficients should be selected such that a value for G^E/RT results from the fitting; these estimates are read as the vector ASTART, which contains NORKAS elements. The values of the virial coefficients are read in as VCCOEF, and if these are known the corresponding element of VCTEST should be set to 1, otherwise the value of Vctest can be set to 0 and an estimate given in the corresponding element of VCCOEF of its value. The integers NOPTS, NOCOEF, NOEQNS, and NORKAS refer respectively to the number of bubble-point,dew-point pairs, the total number of coefficients, the total number of equations, and the number of Redlich-Kister coefficients to be calculated.

```

C
C *****
C THIS PROGRAMME EVALUATES THE CONSTANTS FOR A REDLICH-KISTER TYPE OF
C RELATIONSHIP BETWEEN EXCESS GIBBS FUNCTION AND MOLE FRACTION, X, OF THE
C SECOND COMPONENT IN THE LIQUID PHASE, FOR THE PRESSURE/COMPOSITION
C RESULTS OBTAINED FROM BUBBLE-POINT, DEW-POINT EXPERIMENTS
C
C THE MAIN PROGRAMME IS EFFECTIVELY A DUMMY, AN ARRANGEMENT USED TO
C SIMPLIFY THE PROCESS OF AMENDING THE DIMENSIONALITY OF THE PROGRAMME
C IF THIS IS NECESSARY.
C
C THE DIMENSIONS SHOULD BE SET TO AT LEAST:
C SP1((4*NO.OF POINTS),((4*NO.OF POINTS)+5))
C SP2((NO.OF POINTS),14)
C SP3((4*NO.OF POINTS),(4*NO.OF POINTS))
C *****
C
  DIMENSION SP1(60,65),SP2(15,14),SP3(60,60)
  READ(7,10)NOPTS,NOCOFF,NOFONS,NORKAS
  WRITE(2,10)NOPTS,NOCOFF,NOFONS,NORKAS
10  FORMAT(4(IX,I2))
  IF(NOPTS.GT.15)GO TO 15
  CALL MAINSR(SP1(1,1),SP1(1,2),SP1(1,3),SP1(1,4),SP1(1,5),SP3(1,
1      1),SP2(1,1),SP2(1,2),SP2(1,3),SP2(1,4),SP2(1,5),SP2(1,6)
2      ,SP2(1,7),SP2(1,8),SP2(1,9),SP2(1,10),SP2(1,11),SP2(1,
3      12),SP2(1,13),SP2(1,14),NOPTS,NOCOFF,NOFONS,NORKAS)
  GO TO 30
15  WRITE(7,20)
20  FORMAT(31H TOO MANY POINTS FOR DIMENSIONS)
30  STOP
  END

```

```

SUBROUTINE MAINSB(COFF, WT, DELTAP, RHNORM, JCRIAN, ANORM, PRUR, PDEF,
1 X, Y, Z, WEIGHT, ASTART, RPRUR, RPDEF, RX, RY, RZ, RWEIHT,
2 RASTRT, NOPTS, NOCOEF, NOEONS, NORKAS)

```

```

C *****
C THIS SUBROUTINE IS THE MAIN EXCHANGE ROUTINE. IT READS DATA, THEN
C ORDERS THE TRANSFER OF DATA AND RESULTS BETWEEN THE PROCESSING
C ROUTINES
C *****

```

```

C INTEGER VCTEST, CYCSTP
C REAL JCRIAN
C DIMENSION VCCOEF(3), VCTEST(3), PRUR(NOPTS), PDEF(NOPTS), X(NOPTS),
1 Y(NOPTS), Z(NOPTS), WEIGHT(NOPTS), RPRUR(NOPTS), RPDEF(NOPTS)
2 ), RX(NOPTS), RY(NOPTS), RZ(NOPTS), RWEIHT(NOPTS), ASTART(NOR
3 KAS), RASTRT(NORKAS), COEF(NOCOEF, 1), RHNORM(NOCOEF, 1), WT(N
4 OFONS), DELTAP(NOFONS, 1), JCRIAN(NOEONS, NOCOEF), ANORM(NOCO
5 EF, NOCOEF), RVCOEF(3)

```

```

DO 10 I=1, NOPTS
READ(7, 30) PRUR(I), PDEF(I), WEIGHT(I), X(I), Y(I), Z(I)
WRITE(2, 35) X(I), Y(I), Z(I)

```

```

10 CONTINUE
READ(7, 40) (ASTART(I), I=1, NORKAS)
WRITE(2, 40) (ASTART(I), I=1, NORKAS)
READ(7, 50) (VCCOEF(I), VCTEST(I), I=1, 3)
WRITE(2, 50) (VCCOEF(I), VCTEST(I), I=1, 3)
READ(7, 60) P1, P2, V1, V2, T, CYCSTP
WRITE(2, 60) P1, P2, V1, V2, T, CYCSTP

```

```

30 FORMAT(2(1X, F8.6), 4(1X, F4.2))
35 FORMAT(3(1X, F6.4))
40 FORMAT(F13.6)
50 FORMAT(1X, F7.1, 2X, I1)
60 FORMAT(2(2X, F8.6), 3(2X, F6.2), 2X, I2)
NOCYCL=0

```

```

DO 110 M=1, NORKAS
RASTRT(M)=ASTART(M)

```

```

110 CONTINUE
DO 120 M=1, NOPTS
RPRUR(M)=PRUR(M)
RPDEF(M)=PDEF(M)
RX(M)=X(M)
RY(M)=Y(M)
RZ(M)=Z(M)
RWEIHT(M)=WEIGHT(M)

```

```

120 CONTINUE
DO 130 M=1, 3
RVCOEF(M)=VCCOEF(M)

```

```

130 CONTINUE
DO 145 M=1, NOCOEF
DO 142 N=1, NOEONS
JCRIAN(N, M)=0.0

```

```

142 CONTINUE
145 CONTINUE
ICOUNT=0
DO 147 M=1, NOPTS
DO 146 L=1, 4
ICOUNT=ICOUNT+1
WT(ICOUNT)=WEIGHT(M)

```

```

146 CONTINUE
147 CONTINUE
DO 148 NCOUNT=1, 3

```

```

1         IF(ABS(RVCOEF(NCOUNT)-VCCOEF(NCOUNT)).GT.ABS(VCCOEF(NCOUNT)
1         3.0)) WRITE(2,149)
1         IF(ABS(RVCOEF(NCOUNT)-VCCOEF(NCOUNT)).GT.ABS(VCCOEF(NCOUNT) /
1         3.0)) RETURN
148 CONTINUE
149 FORMAT(/70H VIRIAL COEFF TERM NOT DETERMINATE.SHOULD BE PRESET TO A
1 SUITABLE VALUE)
CALL ASEMBL(P1,P2,V1,V2,VCTEST,RVCOEF,RPRUR,RPDEFW,RX,RY,RZ,NOPTS,
1 RASTRT,NORKAS,DELTAP,JCRIAN,NOCOEF,NOFONS,I)
CALL DEFVPI(NOCYCL,NOFONS,DELTAP,RASTRT,NORKAS,NOCOEF)
CALL SIMEQ4(JCRIAN,DELTAP,WT,NOFONS,NOCOEF,ANORM,RHNORM,COFF,ITEST
1 )
1 IF(ITEST.EQ.1) WRITE(2,160)
WRITE(2,165)
WRITE(2,170) RVCOEF
WRITE(2,155)
WRITE(2,150) COFF
150 FORMAT(7E13.6)
155 FORMAT(/19H COEFFICIENT VECTOR/)
160 FORMAT(/46H SOLUTION OF EQUATIONS SATISFACTORY THIS CYCLE)
165 FORMAT(/20H VIRIAL COEFFICIENTS/)
170 FORMAT(E13.6)
180 FORMAT(16H SINGULAR MATRIX)
IF(ITEST.NE.0)GO TO 250

```

```

C *****
C THE FOLLOWING SECTION EXTRACTS ANY POINT CAUSING SINGULARITY OF THE
C SYSTEM
C *****

```

```

WRITE(2,180)
CALL ASEMBL(P1,P2,V1,V2,VCTEST,RVCOEF,RPRUR,RPDEFW,RX,RY,RZ,NOPTS,
1 RASTRT,NORKAS,DELTAP,JCRIAN,NOCOEF,NOFONS,I)
1 NOCYCL=0
NUMDUF=0
NUMDPT=0
DO 230 I=1,NOPTS
L=(I-1)*4
DO 200 J=1,4
L=L+1
DO 190 K=1,NOCOEF
ANORM(J,K)=JCRIAN(L,K)
CONTINUE
190 CONTINUE
200 M=(I-1)*3
A=ANORM(1,M+2)
R=ANORM(2,M+2)
C=ANORM(3,M+3)
D=ANORM(4,M+3)
DO 210 N=1,NOCOEF
ANORM(1,N)=ANORM(1,N)*B
ANORM(2,N)=ANORM(2,N)*A
ANORM(1,N)=ANORM(1,N)-ANORM(2,N)
ANORM(3,N)=ANORM(3,N)*D
ANORM(4,N)=ANORM(4,N)*C
ANORM(3,N)=ANORM(3,N)-ANORM(4,N)
CONTINUE
210 E=ANORM(1,M+1)
F=ANORM(3,M+1)
DO 220 I1=1,NOCOEF
ANORM(1,I1)=ANORM(1,I1)*F

```

```

ANORM(3,I1)=ANORM(3,I1)*F
ANORM(1,I1)=ANORM(1,I1)-ANORM(3,I1)
IF(I1.GT.(M+3).AND.I1.LE.(M+3+NORKAS).AND.ANORM(1,I1)
).NE.0.0) GO TO 220
NUMDUF=NUMDUF+1
NUMDPT=NUMDPT+1
DELTAP(NUMDPT,1)=FLOAT(1)+0.5
GO TO 230

```

```

220 CONTINUE
230 CONTINUE
WRITE(2,240)NUMDUF
240 FORMAT(11H THERE ARE ,I3,16H SINGULAR POINTS)
WRITE(2,243)
243 FORMAT(18H THOSE POINTS ARE-/)
WRITE(2,244)
244 FORMAT(7H NUMBER/)
DO 247 NWRITE=1,NUMDUF
NUMBER=INT(DELTAP(NWRITE,1))
WRITE(2,245)NUMBER
245 FORMAT(/I5)
247 CONTINUE
RETURN

```

```

250 NOCYCL=NOCYCL+1
260 CALL COFCOR(NOPTS,NORKAS,COFF,VCTEST,RVCOEF,RX,RY,RZ,RASTR1,NOEONS
1,NOCYCL,CYCSTP,NOCOEF,ICRASH)
IF(ICRASH.EQ.1) RETURN
WRITE(2,270)
WRITE(2,280)
DO 265 I =1,NOPTS
WRITE(2,35)RX(I),RY(I),RZ(I)
265 CONTINUE
270 FORMAT(///15H MOLE FRACTIONS/)
280 FORMAT(5X,1HX,6X,1HY,7X,1HZ)
IF(NOCYCL.LT.CYCSTP) GO TO 140
WRITE(2,320)
DO 310 IGIBRS=1,9
XMF=FLOAT(IGIBRS)/10.0
GE=(XMF-XMF**2)*RASTR1(1)
IF(NORKAS.EQ.1) GO TO 300
DO 290 NORK=2,NORKAS
GE=GE+(XMF-XMF**2)*RASTR1(NORK)*(1.0-2.0*XMF)
** (NORK-1)

```

```

290 CONTINUE
300 GE=GE*8.3143*T
WRITE(2,330) XMF,GE
310 CONTINUE
320 FORMAT(1H1,///2H X,8X,3H GE//)
330 FORMAT(1X,F5.4,3X,G13.6/)
WRITE(2,320)
DO 350 IGIBRS=1,NOPTS
XM=RX(IGIBRS)
GE=(XM-XM**2)*RASTR1(1)
IF(NORKAS.EQ.1) GO TO 345
DO 340 NORK=2,NORKAS
GE=GE+(XM-XM**2)*RASTR1(NORK)*(1.0-2.0*XM)**(NORK-1)
CONTINUE
340 GE=GE*8.3143*T
345 WRITE(2,330)XM,GE
350 CONTINUE
RETURN
END

```

```
SUBROUTINE ASEMBL(P1,P2,V1,V2,VCTEST,VCCOEF,PRUR,PDEV,X,Y,Z,NPTS,  
A,NORKAS,DELTAP,JCRIAN,NOCOEF,NEOS,T)
```

C
C
C
C
C
C

```
*****  
THIS SUBROUTINE EMPLOYS THE FUNCTION ROUTINES DIFFL AND PCALC, TO  
CONSTRUCT THE DELTA P VECTOR AND THE JACOBIAN OF THE DIFFERENTIALS  
*****
```

```
INTEGER VCTEST  
REAL JCRIAN  
DIMENSION VCTEST(3),VCCOEF(3),PRUR(NPTS),PDEV(NPTS),X(NPTS),Y(NPTS),  
Z(NPTS),A(NORKAS),JCRIAN(NEOS,NOCOEF),DELTAP(NEOS,1)
```

```
1  
NOROWM=1  
NOCOLM=0  
NOROWA=1  
NOCOLA=3*NPTS  
NOROWV=1  
NOCOLV=3*NPTS+NORKAS  
ISUM=0  
DO 10 N=1,3  
ISUM=ISUM+VCTEST(N)
```

```
10 CONTINUE  
ISUM=3-ISUM  
DO 100 I=1,NPTS
```

```
DO 90 J=1,4
```

```
IF(J.GT.2)GO TO 40  
PC=PCALC(P1,P2,V1,V2,VCCOEF,PRUR(I),X(I),Y(I),Z(I),  
A,NORKAS,T,J)
```

```
1  
P=PRUR(I)  
DELTAP(NOROWM,1)=P-PC  
GO TO 50
```

```
40  
PC=PCALC(P1,P2,V1,V2,VCCOEF,PDEV(I),X(I),Y(I),Z(I),  
A,NORKAS,T,J)
```

```
1  
P=PDEV(I)  
DELTAP(NOROWM,1)=P-PC  
DO 60 K=1,3
```

```
50  
NOCOLM=NOCOLM+1  
IF(J.LT.3.AND.K.EQ.3) GO TO 60  
IF(J.GT.2.AND.K.EQ.2) GO TO 60  
JCRIAN(NOROWM,NOCOLM)=DIFFL(P1,P2,V1,V2,VCCOEF,  
P,X(I),Y(I),Z(I),A,  
NORKAS,T,J,K,0,0,PC)
```

```
1  
2  
60  
CONTINUE  
DO 70 K=1,NORKAS  
NOCOLA=NOCOLA+1  
JCRIAN(NOROWA,NOCOLA)=DIFFL(P1,P2,V1,V2,VCCOEF,  
P,X(I),Y(I),Z(I),A,  
NORKAS,T,J,4,K,0,PC)
```

```
1  
2  
70  
CONTINUE  
DO 80 K=1,3  
NOCOLV=NOCOLV+1  
IF(VCTEST(K).EQ.1)NOCOLV=NOCOLV-1  
IF(VCTEST(K).EQ.1)GO TO 80  
JCRIAN(NOROV,NOCOLV)=DIFFL(P1,P2,V1,V2,VCCOEF,  
P,X(I),Y(I),Z(I),A,  
NORKAS,T,J,5,0,K,PC)
```

```
1  
2  
80  
CONTINUE  
NOCOLM=NOCOLM-3  
NOCOLA=NOCOLA-NORKAS  
NOCOLV=NOCOLV-ISUM  
NOROWM=NOROWM+1
```



```
NOROWA=NOROWA+1  
NOROWV=NOROWV+1
```

```
90 CONTINUE  
NOCOLM=NOCOLM+3  
100 CONTINUE  
RETURN  
END
```

FUNCTION DIFFL(P1,P2,V1,V2,VCCOEF,P,X,Y,Z,A,I,T,NO,ICHGCF,NORK,
NOVCO,PCALCO)

```
C *****  
C THIS SUBROUTINE OBTAINS THE DIFFERENTIALS OF P W.R.T. THE COMPOSITION  
C TERMS, THE REALICH-KISTER A'S ,AND, IF NECESSARY, THE VIRIAL COEFFICIENTS  
C IT DOES THIS BY A NUMERICAL METHOD, USING PCALC TO OBTAIN A VALUE OF P,  
C THEN CHANGING THE VARIABLE VALUE BY A SMALL FRACTION AND RECALCULATING  
C P, THUS OBTAINING THE APPROXIMATE DIFFERENTIAL COEFFICIENT  
C *****  
C  
C DIMENSION RKC(10),VCCFR(3),A(1),VCCOEF(3)  
C IF(ICHGCF.LE.3)GO TO 3  
C IF(ICHGCF.EQ.4)GO TO 20  
C IF(ICHGCF.EQ.5)GO TO 30  
3 GO TO (5,10,15),ICHGCF  
5 VINCR=X+X*1.0E-6  
RINCR=VINCR-X  
PNEW=PCALC(P1,P2,V1,V2,VCCOEF,P,VINCR,Y,Z,A,I,T,NO)  
GO TO 40  
10 VINCR=Y+Y*1.0E-6  
RINCR=VINCR-Y  
PNEW=PCALC(P1,P2,V1,V2,VCCOEF,P,X,VINCR,Z,A,I,T,NO)  
GO TO 40  
15 VINCR=Z+Z*1.0E-6  
RINCR=VINCR-Z  
PNEW=PCALC(P1,P2,V1,V2,VCCOEF,P,X,Y,VINCR,A,I,T,NO)  
GO TO 40  
20 DO 25 NUM=1,I  
RKC(NUM)=A(NUM)  
IF(NUM.EQ.NORK)RKC(NUM)=A(NUM)+A(NUM)*1.0E-6  
IF(NUM.EQ.NORK)RINCR=RKC(NUM)-A(NUM)  
25 CONTINUE  
PNEW=PCALC(P1,P2,V1,V2,VCCOEF,P,X,Y,Z,RKC,I,T,NO)  
GO TO 40  
30 DO 35 NUM=1,3  
VCCFR(NUM)=VCCOEF(NUM)  
IF(NUM.EQ.NOVCO)VCCFR(NUM)=VCCOEF(NUM)+VCCOEF(NUM)*1.0E-6  
IF(NUM.EQ.NOVCO)RINCR=VCCFR(NUM)-VCCOEF(NUM)  
35 CONTINUE  
PNEW=PCALC(P1,P2,V1,V2,VCCFR,P,X,Y,Z,A,I,T,NO)  
40 DIFFL=(PNEW-PCALCO)/RINCR  
RETURN  
END
```

FUNCTION PCALC(P1,P2,V1,V2,VCCOFF,P,X,Y,Z,A,I,T,NO)

C
C
C
C
C
C

THIS SURROUTINE CALCULATES DEW-, OR BUBBLE-POINT PRESSURE FROM THE FOUR
DEW-POINT, BUBBLE-POINT, EQUATIONS

DIMENSION A(I),VCCOFF(3)

DELT12=VCCOFF(2)*2.0-VCCOFF(1)-VCCOFF(3)

AC=X

BC=Y

IF(NO.GT.2) AC=Z

IF(NO.GT.2) BC=X

SUM1=0.0

SUM2=0.0

DO 10 N=1,I

IF(N.EQ.1) SUM1=A(1)*(AC-AC**2)

IF(N.GT.1)SUM1=

1 SUM1+A(N)*(AC-AC**2)*(1.0-2.0*AC)**(N-1)

IF(N.EQ.1) SUM2=A(1)*(1.0-2.0*AC)

1 IF(N.EQ.2) SUM2=SUM2+A(2)*(1.0-2.0*AC)**2-2.0*A(2)*
(AC-AC**2)

1 IF(N.GT.2) SUM2=SUM2+A(N)*(1.0-2.0*AC)**N-2.0*FLOAT(N-1)*
(AC-AC**2)*(1.0-2.0*AC)**(N-2)*A(N)

10 CONTINUE

GF=SUM1*8.3143*T

DGEDX=SUM2*8.3143*T

EMU1=GF-AC*DGEDX

EMU2=GF+(1.0-AC)*DGEDX

IF(NO.EQ.2:OR.NO.EQ.4) GO TO 20

PCALC=EXP((EMU1-(V1-VCCOFF(1))*(P1-P)-DELT12*P*BC**2)/(8.3143*T))*
1 P1*((1.0-AC)/(1.0-BC))

RETURN

20 PCALC=EXP((EMU2-(V2-VCCOFF(3))*(P2-P)-DELT12*P*(1.0-BC)**2)/
1 (8.3143*T))*P2*(AC/BC)

RETURN

END

SUBROUTINE SIMEO4(CAMAT,RHVEC,WT,NEON,NCOEF,ANORM,RHNORM,COEF,I FAL
)

C *****
C THIS SUBROUTINE WEIGTHS THE SETS OF EQUATIONS, NORMALISES THEM, THEN
C OBTAINS A SOLUTION BY A GAUSSIAN PIVOTAL CONDENSATION, PIVOTING ALWAYS
C ABOUT THE LARGEST REMAINING ELEMENT OF THE MATRIX: THE MATRICES WT AND
C AMAT ARE OVERWRITTEN BY THE ROUTINE
C *****

DOUBLE PRECISION DSUM
DIMENSION AMAT(NEON,NCOEF),RHVEC(NEON,1),WT(NEON),ANORM(NCOEF,NCOEF),RHNORM(NCOEF,1),COEF(NCOEF,1)

1 DO 40 N=1,NCOEF
DO 20 M=1,NCOEF
DSUM=0.0
DO 10 L=1,NEON
DSUM=DSUM+AMAT(L,N)*AMAT(L,M)*WT(L)

10 CONTINUE
ANORM(N,M)=DSUM

20 CONTINUE
DSUM=0.0
DO 30 L=1,NEON
DSUM=DSUM+AMAT(L,N)*RHVEC(L,1)*WT(L)

30 CONTINUE
RHNORM(N,1)=DSUM

40 CONTINUE
NO=NCOEF
DO 110 K=1,NCOEF
GTST=0.0
DO 60 M=1,NO
DO 50 N=1,NO
IF(ABS(ANORM(N,M)).GT.ABS(GTST)) I=N
IF(ABS(ANORM(N,M)).GT.ABS(GTST)) J=M
IF(ABS(ANORM(N,M)).GT.ABS(GTST)) GTST=ANORM(N,M)

50 CONTINUE

60 CONTINUE
IF(K.EQ.NCOEF) GO TO 120
DO 70 M=1,NO
AMAT(K,M)=ANORM(I,M)

70 CONTINUE
RHVEC(K,1)=RHNORM(I,1)
WT(K)=FLOAT(J)+0.5
DO 90 N=1,NO
IF(N.EQ.I) GO TO 90
FACTOR=ANORM(N,J)/ANORM(I,J)
DO 80 M=1,NCOEF
ANORM(N,M)=ANORM(N,M)-ANORM(I,M)*FACTOR

80 CONTINUE
RHNORM(N,1)=RHNORM(N,1)-RHNORM(I,1)*FACTOR

90 CONTINUE
DO 100 M=1,NCOEF
ANORM(I,M)=0.0
ANORM(M,J)=0.0

100 CONTINUE
RHNORM(I,1)=0.0

110 CONTINUE

120 DO 130 M=1,NCOEF
COEF(M,1)=0.0

130 CONTINUE
IF(RHNORM(I,1).EQ.0.0.OR.ANORM(I,J).EQ.0.0) WRITE(2,160)

```
IFAIL=0
IF (RHNORM(I,1).EQ.0.0.OR.ANORM(I,J).EQ.0.0) GO TO 170
COEF(J,1)=RHNORM(I,1)/ANORM(I,J)
NFIN=NCOEF-1
DO 150 N=1,NFIN
  NUM=NCOEF-N
  NUM2=INT(WT(NUM))
  DSUM=0.0
  DO 140 K=1,NCOEF
    DSUM=DSUM+COEF(K,1)*AMAT(NUM,K)
140  CONTINUE
  COEF(NUM2,1)=(RHVEC(NUM,1)-DSUM)/AMAT(NUM,NUM2)
150 CONTINUE
IFAIL=1
160 FORMAT(16H SINGULAR MATRIX)
170 RETURN
END
```

SUBROUTINE DEVPOI(NOCYCL,NEQS,DELTAP,A,NORKAS,NOCOEFF)

C
C
C
C
C
C

THIS ROUTINE CALCULATES THE STANDARD DEVIATION OF THE P'S FROM THE
DELTA P VECTOR

DIMENSION DELTAP(NEQS,1),A(NORKAS)
SDPSQ=0.0
DO 10 N=1,NEQS
SDPSQ=SDPSQ+DELTAP(N,1)**2

10 CONTINUE
SDEVP=SQRT(SDPSQ/FLOAT(NEQS-NOCOEFF))
WRITE(2,15)
WRITE(2,20) NOCYCL
WRITE(2,30) SDEVP
WRITE(2,35)
WRITE(2,37)
WRITE(2,40)(A(N),N=1,NORKAS)
15 FORMAT(1H1 ///)
20 FORMAT(///16H CYCLE NUMBER ,I3)
30 FORMAT(///15H STD.DEV. P = ,G13.6)
35 FORMAT(///40H COEFFICIENTS OF REDLICH-KISTER EQUATION)
37 FORMAT (/9X,2HA1,17X,2HA2,17X,2HA3,17X,2HA4,17X,2HA5)
40 FORMAT(/5(5X,G13.6))
RETURN
END

```
SUBROUTINE COFCOR (NPTS,NORKAS,COEF,VCTEST,VCCOEF,X,Y,Z,A,NEQS,  
1 NOCYCL,CYCSTP,NOCOEF,ICRASH)
```

```
C  
C *****  
C THIS ROUTINE INCREMENTS THE COEFFICIENTS, AND TESTS THE VALUES FOR  
C CONVERGENCE TO A SOLUTION  
C *****  
C
```

```
INTEGER VCTEST,CYCSTP  
DIMENSION VCTEST(3),A(NORKAS),COEF(NEQS,1),X(NPTS),Y(NPTS),Z(NPTS)  
1 ,VCCOEF(3)  
M=3*NPTS  
ICOUNT=1  
DO 10 N=1,NPTS  
X(N)=X(N)+COEF(ICOUNT,1)  
Y(N)=Y(N)+COEF(ICOUNT+1,1)  
Z(N)=Z(N)+COEF(ICOUNT+2,1)  
ICOUNT=ICOUNT+3  
10 CONTINUE  
GTSTCF=0.0  
DO 20 N=1,NORKAS  
A(N)=A(N)+COEF(ICOUNT,1)  
IF(ABS(COEF(ICOUNT,1)).GT.GTSTCF)GTSTCF=COEF(ICOUNT,1)  
ICOUNT=ICOUNT+1  
20 CONTINUE  
IF(ABS(GTSTCF).LT.1.0E-6)NOCYCL=CYCSTP  
IF(ABS(GTSTCF).LT.1.0E-6)WRITE(2,40)  
NOVC=3*NPTS+NORKAS+1  
ICRASH=0  
DO 30 N=1,3  
IF(NOVC.GT.NOCOEF)GO TO 30  
IF(VCTEST(N).EQ.0 .AND.ABS(COEF(NOVC,1)).GT.  
1 ABS(VCCOEF(N)/3.0))WRITE(2,50)N  
IF(VCTEST(N).EQ.0 .AND.ABS(COEF(NOVC,1)).GT.  
1 ABS(VCCOEF(N)/3.0))NOCYCL=CYCSTP  
IF(VCTEST(N).EQ.0 .AND.ABS(COEF(NOVC,1)).GT.  
1 ABS(VCCOEF(N)/3.0))ICRASH=1  
IF(VCTEST(N).EQ.0)VCCOEF(N)=VCCOEF(N)+COEF(NOVC,1)  
30 CONTINUE  
40 FORMAT(///47H CONVERGENCE TO 10**-6 IN A PARAMETERS OBTAINED)  
50 FORMAT(/20H VIRIAL COEFFICIENT ,I3,16H NOT DETERMINATE)  
RETURN  
END
```

REFERENCES

- 1* American Petroleum Institute Research Project 44
Carnegie Press 1953
- 2* Barker, J.A.
Austral. J. Chem. 6 207
- 3* Berthelot, D.
C. r. hebdom. Seanc. Acad. Sci., Paris 126 (1898) 1703
- 4* Brewster, E.R. and McGlashan, M.L.
J.C.F.T.A.R. (1973) 12 2046
- 5* Cruickshank, A.J.B., Windsor, M.L. and Young, C.L.
Trans. Faraday Soc. (1966) 62 2341
- 6* Dickinson, E, Hunt, D.C. and McLure, I.A.
J. Chem. Thermodynamics (1975) 2 731
- 7* Dixon, D.T.
Ph.D. Thesis, University of Reading, 1966
- 8* Dixon, D.T. and McGlashan, M.L.
Nature (Lond) 206 (1965) 710
- 9* Ewing, M.B., Marsh, K.N., Stokes, R.H. and Tuxford, C.W
J. Chem Thermodynamics (1970) 2 751
- 10* Faulkner, E.A., McGlashan, M.L. and Stubley, D.

J. Chem. Soc. (1965) 510 2837.

11* Green, M.C., Lappert, M.F., Pedley, J.B., Schmidt, W. and Wilkins, B.T.

J. Organometallic Chem. (1971) 31(3) C55-%c58

12* Guggenheim, E.A.

Mol. Phys. (1965) 9 199

13* Harris, K.R. and Dunlop, P.J.

J. Chem. Thermodynamics (1970) 2 805

14* Harsted, B.S. and Thomsen, E.S.

J. Chem. Thermodynamics (1974) 6 549

15* Hudson, G.H. and McCoubrey, J.C.

Trans. Faraday Soc. (1960) 56 761

16* Huff and Reed

J. Chem. Eng. Data (1963) 8 306

17* Kaye and Laby

Tables of Physical and Chemical Constants. Longman 1973

18* Leland, T.W., Rowlinson, J.S. and Sather, G.A.

Trans. Faraday Soc. (1968) 64 1447

19* Leland, T.W., Rowlinson, J.S., Sather, G.A. and Watson, I.D.

Trans. Faraday Soc. (1969) 65 2034

20* Leonard, P.J., Henderson, D. and Barker, J.A.

Trans. Faraday Soc. (1970) 66 2439

21* Lorentz, H.A.

Annln. Phys. (1881) 12 127

22* Marsh, K.N.

J. Chem. Thermodynamics (1971) 3 355

23* Marsh, K., McGlashan, M.L. and Warr, C.

Trans. Faraday Soc. (1970) 66 2453

24* McGlashan, M.L.

Trans. Faraday Soc. (1970) 66 18

25* McGlashan, M.L. and Stoeckli, H.F.

J. Chem. Thermodynamics (1969) 1 589

26* Murray, R.S. and Martin, M.L.

J. Chem. Thermodynamics (1975) 2 839

27* Myers, D.B. and Scott, R.L.

Ind. Eng. Chem. (1965) 55 no.7 43

28* Prigogine, I.

The Molecular Theory Of Solutions, Chapter 2 (North-Holland
1957)

29* Rowlinson, J.S.

Liquids and Liquid Mixtures (Butterworth 1969)

30* Rowlinson, J.S.

Discussions of the Faraday Society (1970) 49 30

31* Scatchard, G, Wood, S.E. and Mochel, J.M.

J. Phys. Chem. (1939) 43 119

32* Sturtevant, J.M. and Lyons, P.A.

J. Chem. Thermodynamics (1969) 1 201

33* van der Waals, J.D.

Die Continuitat Des Gasformigen Und Flussigen Zustandes
(Barth, Leipzig, 1900)